DISSERTATION

submitted to the

Combined Faculties for the Natural Sciences and for Mathematics of the

Ruperto-Carola University of Heidelberg, Germany

for the degree of

Doctor of Natural Sciences

presented by

MD Beril Doğancı

born in Sakarya, Turkey

The Generation and Characterisation of Mice with Conditional Knock-out of the NMDAR Subunit NR2B

Referees: Prof. Dr. Peter Seeburg

Prof. Dr. Hannah Monyer

Dedicated to my grandfather R. Özdemir , my parents Gülnihal and A. Oktay Doğancı.

Acknowledgements

Many thanks to:

Prof. Dr. Hannah Monyer for interesting project and excellent working conditions.

Prof. Dr. Peter H. Seeburg for continuous scientific input, supervision and valuable ideas.

Dr. Anne Herb for reading the manuscript and critical remarks.

Dr. Jakob von Engelhardt for performing the electrophysiological analysis.

Thorsten Schächinger for his work during the generation of the targeting construct.

Dr. Miyoko Higuchi for her help in organisation and breeding of the mouse lines and for helpful remarks.

Dr. Isabel Aller for continuous moral support, helpful remarks.

Dr. Elke Fuchs for introductory help in ES cell work.

Dr. Valery Grinevich for constructing and providing the viral construct.

Ali Çetin and Dr. Pavel Osten for teaching and helping for the steriotaxy.

Simone Astori for helpful remarks and discussions.

Ulla Amtmann for friendly atmosphere.

Laura Winkel and Catherine Munzig for making the life easy in the department.

All my colleagues and friends from the Department of Clinical Neurobiology.

My uncle Prof. Dr. İ. Bedii Özdemir for his great support, and strengthening my enthusiasm of science.

Jörg Schaefer for constant moral support, making my life in Heidelberg happier and bearable even during challenging and exhausting times.

My parents A. Oktay Doğancı, Gülnihal Doğancı, my sister D. Begüm Doğancı, my brother C. Can Doğancı for their continuous support and love.

Graduate College 791 for financial support .

Summary

The *N*-methyl-*D*-aspartate (NMDA) receptors belong to the family of ionotropic glutamate receptors. They play a critical role in neuronal pattern formation during development and in synaptic plasticity as molecular coincidence detectors. NMDA receptor is a tetrameric protein complex comprised of two obligatory NR1 subunits and two identical or different NR2 subunits, of which four types exist named NR2A-D. In rodents and other mammals, NR1 and NR2B are expressed in the entire central nervous system, already at embryonic stages, whereas NR2A expression starts and increases only postnatally to coexist with NR2B in the adult brain. Mice lacking the NR1 subunit or lacking the NR2B subunit die at birth, whereas mice lacking NR2A are viable. Both NR2A and NR2B containing NMDA receptors are implicated in synaptic plasticity, learning and memory formation but their distinctive functions are unknown. The NR2B subunit received a lot of attention because mice genetically altered to overexpress NR2B showed improved spatial reference memory and enhanced LTP. The lethality of the general NR2B knock-out gives rise to the necessity of a conditional knock-out, by which deleterious effects due to lack of NR2B during embryogenesis are prevented, and the physiological function of NR2B can be elucidated in the postnatal brain. For this purpose, a DNA construct for homologous recombination in embryonic stem (ES) cells was generated with *NR2B* allele exon 6 flanked by loxP sequences. This exon encodes the region preceding the first transmembrane domain of the NR2B subunit. As a selection marker, a neomycin resistance gene flanked by frt sites was introduced in intron 6. The selection marker was subsequently removed by flp recombinase from the targeted *NR2B* allele, and the ES cells were used for blastocyst injection to derive $NR2B^{2lox}$ mice.

$NR2B^{2lox}$ mice were bred with Tg^{Cre4} mice, selectively expressing Cre recombinase in forebrain principal neurons, to generate mice heterozygous for the transgene Tg^{Cre4} and homozygous for the conditional *NR2B* allele ($NR2B^{2lox/2lox}$). In these mice ($NR2B^{\Delta Fb}$), postnatal forebrain principal neurons should lack NMDA receptors containing the NR2B subtype. Deletion of NR2B in $NR2B^{\Delta Fb}$ mice was revealed by electrophysiological measurements. In parallel, in this study, also lentiviral mediated gene delivery was used in vivo for Cre/loxP mediated DNA recombination. Recombinant lentivirus encoding Cre recombinase and the GFP protein under the control of the α-CaMKII promoter was delivered stereotactically to the hippocampal CA1 region of $NR2B^{2lox/2lox}$ mice at P20. Lack of NR2B was assessed by electrophysiological measurements of synaptic and whole-cell NMDA currents, using NR2B specific antagonists. Recordings from CA1 neurons revealed reduced NMDA currents, lack of sensitivity to ifenprodil, a selective blocker of NR2B containing NMDA receptors, and faster than wild type deactivation kinetics of NMDA mediated currents, indicating the effective loss of the NR2B-type NMDA receptors. Frequency and AMPA component of miniature EPSCs were unaltered whereas the NMDA component was reduced. Moreover an impairment of cellular LTP could be shown. Western blot analysis from hippocampal homogenates of $NR2B^{\Delta Fb}$ mice showed a ~ 70% reduction of the NR2B subunit levels, and no significant change in the expression levels of NR2A, and of the AMPA receptor subunits GluR-A and GluR-B. Collectively, these studies describe a conditional mouse model for elucidating the particular physiological functions of the NR2B type of NMDA receptors in the adult forebrain.

Zusammenfassung

N-Methyl-D-Aspartat(NMDA)-Rezeptoren gehören zur Familie der ionotropen Glutamatrezeptoren. Sie spielen eine entscheidende Rolle bei der neuronalen Musterbildung während der Entwicklung sowie bei der synaptischen Plastizität als molekulare Koinzidenzdetektoren. NMDA-Rezeptoren sind tetramere Proteinkomlexe, die aus zwei obligatorischen NR1-Untereinheiten und zwei identischen oder verschiedenen NR2-Untereinheiten, von denen es vier Typen (NR2A-D) gibt, gebildet werden. In Nagern und anderen Säugetieren werden NR1 und NR2B im gesamten zentralen Nervensystem bereits im Embryonalstadium exprimiert, die Expression von NR2A beginnt dagegen erst nach der Geburt und nimmt während der ersten postnatalen Wochen zu, so dass NR2B und NR2A im erwachsenen Hirn gemeinsam vorkommen. Mäuse, denen NR1 oder NR2B fehlen, sterben kurz nach der Geburt, während Mäuse ohne NR2A lebensfähig sind. Sowohl NR2A- als auch NR2B-enthaltende NMDA-Rezeptoren wirken mit bei synaptischer Plastizität, Lernen und Gedächtnisbildung. Die NR2B-Untereinheit erhielt starke Aufmerksamkeit, da Mäuse mit Überexpression von NR2B verbessertes räumliches Referenzzgedächtnis und Verstärkung von LTP zeigten. Die Letalität des generellen NR2B Knock-out erfordert einen konditionellen Knock-out, durch den die nachteiligen Effekte infolge des Fehlens von NR2B während der Embryogenese verhindert werden, und mit dem die physiologische Funktion von NR2B im postnatalen Gehirn aufgeklärt werden kann. Zu diesem Zweck wurde ein DNA-Konstrukt für die homologe Rekombination in embryonalen Stammzellen (ES-Zellen) hergestellt, in dem Exon 6 durch loxP-Sequenzen flankiert wird. Dieses Exon kodiert für die Region N-terminal vor der ersten Transmembrandomäne der NR2B-Untereinheit. Als Selektionsmarker wurde ein von frt-Sequenzen flankiertes Neomycin-Resistenzgen in Intron 6 eingeführt. Der Selektionsmarker wurde anschließend durch Flp-Rekombinase aus dem veränderten *NR2B*-Allel entfernt und die ES-Zellen wurden in Blastozysten injiziert, um $NR2B^{2lox}$ Mäuse zu erhalten.

$NR2B^{2lox}$ Mäuse wurden mit Tg^{Cre4}-Mäusen verpaart, welche Cre-Recombinase ausschliesslich in Prinzipalzellen des Vorderhirns exprimieren, um $NR2B^{\Delta Fb}$-Mäuse zu erhalten, die heterozygot für das Transgen Tg^{Cre4} und homozygot für das konditionelle *NR2B*-Allel ($NR2B^{2lox/2lox}$) sind. In $NR2B^{\Delta Fb}$-Mäusen sollten postnatal in Prinzipalzellen des Vorderhirns NR2B-enthaltende NMDA-Rezeptoren fehlen. Die Deletion von *NR2B* in $NR2B^{\Delta Fb}$-Mäusen wurde durch elektrophysiologische Messungen bestätigt. Parallel dazu wurden auch Versuche unternommen, bei denen in vivo lentiviral induzierte Cre-Expression für die DNA-Rekombination genutzt wurde. Rekombinante Lentiviren, die Cre-Recombinase und GFP unter der Kontrolle des α-CaMKII-Promoters exprimieren, wurden stereotaktisch in die hippocampale CA1-Region von homozygoten $NR2B^{2lox/2lox}$ Mäusen am Tag P20 injiziert. Das Fehlen von NR2B wurde durch elektrophysiologische Messungen von synaptischen und Ganzzell-Strömen untersucht, wobei NR2B-spezifische Antagonisten eingesetzt wurden. Messungen an CA1-Neuronen zeigten reduzierte NMDA-Ströme, das Fehlen von Ifenprodil-Sensitivität sowie Deaktivierungskinetiken von NMDA-vermittelten Strömen, die schneller als in Wildtyp-Mäusen waren, alles Hinweise auf einen effektiven Ausfall von NMDA-Rezeptoren vom NR2B-Typ. Frequenz und AMPA-Komponente von Miniatur-EPSC's blieben unverändert, die NMDA-Komponente war dagegen reduziert. Darüberhinaus konnte eine Verminderung des zellulären LTP gezeigt werden. Die Western-Blot Analyse von hippocampalen Homogenaten aus $NR2B^{\Delta Fb}$-Mäusen ergab eine 70%ige Reduktion der NR2B-Untereinheit und keine signifikante Änderung in der Expressionshöhe von NR2A sowie der AMPA-Rezeptoruntereinheiten GluR-A und GluR-B.

Zusammenfassend beschreiben diese Studien ein konditionelles Mausmodell, um die speziellen physiologischen Funktionen des NR2B-Typs der NMDA-Rezeptoren im erwachsenen Vorderhirn aufzuklären.

1 INTRODUCTION

1.1 Synaptic Transmission

A synapse is the specialized junction where two neurons contact each other. It consists of the terminus of a presynaptic cell apposed to a postsynaptic cell. The process by which nerve cells signal one another at a synapse is termed as synaptic transmission.

Based on the structure of apposition, synapses are categorised into two major groups: electrical and chemical. Electrical synapses occur at specialised sites called gap junctions, which physically connect the cytoplasm of the presynaptic and postsynaptic cells. Synaptic communication in the brain relies mainly on the chemical mechanisms. At chemical synapses, there is no structural continuity between pre- and postsynaptic neurons and the region separating the two cells is named as synaptic cleft. Presynaptic cells contain synaptic vesicles, which contain a neurotransmitter. Arrival of an action potential to the presynaptic axon terminal activates voltage gated calcium channels. The resulting transient elevation of the Ca^{2+} concentration causes vesicles to fuse with the presynaptic membrane, thereby releasing their neurotransmitter into the synaptic cleft. The neurotransmitter diffuses across the synaptic cleft and interacts with the ligand gated ionotropic or metabotropic receptors on the postsynaptic membrane. Ionotropic receptors are membrane proteins that form an ion channel. Upon binding the neurotransmitter the ionotropic receptor undergoes a confirmational change that results in the opening of the channel pore. On the other hand upon interaction with the neurotransmitter metabotropic receptors indirectly activate ion channels in the membrane through signal transduction mechanisms. While ionotropic receptors mediate fast synaptic activity in the range of milliseconds, metabotropic receptors mediate slower synaptic activity lasting seconds to minutes, often associated with changes in neuronal excitability and synaptic strength.

Synaptic transmission in the CNS can be either excitatory or inhibitory. The main excitatory neurotransmitter is glutamate and main inhibitory neurotransmitters are GABA and Glycine. Glutamate activates ionotropic glutamate receptors as well as metabotropic glutamate receptors. These channels are permeable to Na^+ and K^+. Action of glutamate on

ionotropic glutamate receptors is always excitatory whereas on metabotropic glutamate receptors it is either inhibitory or excitatory. GABA acts on ionotropic $GABA_A$ receptors and metabotropic $GABA_B$ receptors. $GABA_A$ receptors gate an intrinsic Cl^- channel and $GABA_B$ receptors act on second messenger cascade often activates K^+ channel.

1.2 Ionotropic Glutamate Receptors

Ionotropic glutamate receptors are ligand gated channels selectively permeable for Na^+ and K^+ and some of them also for Ca^{2+} ions, and they mediate the postsynaptic response at most of the excitatory synapses in the brain. Based on their preferential activation of specific agonists, they are subdivided in different subclasses: *N*-methyl-*D*-aspartate (NMDA) and non-NMDA ionotropic glutamate receptors (Dingledine et al., 1999). The non-NMDA receptors are comprised of the AMPA (α-amino-3-hydroxy-5-methylisoxazole-4-propionic acid) and the kainate receptor families. AMPA receptors are the fast excitatory neurotransmitter receptors in the CNS. They form hetero-oligomeric assemblies consisting of four different subunits termed GluR-A, GluR-B, GluR-C and GluR-D. Kainate receptors are formed by the subunits GluR-5, GluR-6, GluR-7, KA-1 and KA-2 (Hollmann and Heinemann, 1994; Wisden and Seeburg, 1993). NMDA receptors consist of subunits termed NR1, NR2A, NR2B, NR2C, NR2D, NR3A. The different subunits of the AMPA, Kainate and NMDA receptors show amino acid identities higher than 60 per cent within the groups and less than 40 percent identity between the groups (Figure 1). They are mainly expressed in the CNS but there is evidence for the presence of subpopulations in pancreatic islet cells (Inagaki et al., 1995), osteoclasts and osteoblasts (Chenu et al., 1998), skin cells (Ault and Hindebrand, 1993) and cardiac ganglia (Gill et al., 1998). In addition, a fourth class of iGluR is represented by the δ1 and δ2 receptors that share 18-25% amino-acid identity with the other glutamate receptors subunits (Lomeli et al., 1993). These orphan subunits do not form functional channels by themselves, nor have they been shown to modify the function of other subunits. Zuo and co-workers showed their important role with the so called "Lurcher mice" which has a mutation in the δ2 receptor. These mice showed spontaneous degeneration of Purkinje cells and cerebellar ataxia (Zuo et al., 1997).

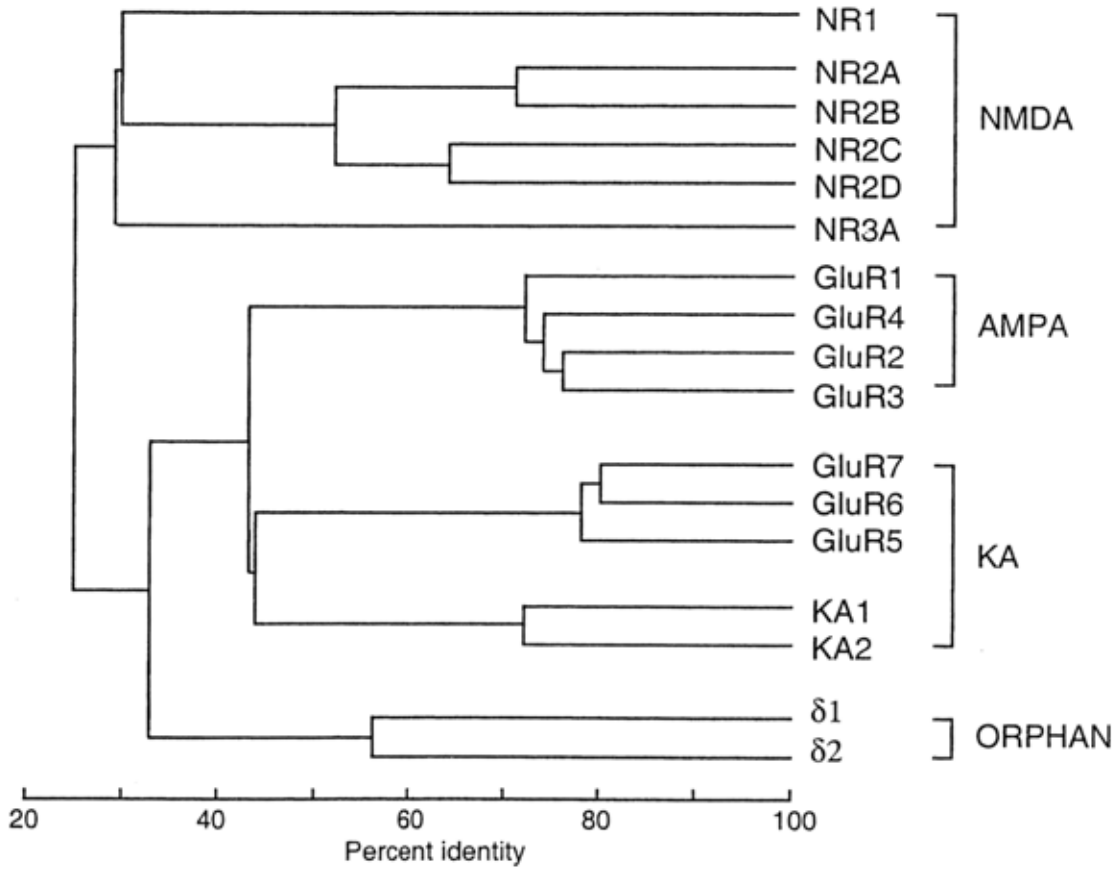

Figure 1: Phylogenetic diagram based on amino acid identities (Egebjerg and Jensen, 2002).

1.2.1 Structure of the Ionotropic Glutamate Receptor Subunits

All ionotropic glutamate receptors share the same transmembrane topology. Various approaches provide compelling evidence for a structure that consists of an extracellular N-terminus, an intracellular C-terminus, and an extracellular loop between M3 and M4. Thus, only three regions (M1, M3, and M4) completely span the membrane, while the channel lining domain is formed by a cytoplasm facing re-entrant loop M2. The N-terminal domain controls proper assembly of receptor complexes (Ayalon and Stern,

2001). Targeting of the receptor to the synapse and its localization depend on series of interactions with other proteins. The C-terminal domain influences receptor function and proper receptor localisation by its interaction with trafficking, motor, signalling and scaffolding proteins (Barry and Ziff, 2002). The M2 domain contains the critical Q/R/N site, and this controls the key permeation properties of the channel. The bipartite ligand binding domain is formed by the two segments within the N-terminal domain (S1) and the extracellular loop between membrane segments M3 and M4 (S2) (Figure 2).

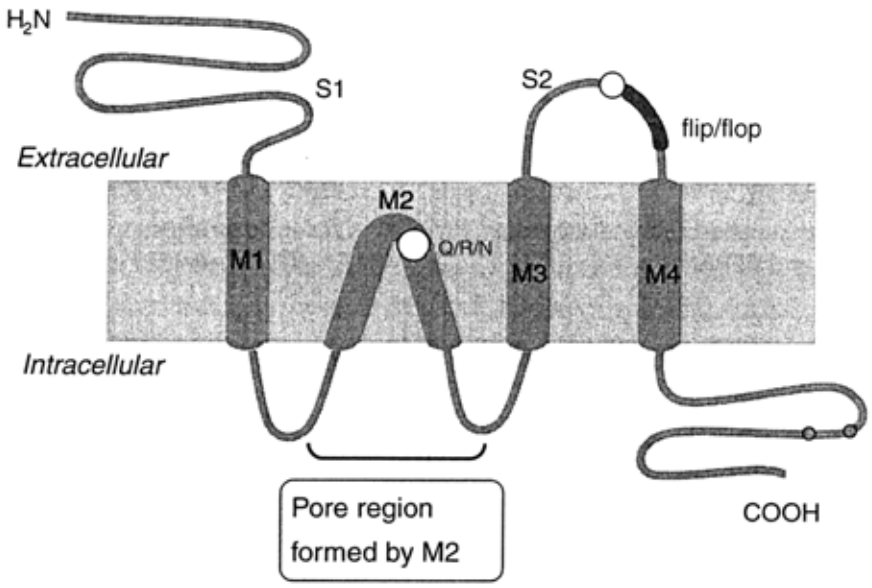

Figure 2: Transmembrane topology of ionotropic glutamate receptors
Three transmemnbrane domains (M1, M3, M4) span the membrane. The pore lining region is generated by M2, which enters the membrane from the intracellular surface forming a pore loop structure. The Q/R/N site is in the pore lining region. The alternatively spliced flip/flop exon exists in AMPA receptors and is located extracellularly. S1 and S2 designate the two parts of the ligand binding domain (Cull-Candy, 2002).

1.2.2 The Q/R/N Site of the Ionotropic Glutamate Receptors

The cation selectivity of the NMDA and non-NMDA receptors depends on a critical residue in the pore-lining region. In this region, NMDA receptor subunits contain an

asparagine (N) at a position homologous to the Q/R (glutamine/arginine) site of the AMPA and kainate receptor subunits. Therefore this site is collectively referred as the Q/R/N site. High Ca^{2+} permeability and voltage dependent blockade of NMDA receptors are critically dependent on the presence of asparagine at this site. Although both NR1 and NR2 subunits contribute to the permeation pathway, they do not contribute equally to the selectivity filter. Thus swapping asparagine for glutamine (N → Q) in NR1 affects the Ca^{2+} permeability of the channel but not its Mg^{2+} block. The same substitution in TM2 region of the NR2 subunits affects the Mg^{2+} block, but not the Ca^{2+} permeability (Burnashev et al., 1992; Cull-Candy, 2002). The amino acid occupying the Q/R site of the AMPA receptor subunits is controlled by RNA editing and determines the conductance, rectification and divalent cation permeability of the ion channel (Sommer et al.,1991; Verdoorn et al., 1991). The presence of an arginine residue at this position in GluR-B renders AMPAR channels impermeable to Ca^{2+}, whereas a glutamine at this position in GluR-A, -C and -D produces Ca^{2+} permeable channels.

1.3 NMDA Receptors

1.3.1 NMDA Receptor Subunits and Splice Variants

The NMDA subtype of the glutamate receptor channel plays an important role in synaptic plasticity as a molecular coincidence detector and in neuronal pattern formation during development (Dingledine et al., 1999). It has also also been implicated in various disease states such as epilepsy and neurodegeneration following ischemia. Three families of NMDA receptor subunits have been identified: the ubiquitously expressed NR1 subunit, (four distinct NR2 subunits (A, B, C and D), and two NR3 subunits (A, B) (Moriyoshi et al., 1991; Sugihara et al., 1992; Monyer et al., 1992,1994; Das et al., 1998; Hollmann et al., 1999). The NR1 subunit has up to eight functional isoforms arising from a single gene due to alternative splicing at three independent sites (Dingledine et al., 1999). Similar to NR1 subunit, NR2 and NR3 subunits (apart from NR2A) has several splice variants although the functional relevance of the different splice variants remains unclear. NMDA receptors are formed as heteromers containing two obligatory NR1 and two NR2 subunits

(Seeburg et al., 1993; Laube et al., 1998; Kuryatov et al., 1998). In the tetrameric receptor complex, identical subunits sit adjacent to each other (Behe et al., 1995; Laube et al., 1998; Schorge and Colquhoun, 2003). Glycine as a co-agonist potentiates the NMDA response by augmenting the NMDA receptor-channel opening frequency and, thus, it increases the open state probability of the channel. While NR2 subunits contain the binding site for glutamate, NR1 carries the binding site for glycine. NR3 subunits co-assemble with NR1 to form excitatory glycine gated receptor channels that are unaffected by glutamate or NMDA (Chatterton et al., 2002). Neurons contain a large pool of NR1, which is unassembled with NR2, and does not reach the cell surface, but is retained in the endoplasmic reticulum (ER) and rapidly degraded (Chazot and Stephenson, 1997a; Huh and Wenthold, 1999). The retention appears to be dependent on a signal in the C terminal domain. It has been suggested that assembly of NR1 with NR2 subunits results in the masking of the retention signal and, therefore, leads to targeting to the membrane (Barria and Malinow, 2002).

1.3.2 Functional Features of NMDA Receptors

1.3.2.1 NMDA Receptors as "Coincidence Detectors" During Synaptic Transmission

For many central synapses, the transmitter activates a mixed population of non-NMDARs and NMDARs. AMPA receptors mediate fast synaptic currents while NMDA receptors mediate currents that are slower and longer lasting. During synaptic transmission, the rates at which the responses of NMDA receptors rise and decline upon application and removal of agonists are markedly slower than those of non-NMDA receptors (Forsythe et al., 1988; Vicini et al., 1998). NMDA receptors first open about 10 ms after glutamate is released into the synaptic cleft and continue to open and close for hundreds of milliseconds until glutamate unbinds from the receptor (Dzubay et al., 1996; Behe et al., 1999). It is the slow deactivation rate of NMDA receptors that governs the duration of the excitatory postsynaptic potential which is a measure of the strength of synaptic signalling (Lester et al., 1990).

NMDARs form cation-selective channels with a high permeability to Ca^{2+} as well as Na^{+} and K^{+} (MacDermott et al., 1986; Jahr and Stevens, 1993). Moreover, they are blocked in a voltage dependent manner by binding of a Mg^{2+} ion to a site within the pore (Nowak et al., 1984; Mayer et al., 1984). The gating of NMDARs is therefore controlled by a combination of ligand(s) and voltage, making them distinct from other types of ligand-gated receptors. High Ca^{2+} permeability and voltage dependent blockade by extracellular Mg^{2+} are considered to be important for the function of receptors in mediating long term changes in synaptic efficacy and cytotoxic effects of glutamate in hypoxic conditions.

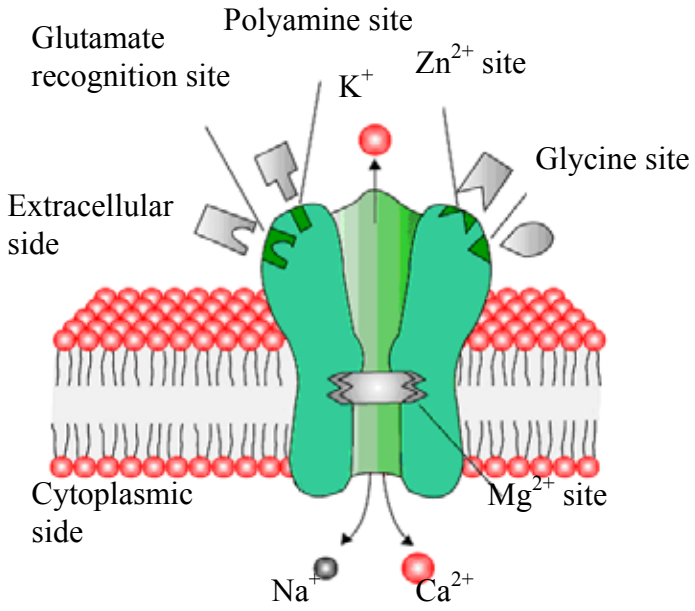

Figure 3: Schematic representation of the NMDA receptor complex.
The NMDA receptor complex possesses a glutamate recognition site to which receptor agonists and competitive antagonists bind, as well as binding sites for glycine, polyamines, and the ions Mg^{2+} and Zn^{2+}. Channel opening permits an influx of Na^{+} and Ca^{2+} ions and an efflux of K^{+} ions (After Scatton, 1993).

This voltage-dependent block by Mg^{2+} is relieved as the postsynaptic cell is depolarised, allowing the NMDAR to function as a coincidence detector of pre- and postsynaptic activity. Thus, the postsynaptic receptor permits an influx of Ca^{2+} and Na^{2+} ions only at those synapses that receive high frequency presynaptic activity (Bourne and Nicoll, 1993). As a result, opening of NMDA receptors leads to an influx of cations including

Ca^{2+} and the permeation of Ca^{2+} through NMDA receptor ion channels initiates signal transduction cascades that in turn modulate synaptic strength (MacDermott et al., 1986).

1.3.2.2 Gating and Pharmacological Properties of NMDA Receptors

As mentioned above, NMDA receptor channels show high permeability to Ca^{2+} ions which, unlike the Ca^{2+} permeability of AMPARs, is independent of the subunit composition. The residue at the N/Q/R site of the NR1 subunit is the main determinant of the Ca^{2+} permeability of NMDARs.

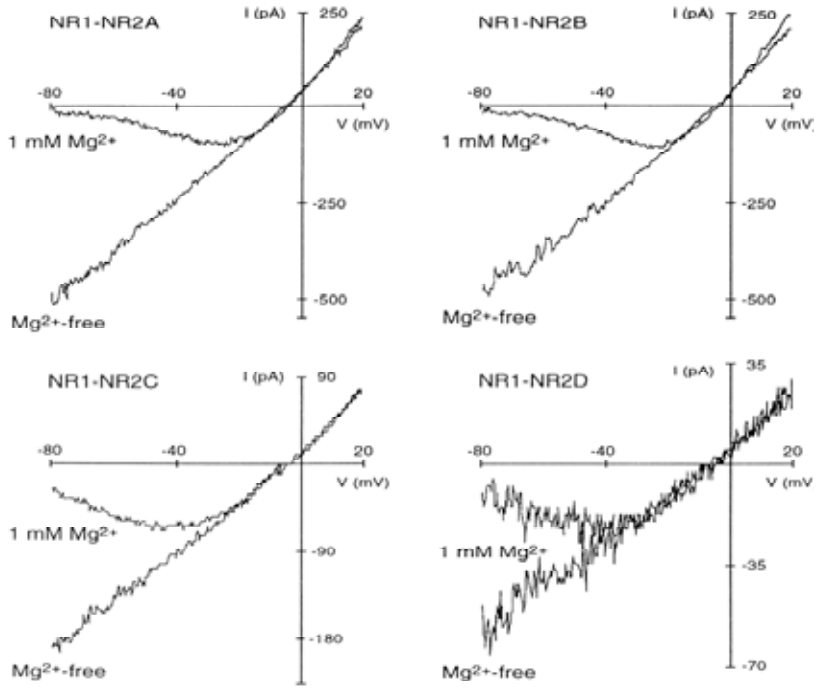

Figure 4: Subunit-specific Mg^{2+} block of recombinant NMDA receptors
A clear difference in the strength of the voltage-dependent block of glutamate induced currents by extracellular Mg^{2+} is observed for different NR1-NR2 channel subtypes. In the presence of 1 mM Mg^{2+} NR1-NR2A and NR1-NR2B channels are characterised by a stronger voltage sensitivity of the Mg^{2+} block. (Monyer et al., 1994).

The extent of blocking of NMDARs by Mg^{2+} is, however, dependent on the NR2 subunit. There is a clear difference in the strength of the voltage-dependent block of glutamate-

induced currents by extracellular Mg^{2+} for different NR1-NR2 channel subtypes (Figure 4). In a heterologous expression system, it has been demonstrated that in physiological concentrations of 1 mM extracellular Mg^{2+}, the NR1-NR2A and NR1-NR2B channels are characterized by stronger voltage sensitivity to Mg^{2+} block than the NR1-NR2C and NR1-NR2D channels (Monyer et al., 1994).

Furthermore, the decay of NMDAR mediating excitatory postsynaptic currents (EPSCs) and the apparent affinity of the receptor for glutamate are both strongly influenced by the identity of the NR2 subunits involved. NR2A-containing receptor channels differ from the other channel subtypes by considerably shorter offset decay time courses after a brief application of L-glutamate, which is thought to be crucial for the coincidence detection of the pre- and postsynaptic activities. NMDA receptor subtypes differ in their pharmacology. D-AP5 is perhaps the most commonly used NMDA receptor antagonist, which shows a selectivity for NR2A and NR2B containing NMDA receptor complexes.

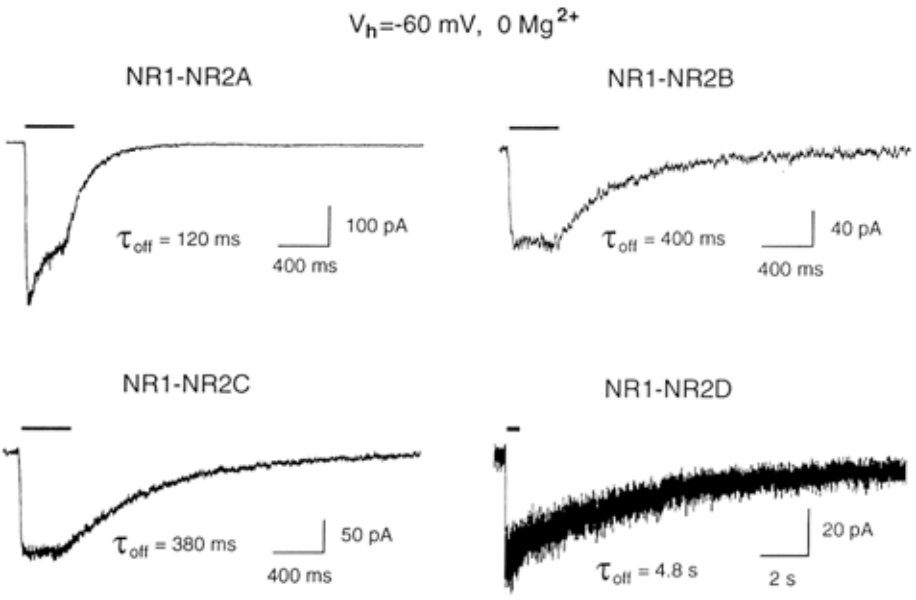

Figure 5. Subunit-specific offset decay time constants of recombinant NMDA receptors.

MK-801 is the NMDA receptor open channel blocker, which acts by binding to the open pore of the NMDA receptor channel. Thus it is a non-competitive antagonist. Ifenprodil

and Ro 25-6981 are the polyamine site antagonists of the NMDARs whose effects are specific for channels containing the NR2B subunit. Furthermore NVP-AAM077 preferentially blocks NR2A containing receptors (9 fold preferance for NR2A compared to NR2B containing receptors) (Paoletti et al., 2006). Thus, the presence of different NR2 subunits confers distinct gating and pharmacological properties to heteromeric NMDARs.

Different NR2 subunits confer different properties to the NMDAR channel. The NR2A subunit has faster deactivation time and increased desensitisation in contrary to the NR2B subunit (Monyer et al., 1994).

1.3.3 Developmental Expression Profile of NMDA Receptors

One indication of the functional importance of NMDAR subunit diversity comes from different regional and developmental expression profiles of the subunits. The NR1 subunit displays ubiquitous expression in all the brain regions and at all stages of development, in keeping with the view that NR1 is indispensable in the formation of functional NMDARs. NR1 subunit mRNA appears as early as E14, peaks around P20, and subsequently declines to adult levels. The expression of the NR1 splice variants, however, shows considerable regional and developmental heterogeneity. In contrast to the NR1 subunit, mRNA for NR2A, NR2B, NR2C and NR2D subunits are differentially distributed. Furthermore, in situ hybridisation studies (Monyer et al., 1994), and immunoprecipitation experiments (Sheng et al., 1994) have demonstrated that their expression is developmentally regulated.

The expression of NR2B and NR2D begins at least as early as E14, whereas NR2A and NR2C are first detected perinatally. At embryonic stages, NR2B mRNA is expressed in the entire brain whereas NR2D mRNA is expressed in the diencephalon and brainstem. After birth, NR2A mRNA appears in the entire brain whereas NR2C mRNA is seen mainly in the cerebellum. The expression of NR2B mRNA becomes restricted to the forebrain where that of NR2D mRNA is strongly reduced (Figure 5).

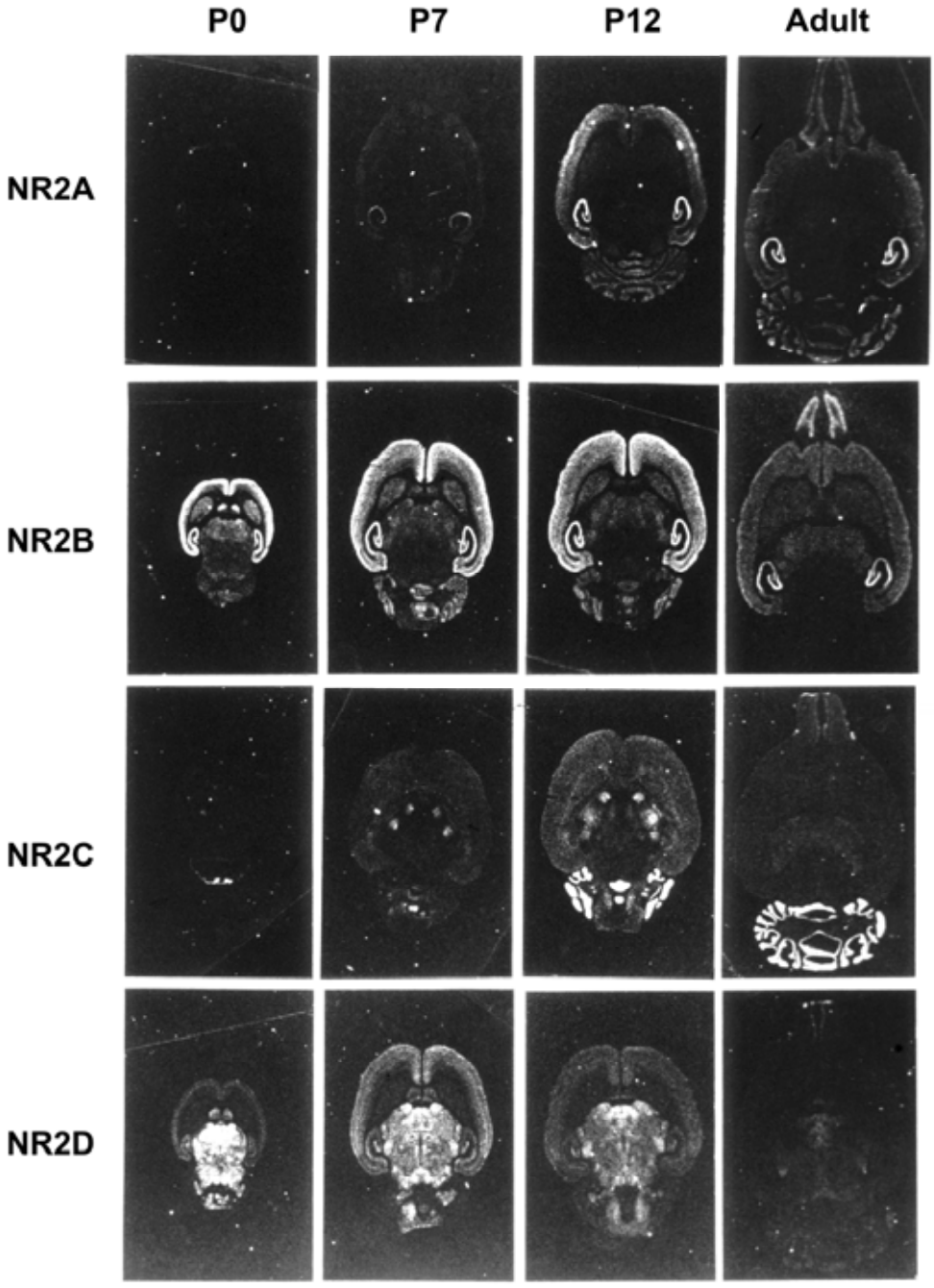

Figure 5. Postnatal developmental profiles of NR2 receptor transcripts in horizontal rat brain sections from P0, P7, P12, and adult animals. NR2A and NR2B are the major subunits expressed in the adult forebrain (Monyer et al., 1999).

All NR2 transcripts reach peak around P20-P25 except for NR2D, which peaks around P7 and subsequently declines to adult levels. In pyramidal neurons of the neocortex and the hippocampus, NR2B is coexpressed with NR2A; in granule cells of the

cerebellum NR2B is replaced by NR2A and NR2C at about P12 (Figure 6). In the adult CNS, NR2A and NR2B are the major subunits expressed in the neocortex and the hippocampus.

1.3.4 Effect of the Subunit Expression Profile on Kinetic Properties

The gradual increase of the NR2A subunit expression in the constant presence of the NR2B subunit results in different kinetic properties of NMDA receptors. It appears that during development, increasing the contribution of NR2A-containing receptors to the synaptic current decreases the contribution from the NR2B subunit. Functional consequence of altering the NR2A/NR2B ratio is a change in the kinetics of EPSCs mediated by NMDARs. *In vitro* NR2A containing NMDARs have shorter current durations than receptors containing the NR2B subunit (Monyer et al., 1994). Also during postnatal development, the duration of currents mediated by NMDA receptors decreases and it has been shown that regardless of the postnatal age, cells expressing NR2A subunit mRNA had faster NMDAR EPSCs than cells with no expression of this subunit (Figure 6) (Flint et al., 1997)**.** The proportion of cells expressing NR2A and displaying fast NMDAR EPSCs increases during postnatal development and, thus, provide a molecular basis for the developmental changes in EPSCs. Furthermore, an appealing hypothesis suggested that an activity-dependent switch in the subunit composition of NMDARs accounts for the shortening of NMDAR currents in visual cortex during development (Philpot et al., 2001). NR2A subunits are incorporated synaptically late in development, whereas NR2B subunits are still highly persistent at extrasynaptic sites (Stocca and Vicini, 1998; Rumbaugh and Vicini, 1999; Tovar and Westbrook, 1999). Moreover, some native NMDAR channels contain more than one type of the NR2 subunit in the same assembly (Dunah et al., 1998; Sheng et al., 1994; Luo et al., 1997). Although studies in a heterologous system suggest the formation of functional triheteromeric assemblies of NR1/NR2A/NR2B (Vicini et al., 1998; Tovar and Westbrook, 1999), it is still unknown to what extent these assemblies are formed *in vivo*.

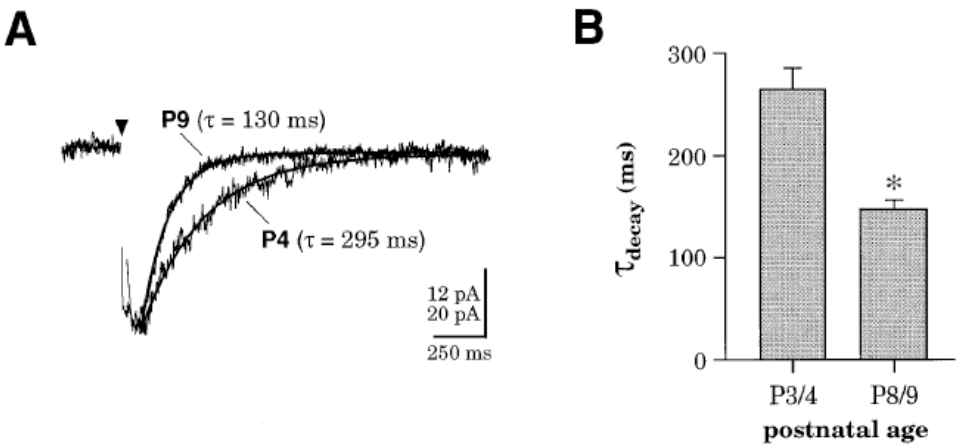

Figure 6: The developmental changes in EPSCs during postnatal development.
Duration of NMDAR EPSCs decreases during postnatal development in somatosensory cortex. The averaged EPSCs from P4 and P9 neurons show a significant difference in the decay time constant (Flint et al., 1997).

1.3.5 Importance of the NR2A and NR2B Subunits for Learning and Memory

According to Hebb´s rule, learning and memory are represented by a change in synaptic strength between two neurons being active at the same time (Hebb et al., 1949). Changes in synaptic strength are referred by the concept of synaptic plasticity. At the molecular level, the synaptic strengthening occurs by a complex process that is initiated by the action of NMDA receptors. In this regard, NMDA receptors play a role as coincidence detectors (Bourne and Nicoll, 1993) since they only open when the neurotransmitter is bound and the postsynaptic membrane is depolarised to a certain extent. This implies that enhanced synaptic coincidence detection would lead to better learning and memory. Understanding how memory works is, by general agreement, one of neurobiology`s central problems. Naturally, many neurobiologists are concerned how synaptic strength is regulated to store information; that is, they are interested in synaptic plasticity. At synaptic levels, it has been proposed that long term potentiation (LTP) and long term depression (LTD) are the key synaptic mechanisms for cortical plasticity (Bliss and Collingridge, 1993; Linden et al., 1994; Lishman et al.,1994; Nicoll and Malenka, 1995; Malenka and Bear, 2004).

"Hippocampus" is the latin word for "sea horse", and early anatomists gave this name to a part of the brain that is shaped somehow like a sea horse. The hippocampus has been identified as brain region concerned with encoding declarative and spatial memories and is therefore typically, but not exclusively, used to study LTP/LTD. Long term potentiation of synaptic transmission in the hippocampus is the primary experimental model for investigating the synaptic basis of learning and memory in vertebrates. Both LTP and LTD in hippocampus require the NMDAR activation (with the exception of mossy fiber-CA3 synapses).

The trigger for both LTP and LTD is Ca^{2+} influx through NMDA receptors. It is believed that the quantity of Ca^{2+} that enters the cell determines the induction of LTP or LTD: little calcium produces LTD and a lot of calcium produces LTP**.** In synapses displaying LTP, a brief high-frequency burst of synaptic activity leads to an immediate and enduring increase in synaptic efficiency (Bliss and Collingridge 1993).

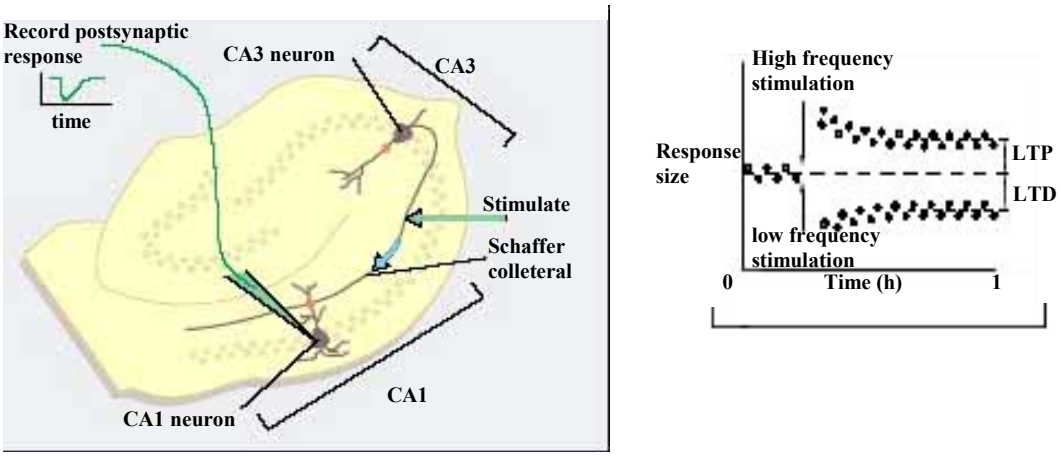

Figure 7: By stimulating a particular pathway (the Schaffer collaterals comprised of axons from pyramidal cells in a region of hippocampus known as CA3) and recording from any of the pyramidal cells in the hippocampal region designated CA1, the electrophysiologist can study direct (monosynaptic) excitatory synaptic connections (Stevens and Sullivan, 1998).

Long term depression as the inverse of LTP is a long lasting reduction in synaptic transmission**.** In contrast to LTP, more prolonged synaptic activity at a lower frequency

gives rise to LTD. In both cases antagonists of the NMDA receptors block induction of the long-lasting change (Bliss and Collingridge 1993; Dudek and Bear, 1992; Mulkey and Malenka, 1992; Bliss and Schoepfer, 2004).

A sufficient rise in Ca^{2+} within the dendritic spine activates intracellular pathways and triggers LTP. Several protein kinases have been implicated in playing roles during these intracellular cascades, like calcium calmodulin–dependent protein kinase II (CaMKII), protein kinase A (PKA) and protein kinase C (PKC) (Bliss and Collingridge, 1993; Malenka and Nicoll, 1999; Lishmann et al., 2002; Lynch et al., 2002; Yasuta et al., 2003; Malenka and Malinow, 2004). Moreover, the mitogen activated protein kinase (MAPK) cascade that activates extracellular signal-regulated kinases (ERKs) has been implicated in LTP (Sweatt et al., 2004; Thomas and Huganir, 2004). The intracellular cascades involved in the induction of LTD accompany the activation of a serine threonine protein phosphatase cascade (Mulkey et al., 1993, 1994, Mulkey and Malenka, 1992). In the last several years, the silent synapse hypothesis has received considerable attention, in that many synapses have only NMDA receptors and LTP occurs by the addition of AMPA receptors (Malenka and Nicoll, 1997).

1.3.6. Characterisation of the Functional Role of NR2B by Overexpression

A large amount of evidence indicates that NMDA receptors are important for synaptic plasticity, learning and memory. In this regard, NR2A and NR2B subunits have become the center of interest because these subunits predominate in the forebrain where they determine many of the functional properties of NMDARs (Monyer et al., 1994). Interestingly, the NR2B subunit received a lot of attention with the generation of the so-called smart mice (Tang et al., 1999). These transgenic mice mice carry additional copies of the NR2B gene under the control of the CaMKII promoter. It has been shown that in neocortex and hippocampus of the transgenic mice the synaptic NR2B protein level is about twice as much as in the wild-type mice. However, it was shown that in visual cortex although the mRNA level of *NR2B* is increased, the synaptic protein level in the visual cortex is unaltered (Philpot et al., 2001). They have proposed that although

overexpression of the *NR2B* transgene alters NMDAR function and synaptic plasticity in hippocampus and insular cortex (Tang et al., 1999; Wei et al., 2001), it does not alter NMDAR function or synaptic plasticity in visual cortex. Yet, in another study using hippocampal neuronal cultures it has been shown that the increased expression of the NR2B subunit does not increase the number of NR2B receptors in the synapse (Barria and Malinow, 2002).

In the "smart mouse" model, overexpression of the NR2B subunit in the forebrain of transgenic mice leads to enhanced activation of NMDA receptors, facilitating synaptic potentiation in response to stimulation at 10-100 Hz. These mice exhibit superior ability in learning and memory in various behavioural tasks, showing that NR2B is critical in gating the age-dependent threshold for plasticity and memory formation. NMDA-receptor dependent modifications of synaptic efficacy, therefore, represent a unifying mechanism for associative learning and memory. Consequently, it has been proposed that the genetic enhancement of mental and cognitive attributes such as intelligence and memory in mammals is feasible. However, the authors did not try to prove that the mentioned effects of the transgenic overexpression of *NR2B* are not simply due to the higher number of NMDA receptors. A possible control would have been transgenic overexpression of *NR2*A. In an other study a transgenic mice with the overexpression of the KIF17 (kinesin superfamily protein 17) in forebrain was generated (Wong et al., 2002). *In vitro* KIF17 was shown to be responsible for the transport of NR2B in neurons (Guillaud et al., 2003). In mice overexpressing *KIF17*, NR2B subunit expression was upregulated. In accordance with the previous results from the smart mouse, these mice also showed superior ability in learning related behavioural tests (Wong et al., 2002). Additionally, in an NR2B knock-down model of aged rats, NR2B anti-sense treatment abolished LTP and impaired spatial learning in behaviour tasks (Clayton et al., 2002). Inconsistent with the previous studies, it has been shown that in adult animals NR2A dependent signalling dominates and activation of NR2A is sufficient to induce LTP, and contribution of the NR2B subunit is redundant (Köhr et al., 2003).

1.3.7 Knock-out Mice and Mice with C-terminally Truncated Receptor Subunits

For each of the known NMDA receptor subunits a knock-out mouse has been generated (Forrest et al., 1994; Li et al., 1994; Ikeda et al., 1995; Sakimura et al., 1995; Ebralidze et al., 1996; Kutsuwada et al., 1996; Das et al., 1998). The absence of NMDARs in NR1 knock-out mice appears to lead to perinatal death (Forrest et al., 1994; Li et al., 1994), which is an indication of important functions for NMDARs in brain physiology. *NR2A* knock-out mice showed impaired hippocampal plasticity (Sakimura et al., 1995). In these mice no morphological or anatomical abnormalities are observed. However, there is a significant decrease of the current mediated by the NMDA receptors and only little LTP. They show moderate behavioural deficits in some learning tasks (Sakimura et al., 1995; Kiyama et al., 1998). Mice lacking a functional *NR2B* gene die at birth (Kutsuwada et al., 1996). *NR2B* knock-out mice which were rescued by hand feeding fail to form the whisker-related neural pattern (barrelets) in the brain stem trigeminal complex and show impaired synaptic plasticity in the hippocampus. Perinatal lethality was found for NR2B knock-out but not for NR2D knock-out mice (Ikeda et al., 1995), indicating that during CNS development, the NR2B subtype is the more important of the two.

In addition to the above mentioned knock-out models, several different gene-targeted mouse lines expressing C-terminally truncated NR2 subunits have been generated (Sprengel et al., 1998; Mori et al., 1998). NMDARs possess extended intracellular C-terminal domains by which they interact with diverse proteins of the postsynaptic density (PSD) for purposes of synaptic localisation, clustering, and signal transduction (Sheng, 1996; Kennedy, 1997, 1998; Kornau et al., 1997; Kim and Huganir, 1999). The C-terminal domains of NR2A and NR2B are potential targets for tyrosine kinases, CaM kinase II, and protein kinases A and C (Moon et al., 1994; Wang and Salter; 1994, Köhr and Seeburg, 1996; Omkumar et al., 1996; Leonard and Hell, 1997; Tingley et al., 1997). The carboxy terminal domains of all four NR2 subunits are large compared to those of other ionotropic glutamate receptors. Thus, the C-terminal domain of NR2A subunit has 627 amino acids, of NR2B subunit has 645, in comparison, the NR1-1 subunit has only 105 amino acids. The regulation of NMDA receptor activity can be caused by direct

phosphorylation of the receptor protein or may involve the phosphorylation of associated postsynaptic proteins (Zheng et al., 1999). Mice expressing C-terminally truncated NR2B subunits die perinatally (Mori et al., 1998; Sprengel et al., 1998), whereas mice expressing C-terminally truncated NR2A subunits show impaired synaptic plasticity and contextual memory (Sprengel et al., 1998). Notably, it has been suggested that C-terminal signalling events are also critical for LTP induction (Köhr et al., 2003). Moreover, in the analysis of mice with truncation of the C-terminal domain an apparent reduction of the truncated NR2A at synaptic sites was seen, which could be due to the impaired targeting, transport or anchoring. Therefore it was proposed that the C-termini of NR2A subunits are necessary for NMDA receptor channels to achieve appropriate densities near release sites (Steigerwald et al., 2000). In mutant mice expressing the truncated NR2B subunit, the effect on synaptic function was examined at hippocampal CA1 synapses during neonatal stages. It has been shown that NMDA receptor mediated excitatory postsynaptic potentials (EPSPs) in the hippocampal CA1 region were strongly reduced in those mice, although the expression level of the truncated protein was comparable to that of the NR2B protein in wild-type mice (Mori et al., 1998). Furthermore, it has been suggested that the carboxy-terminal truncation of the NR2B subunit has little effect on the expression of the subunit protein but does affect its efficient clustering and synaptic localization (Mori et al., 1998). Mice in which the C-terminal domains of the NMDA receptor subunits are truncated show the same severe phenotype as the above mentioned corresponding knock-out mice. Thus, both genetic paradigms independently lead to the functional ablation of NMDAR subunits. Neither with the above mentioned experimental models nor with the knock-out mice and mice with the C-terminal truncation, could the physiological significance of the NR2B subunit in adult mice be clearly characterised.

1.3.8 Pharmacological Approaches to Study the Contribution of NR2A and NR2B Subunits to Synaptic Plasticity

Recent studies using pharmacological blockade of NMDAR subtypes proposed that NR2A-containing receptors are involved in LTP induction, whereas NR2B-containing receptors are involved in LTD induction in the hippocampus and perirhinal cortex (Liu et al., 2004; Massey et al., 2004). Liu and co-workers used two NR2B specific antagonists

(Ifenprodil and Ro25-6981) together with a recently developed NR2A antagonist (NVP-AAM077) to dissect subunit involvement in LTP and LTD at synapses on pyramidal cells in area CA1 of the hippocampus. Both forms of synaptic plasticity can be blocked by the NMDA receptor antagonist D-AP5. The new and unexpected result is that LTP is mediated by NMDA receptors containing NR2A subunits, whereas LTD requires activation of receptors containing NR2B subunits. This finding suggests that the NR2B receptors in the hippocampus may not contribute to learning-related synaptic potentiation, however, no behavioural study has demonstrated the inhibitory effect that NR2B antagonists may have on learning when injected locally in the hippocampus. This result is at odds with the previous findings of Tang and co-workers which showed the important contribution made by NR2B subunits to hippocampal LTP, but not to LTD. In contrast to the conclusions of Liu and co-workers, using a similar pharmacological approach another study demonstrated that LTP induction at CA3 to CA1 synapses with different induction protocols does not require a particular NMDAR subtype (Berberich et al., 2005). It has been proposed that LTP can be induced by tetanic stimulation in the presence of 400 nM NVP via NR2B-type NMDARs, which was not observed by the previously mentioned study. In addition, they showed that LTP induction by repeated tetanic stimulation was not prevented by the NR2A and NR2B specific antagonists. Thus, NR2B-type NMDARs induce LTP when NR2A-type signalling is genetically (Kiyama et al., 1998; Köhr et al., 2003) or pharmacologically impaired. The authors argue that it is not the NMDAR subtype, which determines the polarity of synaptic plasticity. They proposed that it is the pattern of synaptic activation, by triggering different signalling cascades, which directs the response of synaptic plasticity. This view has been challenged by another study (in hippocampal neuronal cell cultures) suggesting that NR2B-containing receptors play a crucial role in synaptic plasticity by recruiting CaMKII to the synapse, a key component of the underlying signalling transduction pathway (Barria and Malinow 2005). Furthermore, it has been suggested that both NR2A and NR2B subunits are critical for the induction of LTD and LTP in anterior cingulate cortex (ACC) (Toyoda et al., 2005; Zhao et al., 2005). Likewise, activation of NR2B in the ACC is important for the acquisition of contextual fear memory, which is consistent with the enhancement of

contextual fear memory in transgenic mice over-expressing NR2B in forebrain (Tang et al., 1999).

1.3.9 NMDA Receptors and Disease

Ca^{2+} influx via NMDAR channels is known to be essential for triggering synaptic plasticity, but excessive calcium influx through NMDA receptors can cause excitotoxic neuronal death. Therefore blockade of NMDARs is neuroprotective in animal models of both stroke and seizure (Lee et al., 1999) and, consequently, NMDA receptors have become a primary focus of excitotoxic research. Excitotoxicity is a critical mechanism contributing to neurodegeneration during ischemia or hypoxia. Major events in the cascade triggered by hypoxia or ischemia include over-stimulation of NMDA receptors, Ca^{2+} entry into cells, activation of Ca^{2+}-sensitive enzymes such as nNOS (neuronal nitric oxide synthase), production of oxygen free radicals, mitochondrial impairment, and subsequent necrosis and apoptosis. Studies indicate that synaptic and extrasynaptic receptor pools have different subunit compositions and form distinct receptor populations: NR2A containing NMDA receptors are predominantly localised at synaptic sites, whereas NR2B containing NMDA receptors are mainly at extrasynaptic sites (Tovar and Westbrook, 1999). It has been proposed that Ca^{2+} entry through the extrasynaptic NR2B containing NMDA receptors are responsible for neuronal cell death (Hardingham et al., 2002). However, inconsistent with this conclusion, a recent study of Coserea (Coserea Dissertation, 2005) shows that both NR2A and NR2B subunits are playing a critical role in excitotoxic neuronal death.

Inappropriate activation of NMDA-receptors is also causally involved in progressive neurodegenerative diseases such as Alzheimer´s disease (AD), Huntington`s disease (HD) and Parkinson´s disease. In animals, overactivation of the NMDA receptors in neostriatum most closely reproduces the neuropathological, neurochemical, and behavioural changes of HD. As well, postmortem analysis of brain tissue from patients with HD suggests that neurons with high expression of NMDA receptors are particularly vulnerable to degeneration (Chen et al., 1999). Selective antagonism of the NR2B subunit

has been shown to improve the treatment of Parkinson`s disease. CP-101,606 has direct antiparkinsonian actions in rodents and monkeys, and it synergistically potentiates the motoric improvements accompanying L-Dopa treatment (Steece and Collier 2000). Some results suggest that NMDA receptor subunits are selectively and differentially reduced in brain areas of AD patients. Modest decrease in the NMDA receptor subunits NR1, NR2A and NR2B was found in the hippocampus and frontal cortex (Loftis et al., 2003).

Some studies suggest that hypofunction of NMDA receptors induced by various NMDA receptor antagonists precipitates a transient psychotic state (a positive symptom of schizophrenia) in healthy individuals (Gao et al., 2000). Mice with reduced NR1 subunit expression (5% of normal levels) (Mohn et al., 1999) or NR2A subunit deletion (Miyamoto et al., 2001) show symptoms related to schizophrenia. The NR2B subunit is also implicated in pain perception. Different from the previously described cognitive enhancement, mice over-expressing the NR2B subunit in the forebrain demonstrate a selective enhancement of persistent pain and allodynia (Wei et al., 2001). This has led to the suggestion that NR2B-selective antagonists may be useful in the treatment of chronic pain.

It is believed that the NR2A and NR2B subunits play important roles in synaptic plasticity, learning and memory. However, none of the investigations using transgenic models, knock-out mice, mice with the C-terminal truncation or pharmacological studies give a definitive explanation and characterisation of the physiological significance of the NR2B subunit in adult mice. Further investigation and characterisation of the functional importance call for a conditional knock-out of the *NR2B* gene.

2.1 Conditonal Knock-out of the *NR2B* Gene Using the Cre/loxP System

The knock-out technology (Capecchi et al., 1989) is instrumental for the understanding of the physiological function of a gene. The technique is also named reverse genetics and differs from the traditional forward genetics technique in which random mutations are introduced to screen a high number of organisms in an effort to search for a certain phenotype. The function of a gene can be indirectly explained from the phenotype of the

corresponding knock-out mouse. A method to study the consequence of a deletion of an important gene is to use behavioural tests. Although this approach to gene inactivation is valuable, for many applications it is important that the inactivation of a particular gene occurs in a conditional manner such as in a predefined cell lineage or at a certain stage of development. Such conditional gene targeting would not only overcome problems posed by the fact that a null mutation in germ line is often lethal, but would also allow a more precise analysis of the impact of a mutation on individual cell lineages. Strategies exploiting site specific DNA recombination have been incorporated into transgenic and gene targeting procedures to allow *in vivo* manipulation of DNA in embryonic stem (ES) cells (Gu et al., 1993; Orban et al., 1992) or living animals (Lakso et al., 1992; Gu et al., 1994). A large number of site-specific DNA recombinases have been described from bacteria and yeast, and the recombination reactions that they catalyse span a wide range of complexity (Kilby et al., 1993). In conjunction with inducible systems for controlling Cre expression and function, these recombination based strategies are likely to have a profound impact on developmental biology and generation of useful animal models of human disease (Sauer et al., 1998)

Cre recombinase from bacteriophage P1 (Sternberg et al., 1981) and Flp recombinase from Saccharomyces cerevisiae are the two members of the integrase family of site specific recombinases (Lewandoski et al., 2001). They are used to conditionally control gene expression by site specific DNA recombination. Cre and Flp recombinases catalyse a conservative DNA recombination (a DNA recombination reaction in which there is no net change in base pairs between the products and the reactants) between 34-bp recognition sites (loxP and FRT). This system allows researchers to create a variety of genetically modified animals and plants with the gene of their choice being externally regulated (Kuhn, et al., 2002; Ghosh, et al., 2002). With the recombinase activity, null alleles could be generated in a tissue-specific and developmentally regulated manner. (Orban et al., 1992). The Cre/loxP system is the most frequently used owing to historical contingency, as it was the first well-developed recombination system. The general strategies are the same for the Flp/Frt system (Lewandoski et al., 2001). The structural biochemistry of the Cre/loxP system showed that Cre is the 38 kDA product of the cre

(cyclization recombination) gene of bactreriophage P1. Its role in the P1 life cycle is believed to include cyclisation of the linear genome following infection of the host cell and resolution of P1 dimers generated by homologous recombination to promote stable segregation of the P1 chromosome to daughter cells (Sternberg et al., 1981). Cre recognises a 34 bp site on the P1 genome called loxP (locus of X-over of P1) and efficiently catalyses reciprocal conservative DNA recombination between pairs of loxP sites. The loxP sites consist of two 13-bp inverted repeats flanking an asymmetric 8-bp spacer region. One molecule of Cre binds per inverted repeat; or two Cre molecules line up at one loxP site. The recombination occurs in the spacer region that gives the loxP site an overall directionality (Sauer and Henderson, 1988). In Cre mediated recombination, resultant DNA structures are dependent upon the orientation of loxP sites. Direct repeats of loxP dictate an excision of intervening sequences leaving one loxP site behind whereas inverted repeats specify inversion. This precise removal of DNA can be used to eliminate an endogenous gene or transgene and to activate a transgene**.**

Figure 8: The loxP site contains two 13 bp inverted repeats and the asymmetric 8 bp spacer region.

To obtain the conditional (meaning tissue and time specific) knock-out, two mouse lines are required. The first line is a conventional transgenic line in which expression of Cre recombinase is driven by a tissue-specific or cell type-specific transcriptional promoter. The second line embodies a target gene to be silenced flanked by two loxP sites (floxed gene) in the same orientation. In offspring derived from intercross between these lines, Cre/loxP site dependent recombination (excision and consequently inactivation of the floxed gene) will occur in cells expressing Cre recombinase under the control of a specific promoter, thereby deleting the target gene. In contrast, the target gene should remain functional in cells of all other tissues, where the Cre transgene is not expressed that is, the promoter controlling the Cre recombinase is inactive. It was shown that Cre could be used at a high efficiency to excise a transgene *in vivo* (Orban et al., 1992). Cre

expressing mice were used to inactivate for the first time an endogenous mouse gene (DNA ploymerase beta gene) (Gu et al., 1994). The terminology of the conditional knock-out was also applied to the NMDA receptor subunit 1 gene (Tsien et al., 1996a, b). The DNA excising capability of Cre recombinase can also be used to turn on a foreign gene by cutting out an intervening stop sequence between the promoter and the coding region of the transgene (Tsien et al., 1996a). The Cre/loxP system is a valuable tool for molecular biology in that, it allows the isolation of individual genes and their functions by establishing tissue specific expression.

Functional inactivation of the *NR2B* alleles is achieved specifically in forebrain principal neurons by breeding with the transgenic mice Tg^{Cre4} in which Cre recombinase is expressed by the α- Ca^{2+} calmodulin dependent protein kinase II (α-CaMKII) promoter (Mantamadiotis et al., 2002). In these mice Cre is expressed in the postnatal forebrain, in pyramidal neurons but not in interneurons.

2.2 The Lentiviral System as a Tool for Gene Delivery

To achieve transgene expression, different viral vectors were applied in different tissues. The most widely used virus types have been adenoviruses (AV), adeno-associated viruses (AAV), herpes simplex virus (HSV), different RNA viruses and retroviruses. In this study the lentivirus, a member of the retroviruses, was used for *in vivo* gene delivery into the mouse hippocampus.

Retroviruses are positive-strand RNA viruses. After entering the host cell the virus reverse transcribes its genome from RNA into DNA. It is this DNA form of the retrovirus that integrates into the host-cell genome. Lentiviruses are a class of retroviruses that cause chronic illnesses in the host organisms they infect. Among retroviruses, they have the distinguishing property of being able to infect non dividing cells in addition to dividing cells, and this ability has led to their development as gene delivery tools (Naldini et al., 1996). Besides, lentiviruses have gained a lot of attention as gene delivery tool due to their very low immunogenicity. Lentivirus based vectors were derived from many different lentiviruses, such as feline immunodeficiency virus (FIV), human

immunodeficiency virus type I (HIV-1), bovine immunodeficiency virus (BIV) (Azzouz et al., 2004; Quinonez and Sutton, 2002). Since they are the best characterised, HIV lentiviruses are the most frequently used in gene delivery.

The lentiviral expression vector system is composed of three plasmids which produce viral particles that are infectious but not contagious (Figure 9): 1) The transfer vector to express the cassette of interest, 2) The packaging vector coding for trans-acting elements necessary for efficient virus replication and maturation, 3) The vector expressing envelope glycoprotein (Naldini et al., 1996).

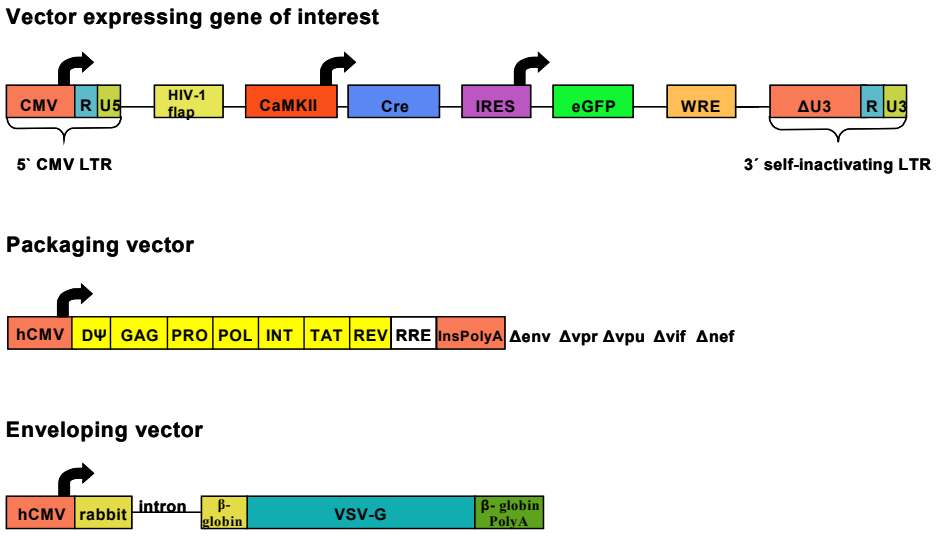

Figure 9: Three components of the self-inactivating lentiviral system (Adapted from A. Cetin Master Thesis, 2004).

A) Vector of gene of interest: expression of Cre recombinase and EGFP is driven by the α-CaMKII promoter. IRES= internal ribosomal entry site, WRE= woodchuck hepatitis virus posttranscriptional regulatory element, LTR= long terminal repeat. B) The packaging vector encodes the information for packing the vector RNA. The RNA encodes for the viral structural proteins: Gag (matrix, capsid and nucleocapsid proteins) and Pol (protease, reverse transcriptase and integrase), in addition the accessory proteins TAT and REV. The vector is devoid of the genes related to HIV pathogenesis (Δvif, Δvpr, Δvpu, Δnef). hCMV (human cytomagalovirus (CMV) promoter, Dψ= packaging signal deletion, RRE= rev-response element. C) the third component is the packaging deficient VSV-g vector (Vesicular Stomatitis virus envelope glycoprotein).

The first component, the transfer vector, contains a packaging signal and will be packed into the newly generated viral particles. This vector is devoid of the gene coding sequences from the original HIV vector. Lacking these cis-acting elements, the transfer vector will be able to transduce target cells but will be unable to replicate. This way, biosafety of the system is enhanced. The HIV-1 flap sequence, which regulates nuclear transport, increases the transduction rate of the infected cells. Introduction of the woodchuck regulatory element (WRE) into the transfer vector close to its 3` end, was shown to facilitate nuclear export of the viral transcript. Its presence also results in higher virus titers (Ramezani et al., 2000).

To achieve efficient gene-of-interest expression from the lentiviral backbone, different internal promoters can be used for targeting different cell types. In this study the α-CaMKII promoter which was characterised by A. Cetin in Prof. Seeburg`s group was used.

The second component, the packaging vector, encodes all necessary and sufficient proteins for packaging. In addition, it lacks the accessory genes vif, nef, vpu, vpr related to HIV pathogenesis but not necessary for infectivity (Kim et al., 1998).

The third component contains the envelope glycoprotein which is necessaray for the tropism and the infectivity of the produced viral particles. When the particles are pseudotyped (the process of generating viral particles that contain the genome of one type of virus and the structural genes of another) with vesicular stomatitis virus glycoprotein (VSV-G), the vector can serve to introduce genes into a broad range of tissues (Burns et al., 1993).

In all 3 vectors of the expression system, U3 from the 5’ LTR (long terminal repeat) was replaced by the CMV (cytomegalovirus) promoter. In addition, the U3 region of the 3’ LTR was also altered. As a result both LTRs became inactive and this makes the transgene vector unable to replicate after infection. These modifications add additional

safety features to the HIV-1 based lentivirus vector system. Such inactive LTR-lentiviral vectors are named as self-inactivating (SIN) vectors.

In this study, lentiviral mediated gene delivery was used *in vivo* for Cre/loxP recombination. The lentiviral particles express Cre recombinase and the GFP protein under the control of the α-CaMKII promoter. The gene of interest to be delivered was cloned by Valerie Grinevich, in Prof. Seeburg´s group.

2.3 Purpose of the Project

It has been hypothesized that the developmental switch from NR2B to NR2B+ NR2A at synaptic sites may be responsible for the decreased plasticity observed in older animals (Carmignoto and Vicini, 1992; Crair and Malenka, 1995). Interestingly, mice overexpressing NR2B show enhanced LTP (Tang et al., 1999) and improved performance in behavioural tests for learning and memory (Tang et al., 1999; Wong et al., 2002) whereas mice lacking the NR2B subunit die at birth (Kutsuwada et al., 1996). Perinatal lethality of *NR2B* knock-out indicates the importance of this subunit during CNS development and calls for a conditional knock-out of the *NR2B* gene.

This dissertation entails 1) generation and analysis of the $NR2B^{2lox}$ mouse line with an exon flanked by loxP sites, 2) generation and analysis of the $NR2B^{\Delta Fb}$ mice by breeding $NR2B^{2lox}$ mice with the transgenic mice Tg^{Cre4} in which Cre recombinase is expressed by the α- Ca^{2+} calmodulin dependent protein kinase II (α-CaMKII) promoter (Mantamadiotis et al., 2002). In $NR2B^{\Delta Fb}$ mice, Cre is expressed in the postnatal forebrain, in pyramidal neurons but not in interneurons. In addition, analysis of the ablation of the *NR2B* in CA1 pyramidal cells of the $NR2B^{2lox}$ mice was performed by using viral mediated gene delivery *in vivo* for Cre/loxP recombination.
Further behavioural studies of the $NR2B^{\Delta Fb}$ mice will help to elucidate the functional importance of the NR2B subunit in learning and memory during adulthood.

2 MATERIALS AND METHODS

2.1 Materials

Common chemicals were purchased from the following companies:

Amersham Biosciences, Freiburg	MBI Fermentas, St.Leon-Rot
AppliChem, Darmstadt	Merck, Darmstadt
Becton & Dickinson, Heidelberg	New England Biolabs (NEB), Frankfurt A.M.
Bio-Rad, München	PEQLAB, Erlangen
Biozym, Hameln	Roche, Mannheim
Fluka, Neu-Ulm	Roth GmbH, Darmstadt
Invitrogen, Karlsruhe	Sigma-Aldrich, München

2.1.1 Special Chemicals

Agar	Invitrogen
Agarose	Invitrogen
Bacto Tryptone	Becton & Dickinson
Bacto Yeast Extract	Becton & Dickinson
5-Brom-4-chlor-3-indolyl-β-D-galactopyranosid (X-Gal)	PEQLAB
Bromophenolblue	CHROMA
Ethidiumbromid	Serva
Ethanol	Sigma-Aldrich
Ficoll, Type 400	Sigma
Isopropyl-β-D-thiogalactosid (IPTG)	PEQLAB
Isopropanol	Applichem
3-(N-Morpholino)-propansulfonic acid (MOPS)	Sigma
Natriumdodecylsulfat (SDS)	AppliChem
Polyethylenglycol 6000 (PEG)	Sigma
Polyvinylpyrrolidon (PVP)	Sigma

PRISM BigDye Terminator cycle sequencing kit	ABI
Quikhyb hybridisation solution	Stratagene
Tris-(hydroxymethyl)-aminomethan (Tris)	Roth

2.1.2 Antibiotics

Ampicillin	Sigma
Chloramphenicol	Sigma
Penicillin/streptomycin	Sigma
Mitomycin C	Sigma

2.1.3 Enzymes and Proteins

RNase inhibitor	Fermentas
5X Buffer Transcription Buffer	Invitrogen
NEB buffer	NEB
0.1 M DTT	Invitrogen
DNAse (RNAse free)	Invitrogen
Reverse Transcriptase	
DNase I (pancreatic nuclease)	Roche
E.coli DNA-Polymerase I (Klenow fragment)	Roche
T4 polynucleotide kinase	NEB
Proteinase K	Roche
RNase A (pancreatic ribonuclease)	Roche
Taq DNA Polymerase	Invitrogen
Pfu DNA Polymerase	Stratagene
T4 DNA Ligase	Roche
Bovine serum albumin (BSA)	Sigma

Restriction endonucleases were purchased from MBI and NEB.

2.1.4 Radioactive Compounds

[γ-^{32}P]ATP	Specific activity:	185TBq/mmol	Amersham
	Radioactive concentration:	370 MBq/ml	
[α-^{32}P]dCTP	Specific activity:	110TBq/mmol	Amersham
	Radioactive concentration:	370 MBq/ml	

2.1.5 Nucleotides

Adenosine triphosphate (ATP)	Amersham
Deoxyribonucleotides (dNTP´s)	MBI

2.1.6 Nucleic Acids

DNA size marker:	λ DNA cut with Sty I	MBI
	pRK7 plasmid DNA cut with Hinf I	MBI
DNA from salmon sperm		Sigma

2.1.7 Vectors

pBluescript II SK (-)	Stratagene

2.1.8 Buffers and Solutions

For the preparation of aquous solutions desalted water from a "MilliQ Water Purification System“ (Millipore) was used.

Chloroform solution	Chloroform/Isoamylalcohol 49:1
Denaturing solution	1.5 M NaCl
	0.5 M NaOH

Loading buffer	30% Glycerol 1% Bromophenolblue and/or 1% Xylencyanol FF 25 mM EDTA
IPTG solution	20 mg IPTG/ml H_2O
10x Ligase buffer	500 mM Tris/HCl pH 8.0 100 mM $MgCl_2$ 10 mM DTT 1 mM EDTA
Phenol solution	1000 g Phenol 250 ml H_2O 1.2 g 8-Hydroxychinolin 52.6 ml Tris-Base (1M) adjust to pH 7 with Tris-HCl (pH 7.6)
Reneutralising solution	1.5 M NaCl 1.5 M Tris-HCl pH 7.5
Solution S1	50 mM Glucose 10 mM EDTA 25 mM Tris-HCl pH 8.0
Solution S2	0.2 N NaOH 1% SDS
Solution S3	3 M Kalium acetate pH 5,2
20x SSC	3 M NaCl 0.3 M Natrium Citrate
TE	10 mM Tris/HCl pH 8,0 or 7,6

	1 mM EDTA
Lysis buffer	
	10 mM Tris
	100 mM EDTA
	0.5% SDS (Sodium Dodecyl Sulfate)
TENS buffer	
	0.14 M NaCl
	20 M Tris
	5 mM EDTA
TFB I	100 mM RbCl
	50 mM $MnCl_2$
	10 mM $CaCl_2$
	30 mM KOAc
	15 % Glycerol (87%)
	adjust to pH 5.8
TFB II	10 mM MOPS
	10 mM RbCl
	75 mM $CaCl_2$
	15 % Glycerol (87%)
	filter sterile
20x TAE Puffer	800 mM Tris/HCl
	400 mM NaOAc
	40 mM EDTA
	adjust to pH 8.3 with acetic acid
X-Gal Solution	20 mg X-Gal/ml DMF

2.1.9 Media for Bacterial Cultures

All Solutions were sterilised in an autoclav.

2YT medium	16 g/l Bacto Tryptone
	5 g/l Bacto Yeast Extract
	5 g/l NaCl
	adjust to pH 7.5 with NaOH
LB medium	10 g/l Bacto Tryptone
	5 g/l Bacto Yeast Extract
	10 g/l NaCl
	4 mM $MgSO_4$
	10 mM KCl
	adjust to pH 7.6 with KOH
TB-A	12 g/l Bacto Tryptone
	24 g/l Bacto Yeast Extract
	0.35% Glycerol 87%
TB-B	0.17 M KH_2PO_4
	0.72 M K_2HPO_4

After autoclaving, 450 ml TB-A are mixed with 50 ml TB-B.

2.1.10 *E.coli* strain

DH5α Invitrogen

2.1.11 Agar Plates

LB medium is autoclaved with 1,5% Select Agar and cooled down to 50°C before preparing plates.

Antibiotics, X-Gal and IPTG are added to the cooled media immediately before use.

Ampicillin plates:	200 mg/l	Ampicillin
Ampicillin/X-Gal plates:	200 mg/l	Ampicillin
	160 mg/l	X-Gal
	160 mg/l	IPTG

2.1.12 Media for ES Cell Culture

DMEM high glucose	Gibco
DMSO	Gibco

2.1.13 Special Buffer and Solutions used in ES Cell Culture

MEM-non-essential amino acids	Invitrogen
Sodium pyruvate	Invitrogen
LIF (leukemia inhibitory factor)	Invitrogen
HEPES buffer	Invitrogen
10x PBS	Invitrogen
Gelatin	SIGMA
Trypsin	Invitrogen
FCS	PAN
Penicillin, Streptomycin	Invitrogen
G418	Invitrogen

ES cell medium

0.1 mM Non-essential aminao acids
1 mM Sodium pyruvate
10^{-4} M β-mercaptoethanol
20% FCS
150 µg Penicillin, Streptomycin
6000 U LIF
0.1 M L-Glutamine

	DMEM high glucose (500ml)
Feeder cell medium	10% FCS
	100 µg Penicillin, Streptomycin
	0.1 M L-Glutamine
Freezing medium	20% DMSO,
	50% FCS
	in ES cell medium
Lysis Buffer	100 mM Tris pH 8.3
	5 mM EDTA
	0.2% SDS
	200 mM NaCl
	0.1 µg/ml Proteinase K

2.1.14 Special Buffer and Solutions for Protein Extraction and Western Blotting

Hepes buffer: (pH 7.4)	ROTH
Solution A) 10 mM Hepes	
Soluton B) 40 mM Hepes	
200 mM NaCl	Applichem
2% Triton	Merck
Protease inhibitor cocktail tablets	Roche
BSA (Bovine Serum Albumin) 10 mg/ml	NEB
Bradford (dye reagent concentrate)	NEB
Triton	Merck
SDS-PAGE gels	
30% Acrylamid/Bis solution	Bio-Rad
10% SDS (Sodium Dodecyl Sulfate)	Applichem
TEMED (N,N,N'N'-Tetra-methylethylenediamine)	Bio-Rad
10% APS (Ammonium Persulfate)	Bio-Rad

Tris (0.5 M,1.5 M)	Tris base	ROTH

Running buffer

Tris base	ROTH
Glycine	Applichem
SDS (Sodium Dodecyl Sulfate)	Merck

Transfer buffer

Tris base	ROTH
Glycine	ROTH
Methanol (10%)	Merck

Loading buffer: Laemmli Sample buffer	Bio-Rad
Milk powder	ROTH
Ponceau S staining solution	Sigma
Tween 20 (electrophoresis reagent)	Sigma
Protein marker: Bench Mark TM Prestained Protein ladder	Invitrogen
Nitrocellulose transfer membrane	Amersham
ECL solution (ECL plus Western Blottiong detection)	Amersham
Hyper film^{TM}ECL	Amersham

Antibodies:

rabbit anti-NR2B polyclonal antibody	Chemicon
mouse anti-NR2A monoclonalantibody	MPI, Heidelberg
rabbit anti-GluRA polyclonal antibody	Upstate
mouse anti-GluRB monoclonal antibody	Chemicon
monoclonal anti-actin antibody	Sigma
rabbit anti-Cre antibody	BAPCO
anti-rabbit Cy3	Jackson Immunoresearch Labaratories
anti-rabbit IgG**,** antibody linked whole peroxidase horseradish	Vector
anti-mouse IgG, antibody linked whole peroxidase horseradish	Vector

Mowiol	20% in 0.2M Tris/HCl pH 8.5	DABCO

2.1.15 Special Articles

Bio-Spin 6 Chromatography columns	Bio-Rad
Filter paper	Schleicher&Schuell
Gene Pulser cuvettes (2 mm, 4 mm)	Bio-Rad
Sterile filter units 185 mm	Millipore
Chromaspin 100 (1000) TE columns	Clontech
Hybond nylon, 0,45 Micron	Amersham
X-ray films Kodak X-OMAT AR	Kodak

2.1.16 Kits

QIAquick Gel Extraction Kit	QIAGEN
QIAquick PCR Purification Kit	QIAGEN
QIAfilter Plasmid Maxi Kit	QIAGEN
Rediprime II DNA Labelling Kit	Amersham

2.1.17 Primers

10 mM	Invitrogen Custom Primers

ex 6-5: GTGGTCATGAAGAGGGCCTACA (22nt)
ex 6-3: CTAAGAAGGCAGAAGGTGACACA (23nt)
ex 5-5: GACCTTTACCTGGTGACCAATG (22nt)
ex 5.5..2:AACAGATGAGGAACCAGGCTAC (20nt)
ex 8.3seq: CAAATCGCTTTGCCCGATGGTGA (20nt)
ex 8-3: CAGGCCGGAAACCTGGTCCA (20nt)
rspcre1: ACCAGGTTCGTTCACTCATGG (21nt)
rspcre2: AGGCTAAGTGCCTTCTCTCTACAC (22nt)
rspneo4: GGCTATTCGGCTATGACTGGGC (22nt)
rspneo5: GGGTAGCCAACGCTATGTCCTG (22nt)
i6-BD3´: GAGTTGCCTCCATCATTGTGTC (22nt)

i6-BD5´ : AGTCTCCTCTTCATCCTCAGTG (22nt)
TS-2Bscr5-f: ATCCACCTGTTTCTGCTTCC (18nt)
TS-2Bscr5-r: CATATTGCTAAGGCTAAGCTAGCTT (23nt)
TS-2Bscr3-f: GATCCCAGGATTCCAAGACC (18nt)
TS-2Bscr3-r: GCCTCCATATGTCAATATTGGAT (21nt)

2.2 Methods

2.2.1 Microbiological Methods

2.2.1.1 Preparation of Competent *E. coli* Cells

a) Chemocompetent Cells

500 ml of LB medium is inoculated with 1 ml of a fresh overnight culture of DH5α bacteria and incubated at 37°C on a shaker until the OD_{600} equals 0.5 to 0.7. The cells are cooled on ice and spun down for 5 minutes at 2600g in a JLA 250-rotor (Beckmann). The bacteria are suspended in 10 ml TFB I, mixed with another 140 ml TFB I and incubated on ice for 2 hours. After a second centrifugation the bacteria are suspended in 20 ml TFB II. Aliquots of 100 µl are frozen in liquid nitrogen and stored at –70°C.

b) Electrocompetent Cells

750 ml LB medium is inoculated with 7.5 ml of a fresh overnight culture and incubated at 37°C on a shaker until the OD_{550} equals 0.75. The cells are spun down at 2600 g, the supernatant is decanted and he pellet is suspended in 750 ml 10% glycerol. This procedure is repeated. The bacterial pellet is finally resuspended in the residual liquid until the OD_{550} is 200-500. Aliquots are prepared as explained above.

2.2.1.2 Plate Culture for *E.coli* Cells

With a sterile wire a colony of E.coli is striked out on an agar plate containing the appropriate antibiotic. After 12 hours of incubation at 37°C the plate is stored at 4°C. The bacterial
plates can be kept up to 4 weeks to set up liquid cultures.

2.2.1.3 Transformation of *E.*coli by Heat-shock

100 µl of chemocompetent cells are mixed with 1 ng plasmid DNA or 10 ng ligated vector and put on ice for 20 minutes. A heat-shock at 37°C for 90 seconds is then performed. Following heat-shock the sample is transferred to ice and 400 µl medium (2YT) is added. After an incubation at 37°C for 15-30 minutes the bacteria are distributed on a agar plate.

2.2.1.4 Transformation of *E.*coli by Electroporation

One third of a butanol precipitated ligation is mixed with 50 µl electrocompetent cells and electroporated in a cuvette with a gap of 2 mm between the electrodes. The electroporator settings are 2.5 kV/25 µF/200-400 Ω. The bacteria is mixed with 1 ml 2 YT medium, incubated at 37°C for 30 minutes and distributed on 3 plates.

2.2.2. Isolation and Purification of Nucleic Acids

2.2.2.1 Preparation of Plasmid DNA by Alkaline Lysis

a) Mini-Preparation
One colony is isolated with tootpick from the plate to a glass tube containing 2 ml TB medium and the appropriate antibiotic. After incubation on a rotating wheel at 37°C for 14 hours (for the growth of the bacteria) the suspension is transferred to a reaction tube and spun down. After discarding the supernatant the bacterial sediment is resuspended in 200 µl S1 (100 ng/µl RNAse A) and mixed with 200 µl S2. The mixture is incubated 5 minutes at room temperature to lyse the cells completely. After the addition of 200 µl of

S3 centrifugation at 13000 rpm for 15 minutes at 4°C is performed. The supernatant is transferred to a fresh tube and precipitated with 400 µl isopropanol, washed with 70% ethanol, dried and dissolved in an appropriate volume of TE buffer.

b) Maxi-Preparation (Qiagen Plasmid Kit)
100 ml of TB overnight culture is centrifuged and resuspended in buffer P1. Addition of buffer P2 is followed by 5 minutes incubation at room temperature. Mixing with buffer P3 is followed by 20 minutes incubation on ice. The precipitate is centrifuged for 30 minutes at 20000g and the supernatant is applied to a column. Using different pH and ionic concentrations of buffer the proteins and the RNA are washed from the column (twice 30 ml buffer QC). The washed plasmid DNA is eluted with 15 ml buffer QF. After isopropanol precipitation and 70% ethanol wash, the DNA is dissolved in TE buffer.

2.2.2.2 Ethanol/Isopropanol Precipitation

Ethanol precipitation is used to concentrate nucleic acids, or to transfer them into a new set of buffer and salts. 0.1 volumes of 3 M sodium acetate, pH 5.5 are added to the DNA solution, together with 2 volumes of absolute ethanol or 0.7 volumes of isopropanol and mixed well. 10-20 minutes centrifugation at 14000 rpm is performed. After decanting the supernatant, in order to remove the salt the pellet is washed with 70% ETOH. The dried pellet is dissolved in TE buffer.

2.2.2.3 Phenol-Chloroform Extraction

Phenol is used to denature and remove proteins from nucleic acid solutions. Equal volumes of phenol and chloroform containing 4% isoamyl alcohol are added to the DNA solution to be purified. The phases are mixed and centrifuged 4 minutes in a microfuge at 14000 rpm at room temperature. Two phases are formed; the phenol (on the bottom) and the aquous (on top) and in between a white interface layer of denaturated proteins. The aqueous phase (which contains the nucleic acids) is transferred to a fresh tube. The phenol extraction can be followed by an extraction with chloroform containing isoamyl

alcohol, to remove residual protein as well as phenol, which might remain from the previous phenol extraction. Again the mix is centrifuged and the aqueous phase (usually the upper phase) is recovered. The upper phase with the nucleic acids is transferred to a fresh tube and precipitated by isopropanol or (100%) ethanol.

2.2.3 Manipulation and Analysis of DNA

2.2.3.1 Restriction Digest of DNA

Restriction digest of DNA serves to linearize circular DNA, to cut out specific fragments from a larger molecule and to cut genomic DNA. It is perfomed for analytical purpose (e.g identification of plasmid, a targeting event in genomic DNA) or preparative purpose (e.g isolation of fragment for cloning). 1 Unit (U) of restriction enzyme is the amount necessary to digest 1 µg of a specific DNA in one hour in a volume of 50 µl. For analytical purposes 100-500 ng of plasmid DNA are digested with one or more restriction enzymes (1-5 units each) in a volume of 10-20 µl for one hour and separated on an agarose gel.

2.2.3.2 Ligation of DNA

The enzyme DNA ligase of the phage T4 catalyses the formation of a phosphodiester bond between a 3´-OH and a 5´-phosphate. In this way fragments with sticky ends (single stranded 5´- or 3´- overhang) or blunt ends can be ligated, if at least one of the fragments has a 5´-phosphate. The enzyme needs ATP as a cofactor. In the ligation mix the molecular ratio of vector to insert in general is 1:5, if the fragments are very small for example adaptors it is 1:1000. The reaction takes place in a volume of 20 µl. This mix contains 10 nmole ATP, 2µl 10X ligation buffer and 1 unit T4 DNA ligase. Incubation can take place at 16°C overnight, in order to prolong the activity of the enzyme, especially for “blunt end”-ligations. In “shutgun”-cloning the fragment to be cloned and the cloning vector are digested together, and then ligated without seperation of the fragments on a gel.

2.2.3.3 Agarose Gel Electrophoresis

Agarose gels serve to separate linear DNA fragments (for identification purification and isolation). Separation takes place in a grid-like matrix of agarose through which smaller fragments can pass more quickly than larger fragments. Ethidium bromide is added to the gel to visualise DNA fragments by its fluorescence in UV light. To determine the length of the fragments a DNA size marker with known fragment sizes is separated in parallel. By varying the concentration of agarose (0.7-2%) separation in the high or low molecular range is favored. The required amount of agarose is dissolved in 100 ml 1X TAE buffer by boiling, ethidium bromide is added to the solution (0.5 µg/ml final) and the gel poured into a gel tray with combs.

2.2.3.4 Cycle Sequencing Reaction

The sequencing method is based on the principle of Frederik Sanger according to which randomly built-in dideoxynucleotides (ddNTP`s) lead to a chain termination of the polymerase reaction. The four ddNTP`s are coupled to dyes fluorescent at different wave lengths. The sequence of the DNA can be determined by laser beam detection after separation in a capillary gel. The reaction occurs in analogy to a PCR reaction, however only one primer is added. The sequencing of plasmid DNA and PCR products takes place according to the “Dye Terminator Cycle Sequencing”-protocol of ABI. A sequencing mix of 10 µl contains approximately 1 µg of plasmid DNA, 5 pmol of primer and 4 µl of “BigDye Ready Reaction Terminator Cycle Sequencing Kit”. The reaction needs 25 cycles with the following conditions: 15 seconds at 95°C, 15 seconds at 55°C, 4 minutes at 60°C. Afterwards the reaction is filled up to 100 µl with H_2O. The DNA is precipitated with acetate and ethanol, washed and dried.

2.2 3.5 Southern Blot Analysis

Southern blotting is the transfer of DNA fragments from an electrophoresis gel to a membrane support. The transfer of DNA fragments is based on the principle of capillary

diffusion from an agarose gel onto a nylon or nitrocellulose membrane, using a high-salt transfer buffer to promote binding of DNA to the membrane. The DNA to be analysed is separated by agarose gel electrophoresis. To have a good quality of seperation low voltage is applied (e.g 50 V). In order to visualise under UV light, staining of the gel with ethidiumbromide is performed after the seperation. The pictures are taken using a fluorescent ruler. In order to facilitate the transfer of bigger fragments (>5kb) the gel is incubated on a shaker in 0.25 M HCl for 30 minutes, followed by 2x 15 minutes in denaturation buffer, twice for 15 minutes in reneutralisation buffer and a final incubation in 5x SSC for 15 minutes. To set up the blot a glass or plastic dish is filled with 20x SSC. A solid support is put inside the dish and covered with a filter paper which is in contact with the solution at both sides. The gel is placed on the filter paper and the surface is covered with a nylon membrane of equal size. 5 filter papers and 5 cm thick paper towels are put on the membrane avoiding air bubbles. A glass plate with a weight on it is placed on top to hold everything on place. The region between the edges of the gel and the dish is covered with plastic wrap. After 6 hours of transfer, the position of the wells in the gel is marked on the membrane and the DNA is fixed using UV cross-linking.

2.2.3.6 Hybridization and Washing of the Membrane

A denaturated radioactive probe binds to DNA fragments with sequences complementary to it. This way DNA fragments can be visualised on the membrane by exposing to X-ray film. Prehybridization is performed by using the Quick-Hyb buffer for 10-20 minutes at 68°C. The labelled probe is mixed with salmon sperm DNA, denaturated and added to the hybridization buffer, after which hybridization takes place for 1-2 hours on a shaker or in rotating glass tubes. After hybridisation, the membrane is washed twice with 5x SSC, 0.1% SDS at room temperature for 15 minutes and once with 1x SSC, 0.1% SDS at 68°C for 20 minutes. The membrane is wrapped in platic film and exposed to a X-ray film.

2.2.3.7 Polymerase Chain Reaction

PCR is an alternative method for amplification of DNA fragments up to 5 kb in a shorter time. Fragments of 50 kb can also be obtained by using special kits. Adjacent sequence of

the fragment of interest has to be known in order to synthesize the two primers. These primers can be elongated by a thermostable DNA-polymerase. The number of DNA molecules increases with the number of elongation cycles in an exponential way. The typical PCR program consists of an initial denaturation step of 1-5 min at 94°C followed by 30 cycles of denaturation for 30 seconds at 94°C, annealing for 30 seconds at 55°C, elongation for 90 seconds at 72°C, and an additional 5 minutes of final elongation at 72°C. The reaction is cooled down to 4°C at the end.

The annealing temperature depends on the primer. It should be 5°C below the calculated melting temperature (T_m). The number of cycles is determined by the number of template molecules. In general 20-25 cycles are performed on cloned DNA, 30-35 cycles on genomic DNA or cDNA, in order to prevent accumulation of false incorporation not more than 25 cycles should be performed for generation of preparative fragments. In addition to the DNA template and in general two primers, $MgCl_2$, dNTP´s, a thermostable DNA-polymerase and the appropriate buffer are necessary.
A polymerase with "proofreading ability" (3' to 5' exonuclease activity) is preferred for preparative purposes.

2.2.4 Propagation and Maintanance of Embryonic Stem (ES) Cells

2.2.4.1 Transfection of Embryonic Stem Cells with the Targeting Construct

All procedures described below are performed in a cell culture room under a laminar flow hood

a) Growing ES Cells for Electroporation
A number of different ES cell lines are available. For this project the cell line R1() was used. The ES cells grow on monolayers of mitotically inactivated fibroblast cells. For this reason mitomycin treated feeder cells (1.3×10^6 cells for 6 cm plate and 4×10^6 cells per 10 cm plate) are thawed at 37°C and resuspended in 5 ml feeder cell medium. After centrifugation at 1000 rpm for 5 minutes, the pellet is resuspended and the cells are distributed to one 6 cm plate and two 10 cm plates containing feeder medium. After 24

hours the medium is changed to ES cell medium. A vial of ES cells is thawed at 37°C and resuspended in 10 ml ES cell medium. After centrifugation at 1000 rpm for 5 minutes, the pellet is dissolved in ES cell medium and transferred to the 6 cm feeder plate prepared previously. The ES cell medium is changed daily until the cells become confluent. The ES cells are split (trypsinized, incubated at 37 °C, spun down at 1000 rpm for 4 min, and resuspended in ES cell medium) when they become confluent and transferred to the two 10 cm plates containing the mitomycin treated feeder cells. The ES cell medium is changed daily until the cells reach confluency and can be used for electroporation.

b) Electroporation of ES Cells

This method is used to introduce DNA into embryonic stem cells for gene targeting experiments. Technically this method is relatively simple compared to others. DNA can be transfected into ES cells by application of a high voltage electrical pulse to the suspension of cells and DNA. After application of this pulse the DNA passes through pores in the cell membrane.

30 µg sterile, linearized plasmid DNA is dissolved in 100 µl PBS. ES cells are trypsinized, centrifuged at 1000 rpm for 5 minutes and the pellet is resuspended in 20 ml ES cell medium, and distributed on a plate covered with gelatin in order to separate the ES cells from the feeder cells. After an incubation of 20 minutes, the medium is collected, the plates are rinsed with ES cell medium, and the cells are pooled in a 50 ml conical tube. This procedure is repeated. The number of cells is adjusted to $10x10^6$ in 0.7 ml PBS. 80-150 µl PBS containing 30 µg of DNA is mixed with 0.7 ml of the cell suspension. The mixture is transferred to a pre-chilled electroporation cuvette and is electroporated at 240 V, 500 µF. After 20 minutes of incubation on ice the cells are transferred to ES cell medium to be distributed on 5 gelatin covered plates. From the third day on 200 µg/ml G 418 is added to the ES cell medium. After growth in this selective medium for 8-10 days clones can be picked.

c) Picking ES Cell Clones

The ES cell clones, surviving the selection in G418 containing medium are picked under a dissecting microscope when the diameter is 0.5-2 mm. On the evening before picking mitomycin treated feeder cells are distributed to flat-bottom 96-well plates. Two hours before picking, the medium on the plates containing the clones is changed to ES cell medium. The plates are washed twice with PBS before picking under the microscope. Picking is performed, by sucking a clone into a 200µl pipet tip. The picked clones are distributed to a round-bottom 96 well dish containing 50 µl 1/2x trypsin (1:1 trypsin:PBS) per well. The picked trypsinised colonies are then split to the flat-bottom 96 well master plates containing feeder cells, and to 24 well plates covered with gelatin.

d) DNA Isolation from ES Cell Clones for Genomic Southern Blot

DNA is prepared from cells, which are grown on gelatin to confluency. Cells are washed twice with PBS. 500 µl lysis buffer is added to each well. The suspension is incubated at 37°C overnight. Thus, the cells are lysed and DNAses are digested. Isopropanol (500 µl) is added and incubated on a shaker at room temperature for 10-15 minutes. The precipitated DNA is spooled out of the wells, rinsed in 500 µl ETOH 70%, dissolved in 100-200 µl TE and stored at 4°C.

e) Freezing ES Cell Clones in 96 Well Master Plates

The media of the 96 well master plate is changed. After two hours the cells containing the clones are washed two times with PBS, then 25 µl trypsin is added and left at 37°C for 4-6 minutes. After checking under the microscope to confirm that the ES cells are split, 75 µl of pre-chilled freezing medium is added. The plate is sealed in plastic, labelled and left at -20°C 1 hour before it is transferred to -70°C.

f) Expansion of the Positive ES Cell Clones

Positive clones from a master plate are thawed and transferred into falcon tubes containing 5 ml ES cell medium. Centrifugation for 5 min at 1000 rpm is followed by suspension of the pellet in 3 ml ES cell media and distribution in 3 wells of a 24 well plate on feeder cells. After growing to a certain (40%) confluency, the cells are washed 2 times with PBS and 1.5 ml trypsin is added and incubated at 37°C for 3 minutes. After

trituration the cells are transferred in tubes containing 8 ml ES cell medium and centrifuged for 4 minutes at 1000 rpm. The pellet is resuspended in 1.5 ml ES cell medium and an equal amount of pre-chilled freezing medium is added on ice. The vials are left for 1 hour at -20°C, then they are transferred to -70°C.

g) Preparation of ES Cells for Blastocyst Injection

7 day prior to injection, mitomycin treated feeder cells (1.3 x 10^6 cells per 6 cm plate and 4 x 10^6 cells per 10 cm plate) are thawed at 37°C and resuspended in 5 ml feeder medium. After centrifugation at 1000 rpm for 5 minutes, the pellet is resuspended and the cells are distributed to one 6 cm plate and two 10 cm plates containing 4 ml and 9 ml feeder medium, respectively. A vial of ES cells containing the correctly targeted clone is thawed and plated onto the 6 cm plate. The ES cell medium is changed daily until the cells become confluent. Meanwhile the medium of the other two 10 cm plates containing the feeder cells is changed every 48 hours to feeder medium. On the 4^{th} or the 5^{th} day the ES cells are at the appropriate density. The cells are washed two times with PBS and 800µl of trypsin is added. After 3 minutes of incubation at 37°C the cells are triturated and collected into an falcon tube. Centrifugation at 1000 rpm for 4 minutes is followed by resuspension in 5 ml ES cell media. The suspended ES cells are distributed in three 10 cm feeder cell containing plates at different volumes (3 ml, 1.5 ml, 0.5 ml). The medium is changed daily until the day of injection. At the day of injection the medium is changed 2 hours before the procedure. Four 10 cm gelatin coated plates are prepared. 1.5 hours before the injection splitting procedure is performed (wash with 2 times with 1X PBS, trypsinisation ,incubation at 37°C for 3 minutes, trituration, centrifugation at 1000 rpm for 5 minutes). Cells are suspended in 10 ml of ES cell media and transferred into the prepared gelatin plates for seperation from the feeder cells. Incubation at 37°C. 20 minutes incubation is followed by another transfer to a second gelatin plate for another 20 minutes incubation at 37°C. This way the feeder cells are cleaned and ES cells are isolated. Transfer of the cells to a tube and centrifugation (1000 rpm, 5 min) are followed by resuspension of the cells in pre-chilled feeder medium containing 100 µl hepes buffer (20 µl/ml). After this step the cells are ready for blastocyst injection. Blastocyst injection was performed by F. Zimmerman.

2.2.5 Protein Extraction and Immunoblot (Western Blot) Analysis

Mice are decapitated under anesthesia, and the brains are removed. The hippocampi are taken out in 600 µl Hepes buffer A, homogenized and left on ice for 10 min. Centrifugation at 1000 g for 10 min at 4°C is followed by addition of Hepes buffer B (equal volume as the supernatant) to the supernatant. The potein solution containing the combined membrane and cytosolic fractions is mixed for 30 min on a shaker at 4°C. The protein concentration is determined by the method of Bradford. Equal amounts of the protein are seperated by 10% SDS-PAGE and the proteins are transferred onto nitrocellulose membranes by electroblotting. Membranes are blocked with Tris-buffered saline containing 0.1% Tween 20 and 5% non-fat dry milk for 1 hour at room temperature. The blotted proteins are probed with the following primary antibodies: rabbit polyclonal C-terminal anti-NR2B, 1:500; mouse monoclonal C-terminal anti-NR2A, 1:1000 (provided by MPI Heidelberg); β-actin mouse monoclonal β-actin clone AC-15 ascites, 1:8000) Membranes are washed 3 times 15 min for each and are incubated with horseradish peroxidase-conjugated anti-rabbit or anti-mouse IgG (1:8000) for 1 hour. After washing three times bound antibodies are visualized by chemiluminescence (ECL Plus; Amersham) and exposed to Hyper film^{TM} ECL. Quantification of the expression levels from western blots were performed by using, adope photoshop, image J and microsoft exel programs.

2.2.6 RT PCR

2.2.6.1 RNA Extraction

Total RNA is prepared according to the protocol supplied with TRI REAGENT (Molecular Research Labs). RNA is prepared from total brain. Mice are decapitated under anesthesia, and the brain is removed. The tissue is homogenized in 2.5 ml of trizol in a 15 ml tube, then 500 µl chloroform is added. The phases are mixed well, and centrifuged for 20 min. at 4 ˚C, 14 000 rpm. The supernatant containing the RNA is taken into a new tube. The RNA is precipitated by addition of 2.5 ml isopropanol. After

centrifugation at 14.000 rpm for 20 min at 4 ˚C the supernatant is removed. The RNA pellet is washed with 70% ethanol, dried briefly and resuspended in 100 µl DEPC water.

2.2.6.2 Reverse Transcription and PCR

Reverse Transcription-PCR (RT-PCR) is a method used to amplify cDNA copies of a RNA: The first step is the enzymatic conversion of RNA to a single-stranded cDNA templete. An oligodeoxynucleotide primer is hybridized to the mRNA and is then extended by an RNA-dependent DNA polymerase to create a cDNA copy that can be amplified by PCR.

a) Reverse Transcription
50 µg of total RNA, 10 ml of RNase free NEB buffer 2, 1 µg of placental RNAse inhibitor (25 u/µg) and 1.5 µl DNAse I (10 u/µl RNAse free) are mixed in a total volume of 100 µl and incubated for 1 hour 37 ˚C. After phenol chloroform extraction and ethanol precipitation, the RNA is resuspended in 16 µl of DEPC treated water. Subsequently 16 µl of DNAse treated RNA, 0.5 µl of p(dN)6 (random hexamer primers,1 µg/µl) are mixed and incubated for 10 min at 80˚C, and then stored on ice for 5 min. 6 µl of 5x reverse transcription buffer, 3 µl dNTPs, 3 µl of 0.1 M dithiothreitol, 1 µl RNase inhibitor (20 u/µl) are then added, to obtain a final volume of 29 µl. 5 µl of this mixture is taken as untranscribed control for mock-reverse transcription. To the remaining 28 µl 1µl of MMLV-reverse transcriptase (200 u/µl) is added. Reverse transcription is performed for 1 hour at 42˚C and then stopped by heat inactivation at 72˚C for 10 min.
b) PCR
PCR is performed on 1 µl of transcribed cDNA and 1 µl of untranscribed control (to exclude DNA contaminations). PCR is performed for 32 cycles in a total volume of 70 µl.

2.2.7 Genotyping of Mice

a) By PCR
For genotyping DNA is prepared from the tip of a mouse tail (0.3-0.5 cm). The tails are lysed overnight on a shaker at 1000 rpm at 55 °C in 500µl of TENS buffer containing 0.5

mg of proteinase K at 55°C. Afterwards the debris is spun down at 13000 rpm for 5 min. 600µl of isopropanol is added to the supernatant, mixed, and spun down for another 10 min. The supernatant is discarded and the DNA pellet is washed with 70% ethanol, dried and dissolved in 100 µl TE buffer. PCR reaction is performed for 35 cycles.

B) By Genomic Southern Blot

For Southern blot analysis liver DNA is prepared because the quality of the DNA is better compared to tail DNA.

Mice are decapitated under anesthesia, and the liver is removed. 1/3 volume of the liver is taken into 2 ml of TENS buffer containing 1.5 mg of proteinase K and lysed overnight on a shaker at 55°C. Afterwards 2 ml of phenol-chloroform (1:1) mixture is added to the debris and mixed on a shaker at room temperature (RT). The mixture is centrifuged at 3000 x g for 5 min (RT). The supernatant is taken into a fresh 15 ml tube containing 2 ml phenol-chloroform (1:1). Mixing on a shaker for 20 minutes is followed by another centrifugation (3000 x g for 5 min RT). To the upper phase the same volume of chloroform is added and mixed on a shaker for 20 minutes (RT). After centrifugation (3000 x g for 5 min RT) the upper phase is extracted a second time with chloroform. The upper phase containing the DNA is then precipitated by addition of ethanol. The pellet is dried and according to the size dissolved in 500-800 µl of TE buffer.

The Southern blot analysis is explained in detail in the previous section (2.2.3.5).

2.2.8 Immunohistochemistry

250 µm thick hippocampal slices are fixed with 4% paraformaldehyde in PBS for 3 to 4 hours. The sections are washed in PBS 3 times for 10 minutes at room temperature, permeabilisation and blocking are achieved by incubation in 1% triton and 10% NGS in PBS on a shaker at room temperature overnight. The slices are incubated in PBS with 1% NGS and 0.5% Triton X-100 with the primary antibody, for 4 hours at room temperature. For visualisation of the primary antibody, the slices are washed three times in PBS and incubated with the secondary antibody in PBS with 1% NGS and 0.5% Triton X-100 for 2 hours at room temperature. As a primary antibody rabbit anti-Cre (BAPCO), 1:5000, and as secondary antibody antirabbit Cy3 (Jackson Immuno Research Labaratories Inc.,

West Grove, PA), 1:250, are used. After incubation with the secondary antibody the slices are washed three times for 10 minutes with PBS and mounted on glass slides, embedded in Mowiol and coverslipped. For analysis an upright fluorescent microscope (Zeiss Axioplan 2; Zeiss Goettingen, Germany), containing a Zeiss filter set 10 for detection of EGFP (excitation filter BP 450-490; dichroic mirror FT 510; emission filter BP 515-565) and filter set 15 for detection of Cy3 (excitation filter BP 546/12; dichroic mirror FT 580; emission filter LP 590) is used.

2.2.9 Stereotactic Injection of Lentivirus into Hippocampus CA1

Lentivirus preparation and purification was done by Prof. Seeburg´s group, according to production protocols of Carlos Lois.

A calibrated stereotactic instrument is used to precisely locate the site and depth of injections for delivery of the lenti-viruses. The injections are made with a fine glass capillary which is prepared with a capillary puller. The fine tip of the capillary is cut at 1-2 mm from the end for smooth loading and injection. All surgery instruments are kept in sterile solution, and washed in distilled water before use. To start a surgery the animal is anesthesized with ("ketamine + xylasine") mix in PBS (6.5mg/ml of ketamine, 1.4 mg/ml of xylasine) at a volume of 10 µl/g according to the body weight of the animal. The anesthetic solution is injected subcutaneously to the abdominal region. After the animal is deeply sedated, the fur covering the region of surgery is shaved. The animal is then put on a heat blanket to keep the body temperature at 37°C. After checking the reflexes to make sure that animal is deeply anesthesized, the head is fixed in the stereotactic frame with appropriate ear bars, by targeting the ear canal. The region for surgery is then cleaned with ethanol and the eyes are covered with PBS soaked tissue. The head skin is cut in a saggital direction, and fixed with hooks at each side. A tiny hole (~ 1mm in diameter) is opened in the skull using a dental grill until right before the dura mater at the region of interest. The thin layer of bone that is left between the dura and the outside is then very carefully opened with the tip of a needle to the side avoiding any damage to the brain. To proceed for the injection, sometimes a very fine cut in the dura mater is necessary, especially if the animal is old. To inject the virus, first the virus solution is back-loaded into a capillary from the tip by applying suction at the open end of the

capillary from a 50 ml syringe. The virus is then injected to the area of interest by controlling the coordinates via stereotaxy. Once the desired depth is reached the virus solution is injected by applying very little pressure with the syringe. The amount of injection is determined by the distance covered by the upper surface of the viral solution in the capillary. Usually ~ 50-100 nl of volume is injected. To avoid spill-over of the virus solution the tip of the needle is left at the injection site for additional 2 minutes. The skin is the sewed and 50 µl of lidocaine is injected subcutaneously at the area of surgery to avoid pain after the recovery from general anesthesia. During the recovery period the animal is kept on a heat blanket. After the recovery it is transferred to its cage and fed with wet food. Animals are kept for 3 weeks before analysis.

2.3 Computer Programs

Adope Photoshop
Canvas 8.0.3
DNA Strider 1.3
EditSeq
EndNote 6.0
ImageJ version 1.30
Microsoft Word
Microsoft Excel
Microsoft Explorer

3 RESULTS

3.1 Generation of Mouse Line *NR2B*^{2lox}

3.1.1 Generation of the Targeting Construct

Since the general *NR2B* knock-out is lethal, a conditional knock-out of the *NR2*B gene might elucidate the physiological function of NR2B subunit.

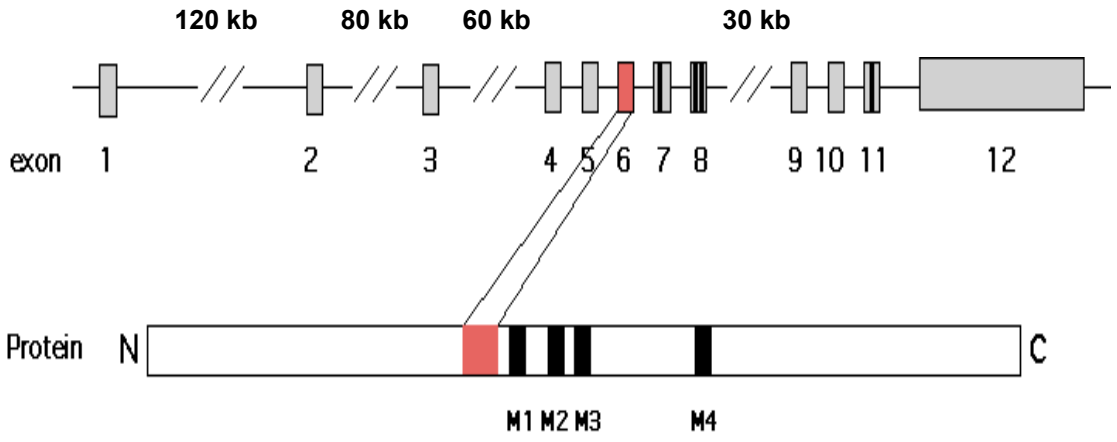

Figure 10: Organisation of the mouse *NR2B* gene.
The mouse *NR2B* gene consists of 12 exons and covers 314 kilobase pairs (kb).The protein contains four transmembrane domains. Exon 6 encodes the region immediately preceding the first transmembrane domain. M1 is encoded by exon 7, M2 and M3 are encoded by exon 8 and M4 is encoded by exon 11.

For this purpose, a DNA construct for homologous recombination in embryonic stem (ES) cells has been generated in our group. To obtain the genomic fragment containing exon 6 of the *NR2B* gene, a mouse genomic library in the vector lambda FIX II was screened using two oligonucleotides complementary to intronic regions flanking exon 6. This exon encodes the region preceding the first transmembrane domain of the NR2B subunit (Figure 10). A loxP site was cloned into intron 5 as well as a Hind III site for screening by Southern blot. A second loxP site was introduced in intron 6. To enable

mRNA quantification from the wild-type allele versus the mutant allele in heterozygous mice, a silent mutation creating an Age I site was introduced into the exon 6 (Figure 11). PCR primers were designed for RT-PCR and sequencing, which will be explained in detail in chapter 3.2.1. As a positive selection marker, a neomycin resistance gene (*neo*) under the control of the HSV promoter and flanked by two frt sites was also introduced in intron 6. Due to possible interference with the splicing process, the neomycin cassette can lead to an alteration of gene expression. Thus, it is desirable to remove the neomycin cassette either in embryonic stem cells by transient expression of the Flp recombinase or in the heterozygous mouse by mating with a so-called "deleter mouse" expressing the Flp recombinase under the control of the actin promoter (Rodriguez et al., 2000). Two arms of 3.4 kb and 5.1 kb, respectively, serve for homologous recombination (Figure 11).

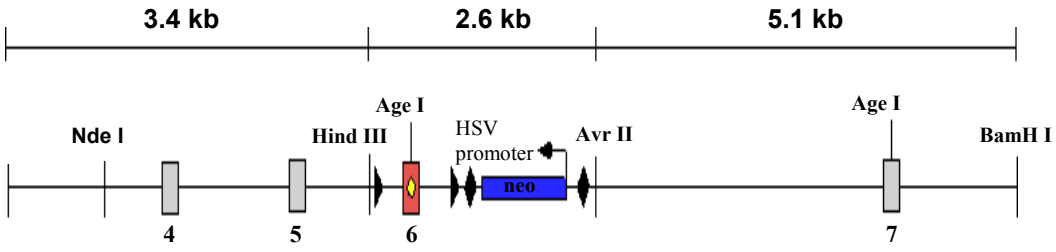

Figure 11: Targeting construct for the conditional knock-out of the *NR2B* gene. In the targeting construct exon 6, carrying two silent mutations (yellow dot), is flanked by loxP sites. A neomycin resistance gene flanked by frt sites is inserted in intron 6.

3.1.2 Transfection of Mouse Embryonic Stem Cells with the Targeting Construct for the *NR2B* Allele and Screening by Genomic Southern Blot

After digestion with Not I, 100 µg of linearized plasmid containing the targeting construct (Figure 11) was electroporated into R1 embryonic stem cells which are derived from agouti coloured 129/Sv mice (Nagy et al., 1993). Electroporated cells were grown in selective media containing G418 in order to select for neomycin resistant colonies indicative of the presence of the neomycin gene. After insertion of the targeting construct

into the embryonic stem cells, it is in most cases randomly integrated into the mouse genome. To ascertain that not only homologous recombination in ES cells has occurred but also to guarantee the presence of the neomycin cassette and both loxP sites, a Southern blot analysis was performed. For this reason, a 5' and a 3' outside probe of 580 bp and 425 bp, respectively, were generated by PCR. The location of the two probes is indicated in figure 12. Both fragments were tested on wild-type (wt) genomic DNA from mouse tails.

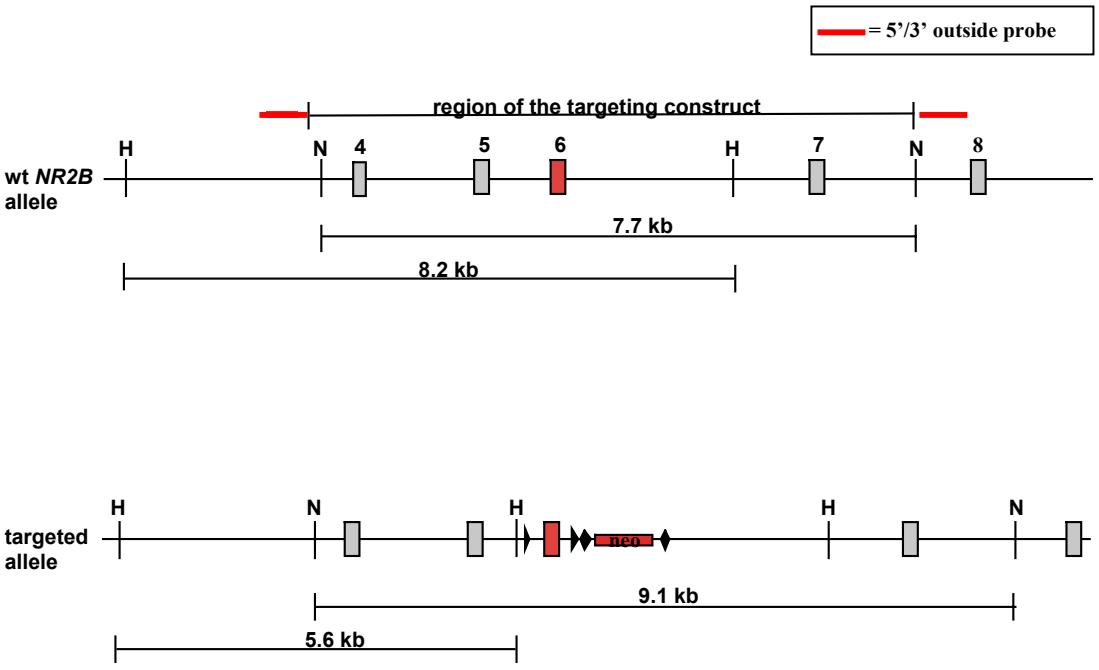

Figure 12: Screening strategy with restriction enzymes Nde I (N) and Hind III (H) for the identification of ES cells positive for homologous recombination.

Digestion of the genomic DNA with Hind III should reveal the following bands on a Southern blot when probed with the 5' outside probe (Figure 12):

No homologous recombination (wild-type):	8.2 kb
Only insertion of the neomycin resistance gene:	9.5 kb
Correct insertion of both loxP sites and neomycin cassette:	5.6 kb

For confirmation of the primary analysis a Nde I digest of the genomic DNA was performed. It revealed the following bands on a Southern blot probed with the 3' outside probe (Figure 12):

No homologous recombination (wild-type):	7.7 kb
Correct insertion by homologous recombination:	9.1 kb

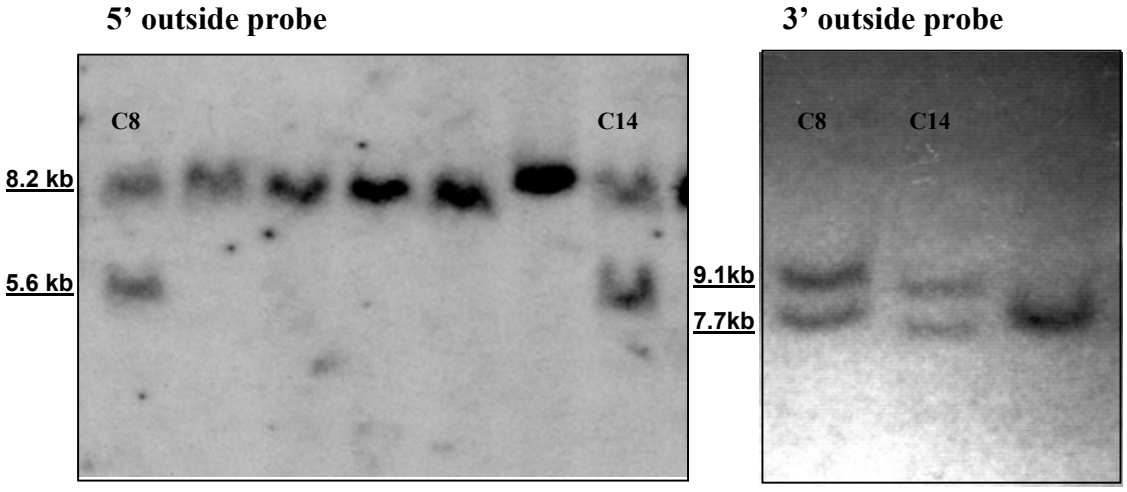

Figure 13: The genomic Southern blots show two putative positive clones (C8 and C 14) with the expected fragment sizes when probed with the 5' and 3' probes.

Genomic Southern blots of 500 clones surviving the selection identified 4 clones with DNA fragments of the size expected for the mutant allele. After confirmation of 3 of the positive clones by the second probe, ES cells from one of the positive clones were selected for the second recombination step in order to take out the neomycin resistance gene in culture.

3.1.3 Removal of the Neomycin Cassette by Flp Recombination

Although Cre is a remarkable aid for genetic engineering in the mouse, a variety of experiments could benefit from the use of two site specific recombinations. Most prominently, conditional strategies to engineer the mouse genome rely upon the good

properties of Cre in mice, however, the removal of the selectable marker used to generate the conditional allele is also accomplished by use of Flp recombinase. In order to remove the frt-flanked neomycin resistance gene, we used the vector pCAGCGC-FLPe (Schaft et al., 2001) for transient expression of the Flp recombinase in mouse ES cells. 15 µg of the circular plasmid (pCAGCGC-FLPe) was electroporated into embryonic stem cells from the clone C8 in which homologous recombination was successful. 8 days after electroporation the clones were grown to the right size for picking. The picked clones were distributed in three 96 well master plates containing neomycine resisitant feeder cell layers. One of these plates was used for G418 selection in order to differentiate the clones lacking the neomycin resistance gene. These clones should not survive the selection. After 8 days of selection among the 360 picked clones, 8 candidate clones were found.

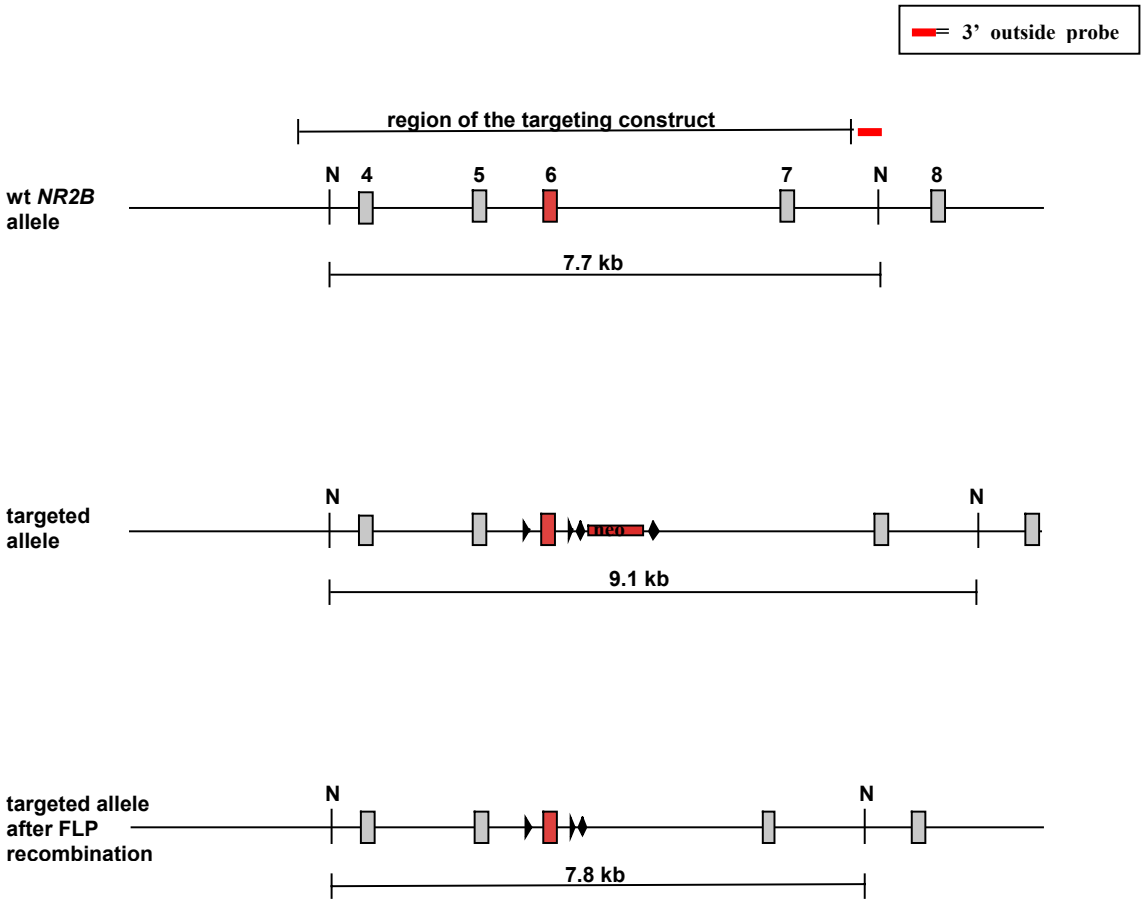

Figure 14 : Screening strategy with the restriction enzyme Nde I (N) for identification of ES cells in which neomycin cassette was removed.

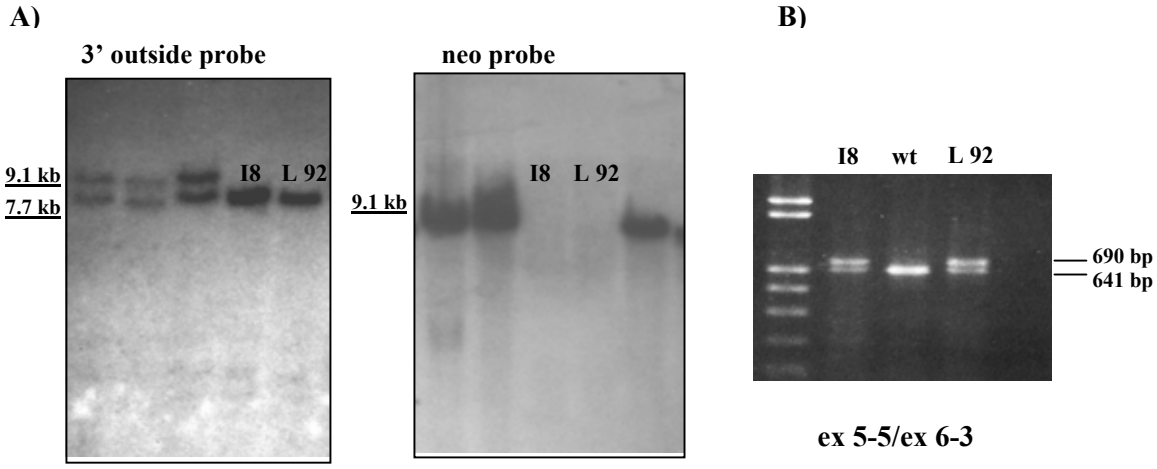

Figure 15: A) Southern blots of the Nde I digested genomic DNA with the 3´ outside probe and the neo probe (I8 and L92 are two putative clones where neo was removed. B) PCR confirms the presence of the 5' loxP site in the two putative positive clones with the expected size of the fragments.

These clones were analysed by genomic Southern blot and PCR for confirmation of the successful Flp recombination and consequently lack of the neomycin cassette. Absence of the neomycin cassette was confirmed with a 1.2 kb neo probe. To ascertain not only the absence of neomycin cassette but also the correct targeting event, also the 3' outside probe was used. A Nde I digest of the genomic DNA should reveal the following bands on a Southern blot probed with the 3' outside probe (Figure 14):

No homologous recombination (wild-type):	7.7 kb
Fragment with neomycin resistance gene (*neo*):	9.1 kb
Fragment where *neo* is removed:	7.8 kb

When hybridised with the neo probe the same digest should not reveal any signal on wild-type or on the mutated allele, which does not contain neomycin resistance gene (*neo)*. In order to reconfirm the presence of the 5' loxP site a PCR was performed. For this purpose two oligonucleotide primers were designed (ex 5-5 and ex 6-3). The amplification of the genomic DNA with this primer pair should reveal a fragment of 641 bp in wt and 690 bp in the mutant allele.

3.1.4 Generation of the Mouse Line *NR2B^{2lox}*

Among 360 ES cell clones, 6 did not survive the selection procedure and were confirmed to lack the neomycin cassette. One of the positive ES cell clones (I8) was injected into mouse blastocysts derived from C57Bl6 strain. The blastocysts were implanted in pseudopregnant foster mothers, which gave birth to 3 highly chimeric males (F0 generation). These males were further bred with the C57Bl6 females. In order to prove the germline transmission of the mutant allele, 4 weeks after birth a small piece of the tail from brown (Agouti) coloured F1 generation litters was taken for DNA preparation and analysis by PCR. The F1 offspring from one of the highly chimeric males showed mice heterozygous for the mutated allele and wild-type mice in concordance with the mendelian rules of 50% probability. As a name *NR2B^{2lox}* was given to the mouse line.

3.1.5 Genotyping of the *NR2B^{2lox}* Mice

Genotyping of the mice was performed by PCR using DNA obtained from mouse tails. Figure 15 shows the organisation of wild-type and targeted alleles and alignment of the PCR primers. Two separate PCRs were used to determine the genotype of each animal. Each PCR was designed to amplify over the insertion site of the loxP sites. This resulted in PCR fragments of different lengths for the wild-type and *NR2B^{2lox}* allele. Presence of the 3' loxP site together with the frt site in the absence of the neomycin resistance gene was tested by a PCR with the primer pair BD-i6 5' and BD-i6 3'. The reaction products in the wild-type allele and the mutated allele are 213 bp and 328 bp, respectively.

To confirm the presence of the 5´ loxP site and exon 6, PCR with the primers ex 5-5 and ex 6-3 was performed. It revealed 641 bp in the wild-type and 690 bp in the mutated allele. Southern blot analysis was performed on genomic DNA obtained from mouse liver to confirm the correct targeting in mice. For this purpose the same probes were used as explained during the screening procedure (Chapter 3.1.2).

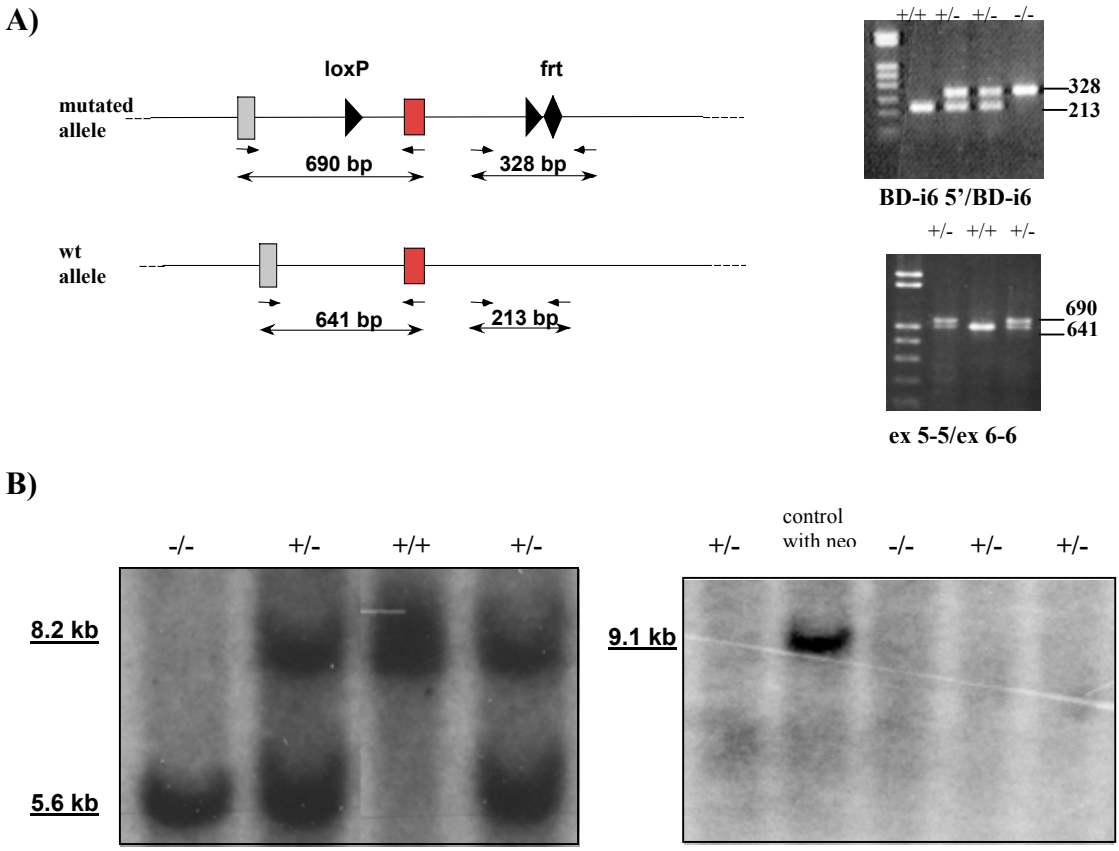

Figure 16: A) Genotyping strategy by PCR with primer pairs BD-i6 5', BD-i6 3´and ex 5-5, ex 6-3 resulting in the expected bands of 328 bp, 213 bp and 690 bp, 641 bp, respectively. B) Southern blots with 5' outside probe (left) and neo probe (right) from genomic liver DNA of the F2 generation confirm the correct targeting event and absence of the neomycin cassette (see chapter 3.1.2, 3.1.3).

3.2 Confirmation of the NR2B Expression in Mutant Mice

Since the loxP sites are located in introns, they should not interfere with the *NR2B* expression in the mutated allele. For confirmation of the intact NR2B expression at the mRNA and protein level, RT-PCR and western blot analysis were performed.

3.2.1 Analysis of the mRNA Expression by RT- PCR

Heterozygous mice were used to quantify the mRNA ratio from wild-type versus the mutated allele. For this purpose two silent mutations generating an Age I site had been introduced into exon 6. RT-PCR (reverse transcription-polymerase chain reaction) is the most sensitive technique for mRNA detection and quantification. It was performed on RNA from the brain of adult animals.

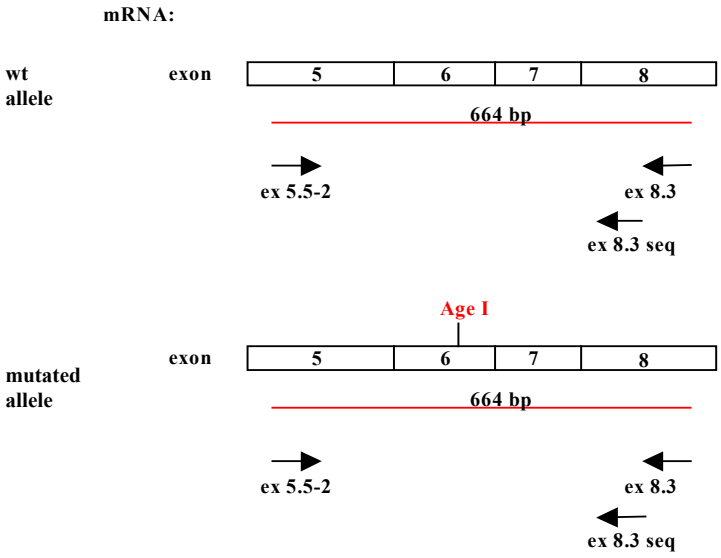

Figure 17: Schematic representation of the mRNA from wild-type and the mutated allele.
The PCR primers (ex 5.5-2 and ex 8.3) amplify the region covering the silent mutation. The sequencing reaction was performed on the 644 bp PCR product using ex 8.3 seq as a primer.

PCR primers were designed to amplify a 644 bp fragment covering the mutation: a sense primer corresponding to exon 5 (ex 5.5-2) and an antisense primer corresponding to exon 8 (ex 8.3). The sequencing reaction is performed on the PCR product using internal primer (ex 8.3seq) (Figure 17).

In the analysis, the peaks corresponding to the sequences of the wild-type and the mutated allele ideally were equal in height in cDNA from heterozygous mice (Figure 18). Thus, sequencing analysis indicated equal level of expression of the mutated allele compared to wild-type. Figure 18 shows the two silent mutations created by insertion of

the Age I site in the *NR2B*$^{2lox/2lox}$ mice (C and T) in the codons for the amino acids thymidine and glycine, respectively.

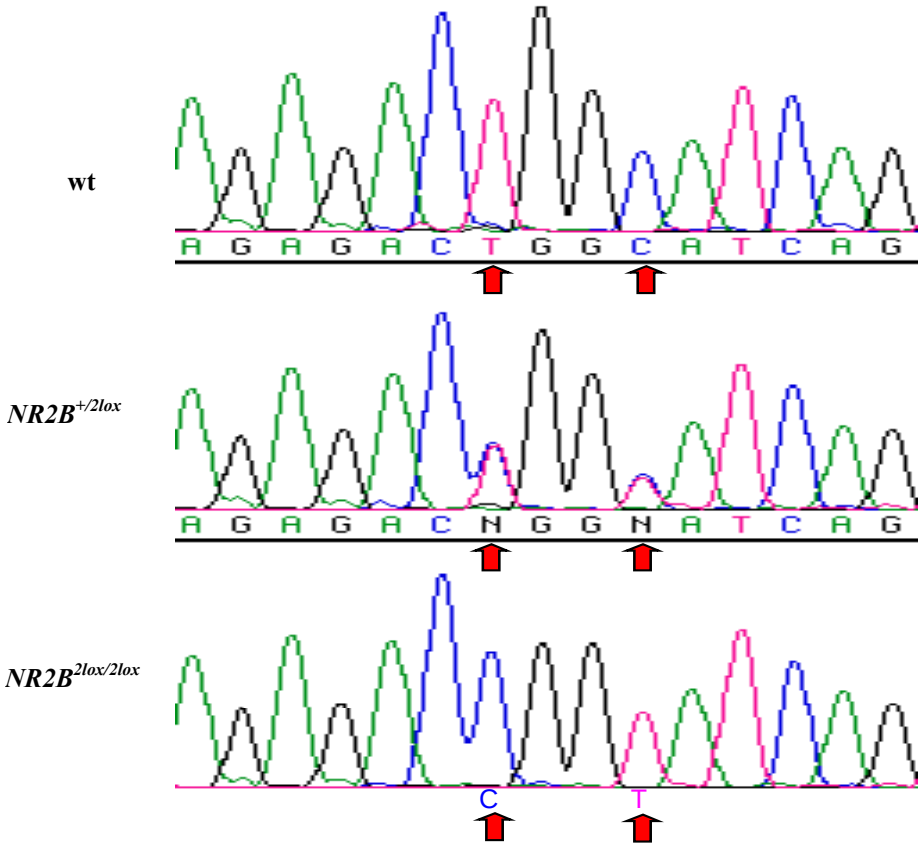

Figure 18: RT-PCR was performed on RNA obtained from animals with three different genotypes (wt, *NR2B*$^{+/2lox}$, *NR2B*$^{2lox/2lox}$) with at least three different animals from each genotype. The figure shows the wild-type sequence (top), the sequence with the two silent mutations in homozygous mice (bottom) and the overlapping peaks of the equal height (indicating the comparable expression of mutated allele compared to wild-type) from the sequence of the heterozygous mice (middle).

3.2.2 NR2B Protein Expression

In homozygous mice with the mutated allele (*NR2B*$^{2lox/2lox}$), the expression level of the NR2B subunit should be same as the expression in the wild-type. In order to confirm the equal expression at the protein level, 20 µg of whole brain homogenates were separated on SDS-PAGE. Western blot analysis was performed on whole brain homogenates of

adult (P 60) wild-type and homozygous (*NR2B*$^{2lox/2lox}$) mice. The analysis indicated that the NR2B subunit is expressed at levels comparable to wild-type.

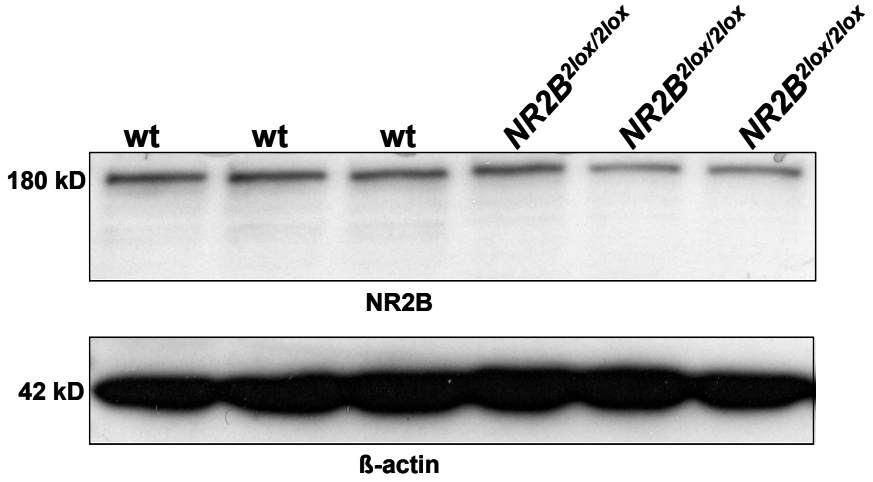

Figure 19: Western blot analysis of whole brain homogenates.
Expression of the NR2B subunit in wt and *NR2B*$^{2lox/2lox}$ mice is comparable. β-actin, a ubiquitously expressed protein was used as an internal control.

3.3. Conditional Ablation of the NR2B Subunit

3.3.1 The Transgenic Cre4 line and Generation of *NR2B*$^{\Delta Fb}$ Mice

To determine the consequences of NR2B subunit deletion in principal cells of the forebrain, we crossed *NR2B*$^{2lox/2lox}$ mice with the transgenic mice Tg^{Cre4} (Mantamadiotis et al., 2002) to establish the line *NR2B*$^{\Delta Fb}$ (*NR2B*$^{2lox/2lox}$/Tg^{Cre4}).

Expression of α-CaMKII mRNA starts postnatally in the forebrain (Burgin et al., 1990). Regional specifity of the 8.5 kb promoter fragment in the Tg^{Cre4} of the calcium/calmodulin-dependent protein kinase II-α gene in Tg^{Cre4} mice gives the Cre recombinase possibility of a gene knock-out restricted to hippocampal and neocortical tissues known to play central roles in learning and memory. Furthermore, the lack of activity of the Cre recombinase during prenatal and perinatal periods reduces the possibility of developmental defects caused by a gene knock-out during early development (Figure 20).

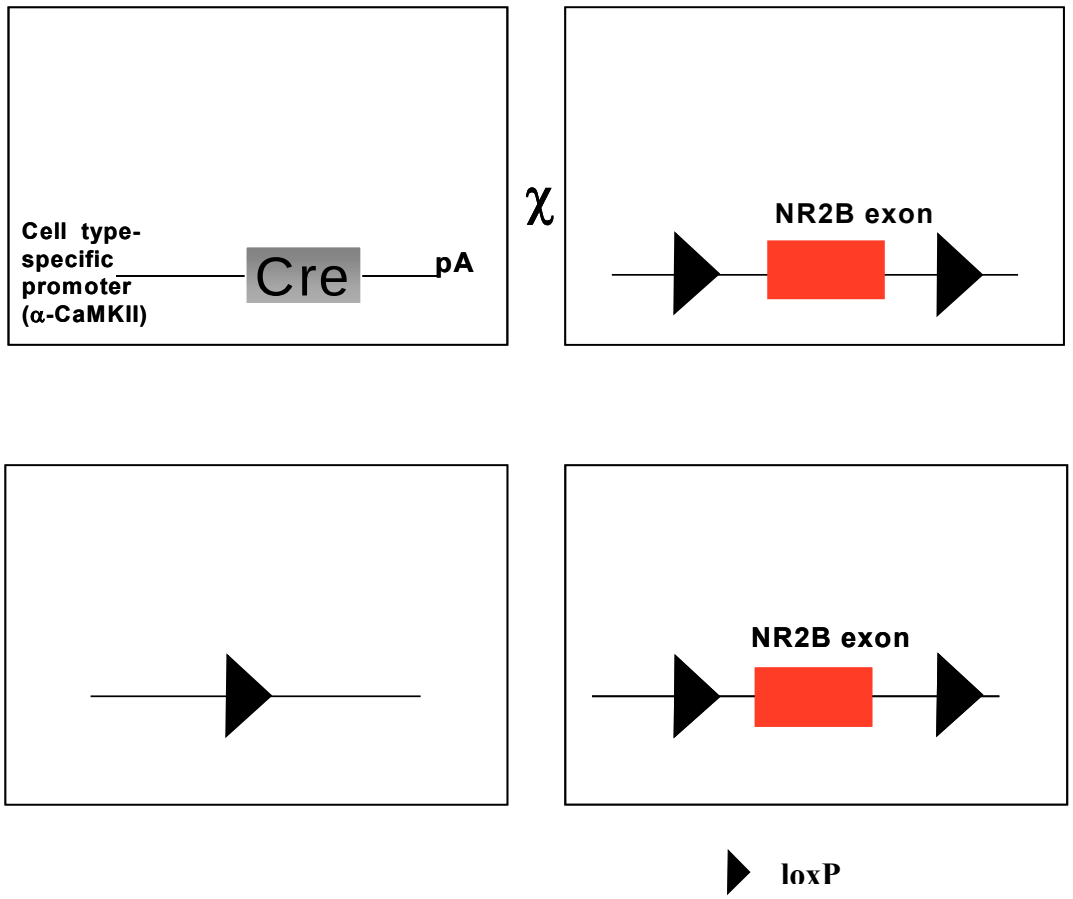

Figure 20: Schematic representation of the Cre/loxP recombination by crossing of the *NR2B*$^{2lox/2lox}$ and Tg$^{Cre\ 4}$ mice. The α-CaMKII promoter fragment guarantees the expression of the Cre recombinase postnatally only in the principal cells of the forebrain.

3.3.2 NR2B Subunit Expression in *NR2B*$^{\Delta Fb}$ Mice

Hippocampal homogenates were prepared from adult (P60-P120) *NR2B*$^{2lox/2lox}$ (control) and *NR2B*$^{\Delta Fb}$ mice. 10 µg of the protein was separated on a SDS-PAGE. Western blot analysis indicated a reduction of the NR2B subunit level. Quantification of the immunoblot results documented a ~70% reduction of the NR2B subunit in *NR2B*$^{\Delta Fb}$ mice compared to control littermates (*NR2B*$^{2lox/2lox}$= 100±20, n= 6 and *NR2B*$^{\Delta Fb}$= 32±7, n= 6). This way consistent with the electrophysiological studies the conditional ablation of the NR2B subunit from the hippocampus is demonstrated. The remaining ~30% expression might come from the expression of NR2B in cell populations other than pyramidal cells, most probably in interneurons.

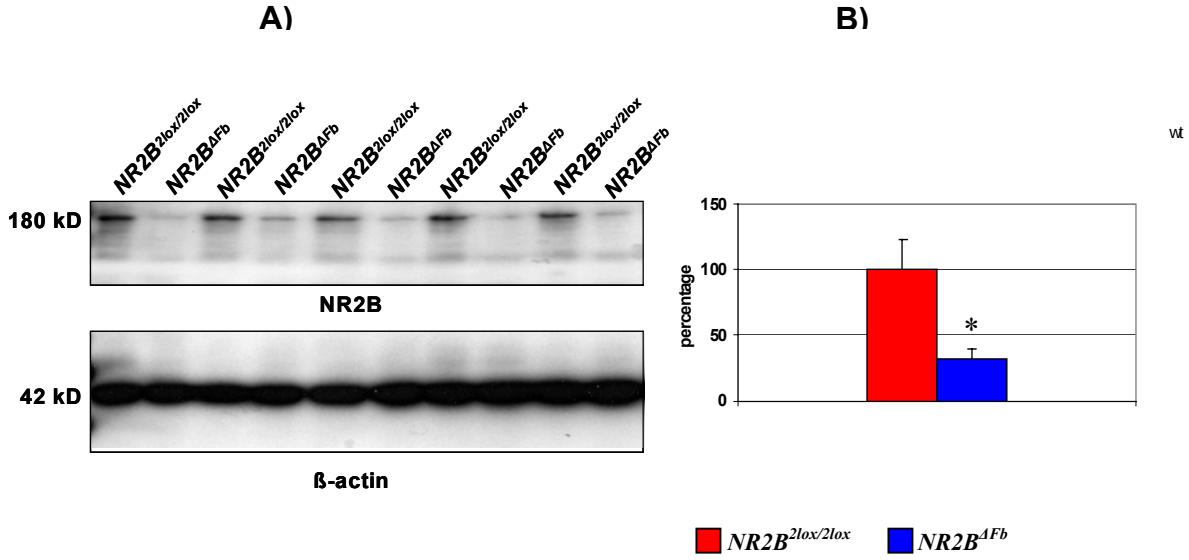

Figure 21: Expression of the NR2B protein

A) Western blot analysis demonstrates the reduced expression of the NR2B subunit in the hippocampus of *NR2B*$^{\Delta Fb}$ mice compared to control (*NR2B*$^{2lox/2lox}$) littermates. Values on left show the corresponding molecular weight (kD: kilodalton). Hippocampal homogenates were prepared from 6 adult mice (P60-P120) of each genotype and separated by SDS-PAGE. Expression profile of NR2B and β-actin (used as an internal control) was determined using specific antibodies against NR2B and β-actin. B) Quantification showed ~70% reduction of the expression of NR2B in *NR2B*$^{\Delta Fb}$ mice (n= 6). Values represent average of three different experiments from 6 different animals of each genotype. Statistical significance was evaluated by unpaired Student's t-test, *= $p < 0.05$, error bars= SD.

3.3.3 Expression Levels of NR2A, GluR-A and GluR-B

Deletion of the NR2B subunit might cause an compensatory increase in the expression level of the NR2A subunit. On the other hand it has been shown in neuronal cultures that initially the NR2B subunit is important for the proper targeting of NR2A to the membrane (Barria and Malinow, 2002). Consequently absence of NR2B might cause a decrease of the NR2A expression. Therefore I checked the NR2A expression profile by seperating 10 µg of hippocampal homogenates on SDS-Page. Western blot and quantification showed an unchanged level of the NR2A subunit expression in *NR2B*$^{\Delta Fb}$ mice.

A previous study had shown that NMDAR activation can have differential effects on AMPAR trafficking, depending on subunit composition of NMDARs (Kim et al., 2005). It has been suggested that in mature neurons NR2A and NR2B subunits have opposing actions on the surface insertion of the GluR-A subunit. The NR2B subunit inhibits the insertion whereas the NR2A subunit enhances the insertion. Since overexpression of NR2B in culture inhibits the surface expression of GluR-A, I checked if the expression of the GluR-A subunit is affected in absence of NR2B in *NR2B*$^{\Delta Fb}$ mice at an age between P60 and P120. Western blot analysis of hippocampal homogenates did not show a significant difference in the expression level of the GluR-A subunit from wild-type littermates. Since hippocampal AMPA receptors are mostly heteromers of GluR-A and GluR-B, I also checked the possible change in the expression level of the GluR-B subunit. The analysis showed no significant difference in the expression profile of GluR-B between *NR2B*$^{\Delta Fb}$ and *NR2B*$^{2lox/2lox}$ mice.

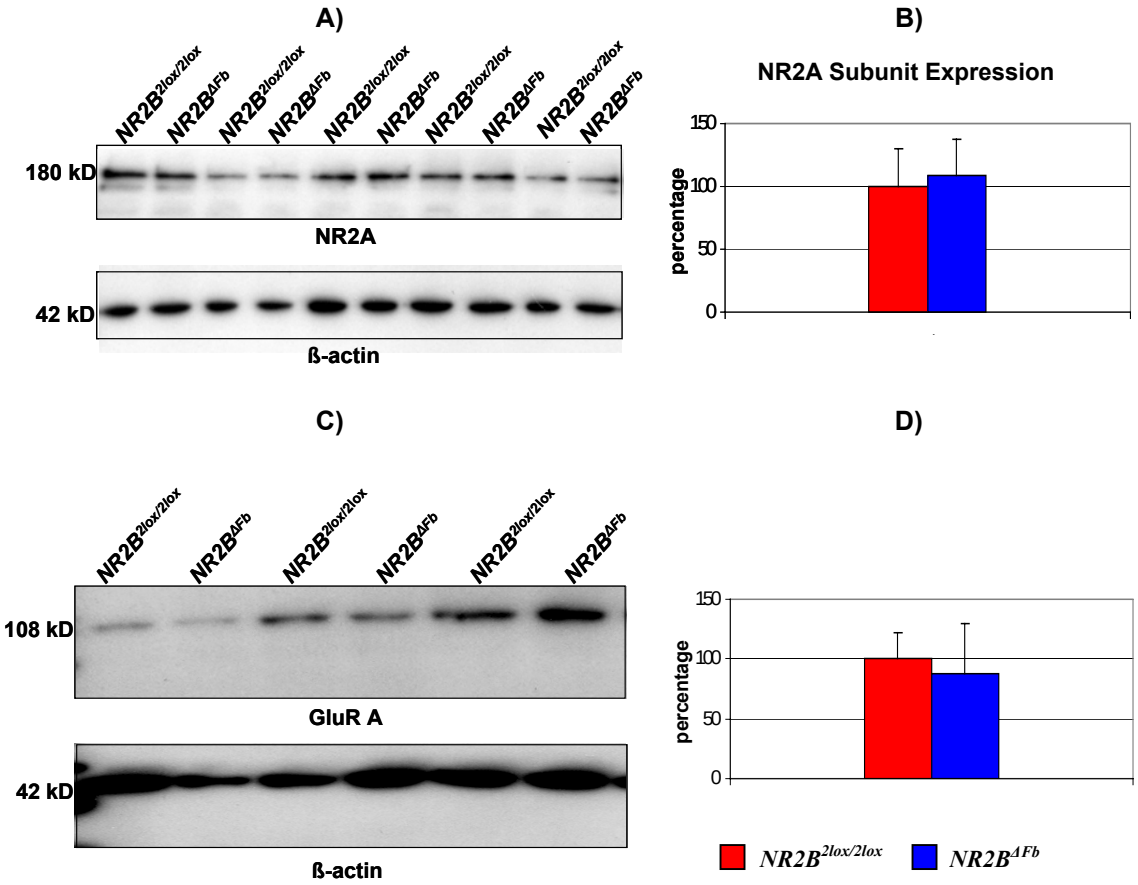

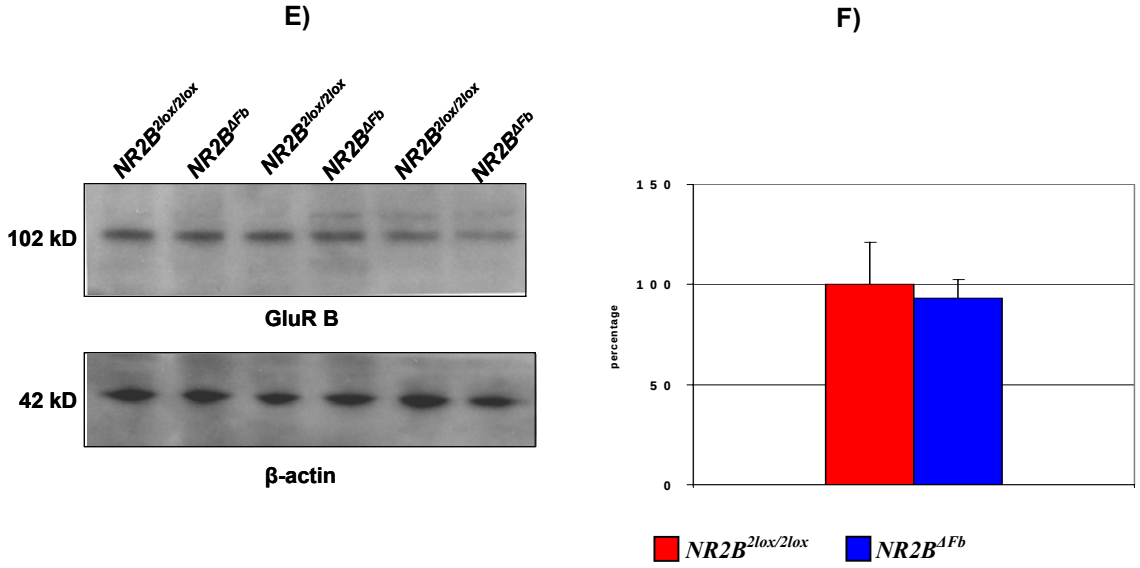

Figure 22: Expression analysis of NR2A, GluR-A and GluR-B.

Hippocampal homogenates from 6 adult mice (P45-P120) for each genotype (*NR2B*$^{\Delta Fb}$, *NR2B*$^{2lox/2lox}$) were separated by SDS-PAGE and transferred to nitrocellulose membrane. The proteins were visualised with antibodies specific for NR2A, GluR-A and GluR-B and compared to the corresponding β actin band (A), (C), (E). Quantification did not show any change in the expression of the NR2A, GluR-A and GluR-B subunits in *NR2B*$^{\Delta Fb}$ mice compared to *NR2B*$^{2lox/2lox}$ mice. Values represent average of three different experiments of from 6 different animals (B), (D), (F). Statistical significance was evaluated by unpaired Student's t-test (error bars= SD).

3.3.4 *In vivo* Cre/loxP Recombination by Using the Lentiviral System

In parallel to the breeding with the Tg^{Cre4} line, the lentiviral system was used for *in vivo* Cre/loxP recombination. Lentiviral particles expressing the Cre recombinase and the GFP protein under the control of the α-CaMKII promoter (Figure 23 A) were delivered steriotactically to the hippocampal CA1 region of *NR2B*$^{2lox/2lox}$ mice at P20. GFP-mediated fluorescence enables identification of the cells expected to lack the NR2B subunit. 3 weeks after the injection, mice named as *NR2B*$^{\Delta lenti}$ were sacrificed for further electrophysiological (EP) and immunohistochemical analysis. Following EP analysis the 250 µM thick hippocampal sections were processed for immunohistochemistry. They were incubated with anti-Cre primary antibody and Cy3 secondary antibody. Figure 23 B

shows the staining of Cre recombinase in the hippocampal CA1 region (right), and the unenhanced EGFP fluorescence (left) from the same section. The expression of Cre recombinase together with GFP and the correct targeting of the injected area were proven as a control in parallel to the EP studies.

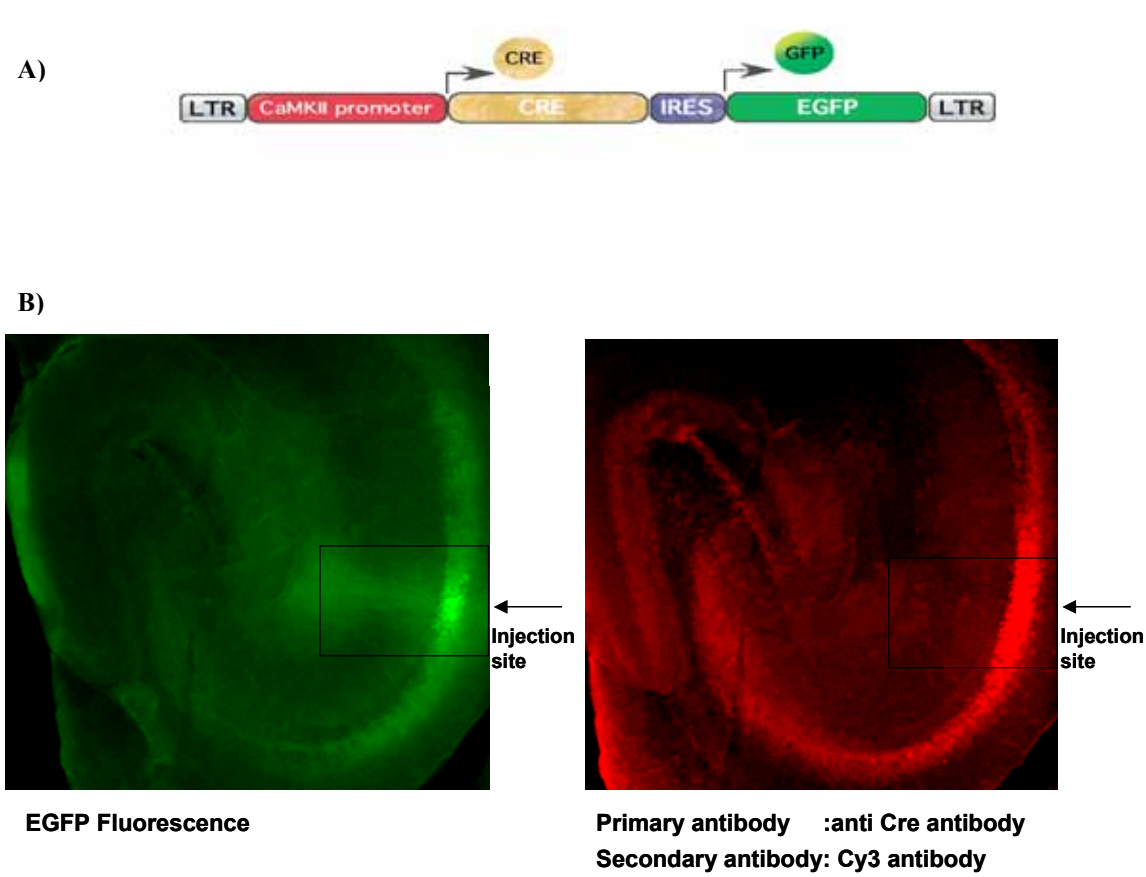

Figure 23: The lentiviral expression system was used for *in vivo* Cre/loxP recombination.

A) The lentiviral vector for the expression of Cre recombinase and GFP under the control of the α-CaMKII promoter was constructed by Valery Grinevich and Pavel Osten. B) Virus particles were delivered steriotactically to the hippocampal CA1 region of *NR2B*$^{2lox/2lox}$ mice at P20. GFP mediated fluorescence allows to identify and patch clamp cells expected to lack the NR2B subunit.

3.4 Electrophysiological Characterisation of the *NR2B$^{\Delta Fb}$* Mice

3.4.1 Increased AMPA/NMDA Ratio and Decreased Ifenprodil Sensitivity

Synaptic EPSCs were evoked by Schaffer collateral stimulation in hippocampal acute slices from P 42-45 mice in the presence of 0 mM Mg^{2+}. After recording of total AMPAR and NMDAR mediated EPSCs at holding potential of –70 mV from CA1 pyramidal cells, 5 μM NBQX (AMPA receptor antagonist) was added to the extracellular medium in order to isolate NMDAR currents. The NMDA component was then substracted from the total synaptic current to calculate AMPAR component. Figure 24 A shows AMPAR mediated EPSCs (traces in red) which were normalised and NMDAR mediated EPSC (traces in blue). The AMPA/NMDA ratio was increased two fold in the absence of the NR2B subunit (*NR2B$^{2lox/2lox}$*= 1.73± 0.87, n= 8, *NR2B$^{\Delta lenti}$*= 3.35± 1.35, n= 6 and *NR2B$^{\Delta Fb}$*= 3.62± 0.94, n= 3). NMDAR mediated currents were significantly reduced assuming that there is no change in the currents mediated by AMPARs. Applicaton of the NR2B specific antagonist ifenprodil (10 μM) showed ~45% reduction of the amplitude of the NMDAR mediated synaptic currents in *NR2B$^{2lox/2lox}$* mice (54.7± 7, n= 6) whereas it did not cause a significant reduction in *NR2B$^{\Delta lenti}$* and *NR2B$^{\Delta Fb}$* mice (92.6± 13.9, n= 5; 94.5± 10.1, n= 4) (traces in green). Furthermore a decrease in the decay time (from 38.7± 6.7 ms in *NR2B$^{2lox/2lox}$*, n= 11, to 28.1± 6.6 ms in *NR2B$^{\Delta lenti}$*, n= 8, and to 28.7± 5.2 ms in *NR2B$^{\Delta Fb}$*, n= 4) could also be seen. NR2B containing receptors have been shown to have slower decay times compared to NR2A containing receptors (Monyer et al., 1994; Flint et al., 1997). Therefore the faster decay time of the NMDA EPSCs in the mutant can be explained by the predominance of NR2A containing receptors. This way it was shown that the number of synaptic NMDA receptors is reduced which can be explained by the increased AMPA/NMDA ratio. Moreover, lack of sensitivity to ifenprodil and faster decay time confirm the absence of synaptic NR2B containing receptors in *NR2B$^{\Delta lenti}$* and *NR2B$^{\Delta Fb}$* mice.

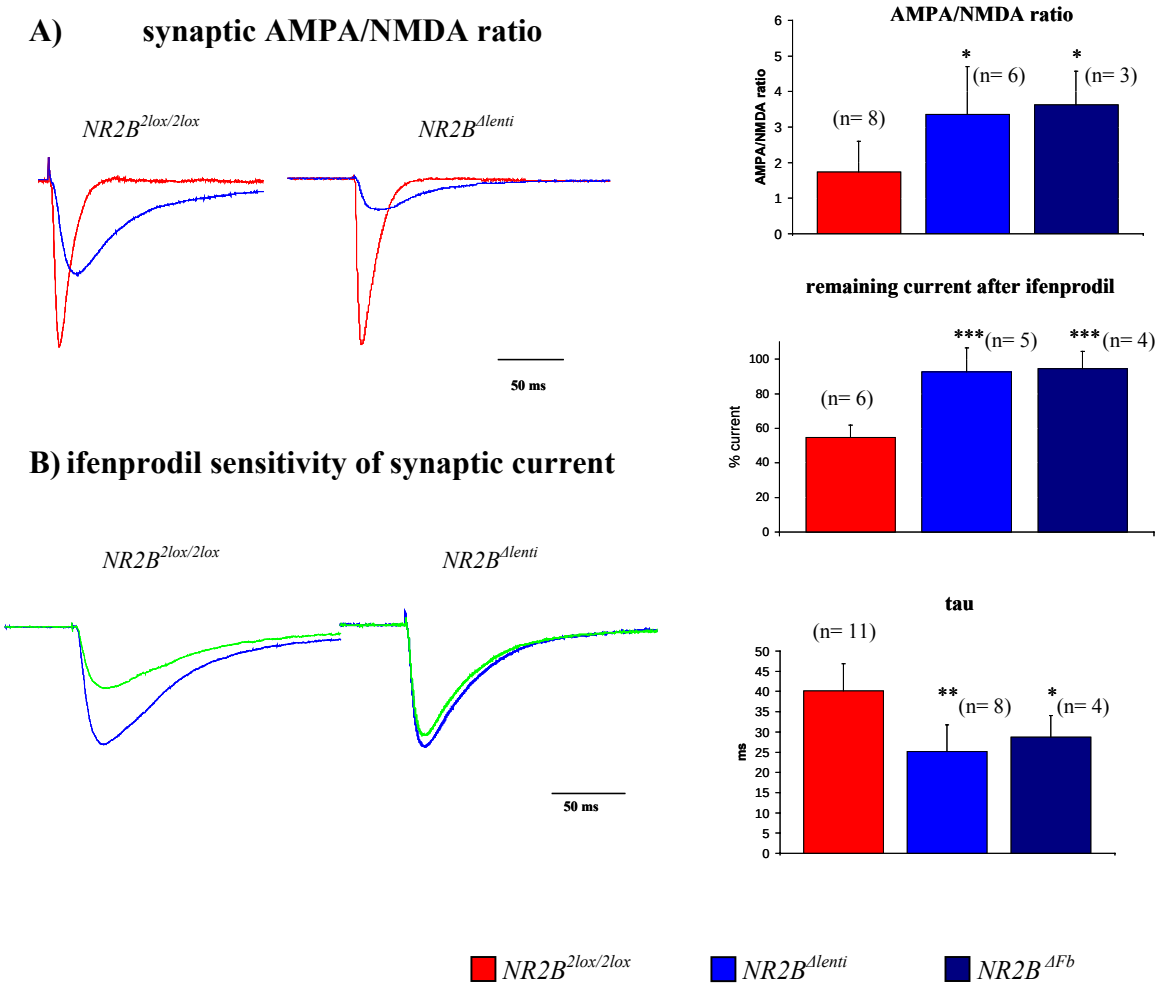

Figure 24: Synaptic EPSCs and ifenprodil sensitivity in the absence of NR2B containing receptors.
250 µm thick slices from P42-P45 *NR2B*$^{2lox/2lox}$, *NR2B*$^{\Delta lenti}$ and *NR2B*$^{\Delta Fb}$ mice were perfused with carbonated ACSF (artificial cerebrospinal fluid). Data in the graphs ae given as mean +/- SD. Differences between two groups were evaluated using the unpaired two-tailed Student's t-test. P values <0.05 were considered statistically significant ($p<0.05$=*; $p<0.01$=**; $p<0.001$=***). A) Amplitudes of synaptic EPSCs mediated by NMDARs were reduced in mice with the ablation of the NR2B subunit in CA1 (*NR2B*$^{\Delta lenti}$ and *NR2B*$^{\Delta Fb}$) compared to wild-type littermates (*NR2B*$^{2lox/2lox}$), which was reflected as a two fold increase in AMPA/NMDA ratio. B) There is a significant decrease in the ifenprodil sensitivity and decay time in *NR2B*$^{\Delta lenti}$ and *NR2B*$^{\Delta Fb}$ mice. Number of cells is shown in parenthesis.

3.4.2 Reduced NMDAR Component of mEPSCs

Spontaneous vesicular release of glutamate in the absence of action potentials provides information about presynaptic release probability (frequency of events) and the number of postsynaptic receptors (amplitudes of events).

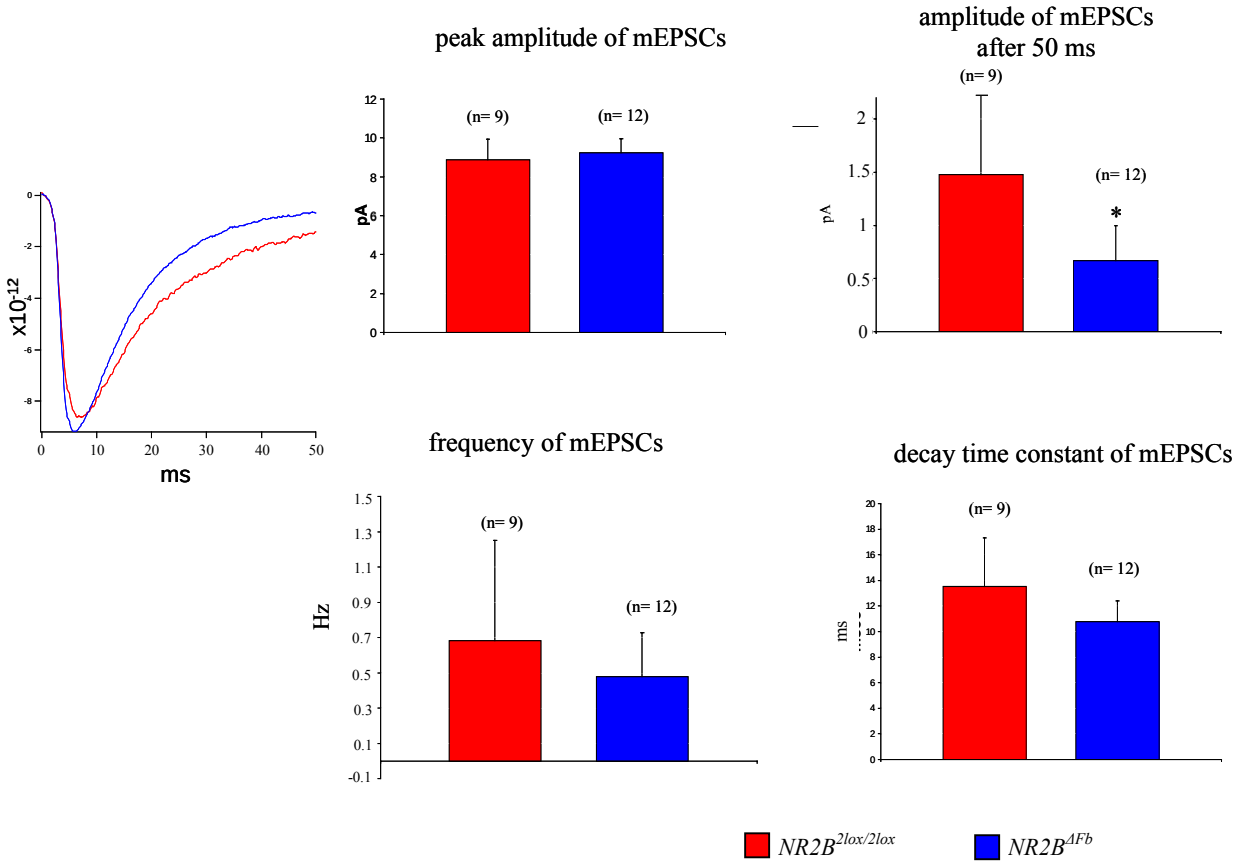

Figure 25: NMDAR component of mEPSCs is strongly reduced.
mEPSCs in P42-P45 *NR2B*$^{\Delta Fb}$ and wild-type mice were recorded at –70 mV in TTX (1 µM), bicuculline (10 µM), glycine (10 µM), and low Mg^{2+} (0.1 mM). In both genotypes, mEPSCs with AMPAR components displayed comparable amplitudes, however there was a decrease of the NMDAR component reflected as a significant reduction of the amplitude after 50 ms. Data in the graphs are given as mean +/- SD. Differences between two groups were evaluated using the unpaired two-tailed Student's t-test. P values <0.05 were considered statistically significant (p<0.05=*; p<0.01=**; p<0.001=***).

Therefore, mEPSCs in P42-P45 *NR2B*$^{\Delta Fb}$ and wild-type mice were recorded at –70 mV in TTX (1 µM), bicuculline (10 µM), glycine (10 µM), and low Mg^{2+} (0.1 mM). This analysis revealed no significant difference initial peak in amplitude and frequency

between both genotypes indicating that there are no changes in the vesicular release and number of postsynaptic receptors. This also strongly suggests that the number of AMPA receptors in the postsynaptic site is unaltered. Moreover, the decay time constant was not significantly changed. AMPA receptors mediate fast synaptic currents and NMDA receptors mediate currents that are slower and longer lasting. Therefore the amplitude of mEPSCs after 50 ms was assumed as a measure of the NMDAR contribution. The reduced amplitude after 50 ms (Figure 25, $NR2B^{2lox/2lox}$= 1.47± 0.67 pA, n= 9 and $NR2B^{\Delta Fb}$= 0.67± 0.32 pA, n= 12) gives further evidence for a reduced number of synaptic NMDA receptors.

3.4.3 Reduced NMDAR Currents at Somatic Sites

It has been suggested that extrasynaptic NMDARs mainly contain NR2B subunit (Tovar and Westbrook, 1999). In order to assess the effect of *NR2B* ablation, somatic currents were recorded in nucleated whole-soma patches from CA1 neurons. Consistent with the synaptic recordings the peak amplitude and the decay time of AMPAR currents evoked upon application of glutamate did not show any change, indicating that the AMPAR component was unaltered (Figure 26 A, B). The observed increase in AMPA/NMDA ratio (Figure 26 C, $NR2B^{2lox/2lox}$= 8.76± 2.36, n= 16, and $NR2B^{\Delta Fb}$= 25.58± 6.32, n= 14) was attributable to the reduced number of NMDA receptors at extrasynaptic sites as it was found at synaptic sites. A significant decrease in the peak amplitude of NMDAR currents (Figure 26 D, $NR2B^{2lox/2lox}$= 308.9± 107.1 pA, n= 16, $NR2B^{\Delta Fb}$= 106.5± 36.7 pA, n= 16) and decreased ifenprodil (NR2B specific antagonist) sensitivity confirm the lack of the NR2B subunit. Moreover, due to lack of NR2B subunits, the kinetics of NMDAR currents became faster, which was also reflected by a two fold decrease in the decay time ($NR2B^{2lox/2lox}$= 81.43± 24.43 ms, n= 16, $NR2B^{\Delta Fb}$= 37.46± 19.38 ms, n= 17). There was no reduction of absolute currents mediated by NMDARs (in $NR2B^{\Delta Fb}$ mice) after ifenprodil application, probably due to unaltered NR2A component (Figure 26 F). A puzzling finding was the unchanged decay time (Figure 26 H) after ifenprodil application in wild-type mice. The results collected so far were confirmed by experiments in which the specific NR2B antagonist CP101,606 was applied instead of ifenprodil (Figure 26 E,

F, H). The decay time of the NMDAR currents in wild-type did not change also in the presence of CP101,606. This could be due to the contribution of triheteromeric NR1/NR2A/NR2B complexes at extrasynaptic sites (Vicini et al., 1998; Tovar and Westbrook, 1999) that might have less sensitivity to NR2B antagonists.

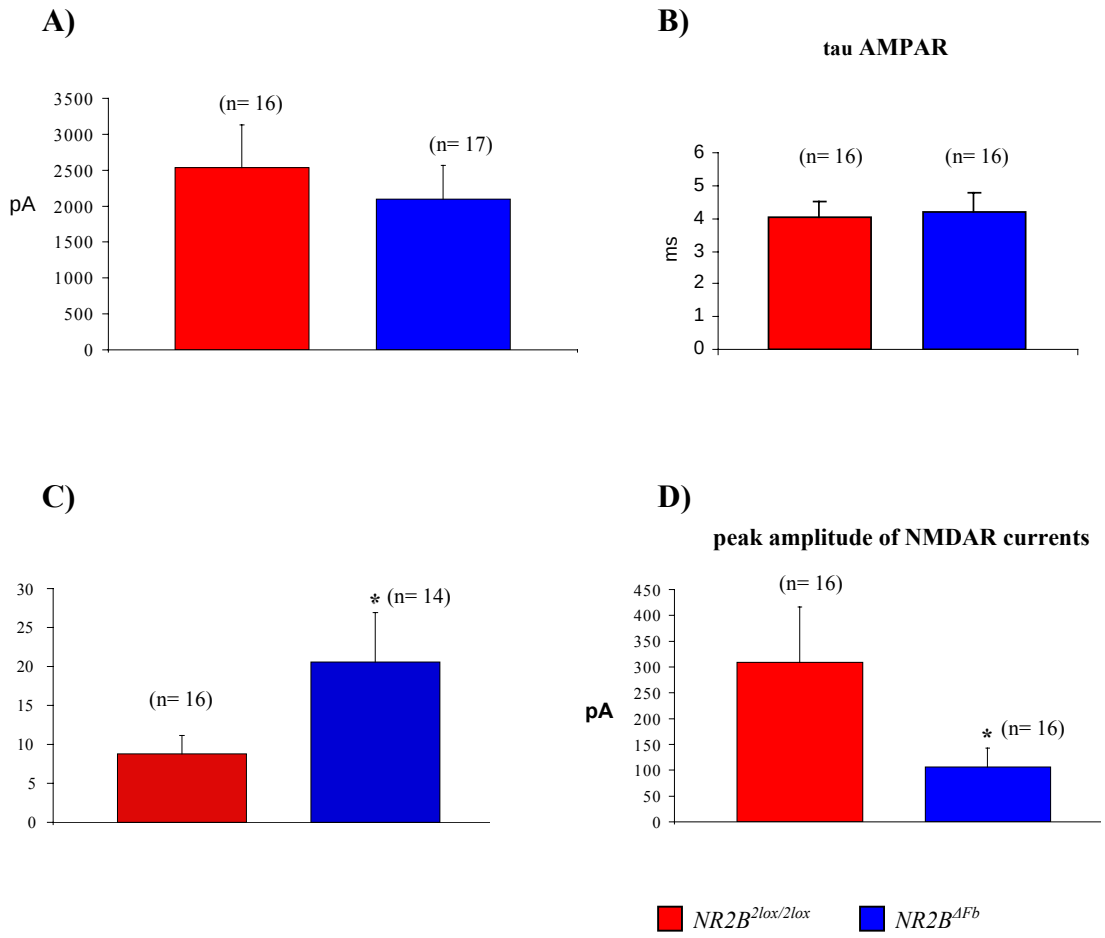

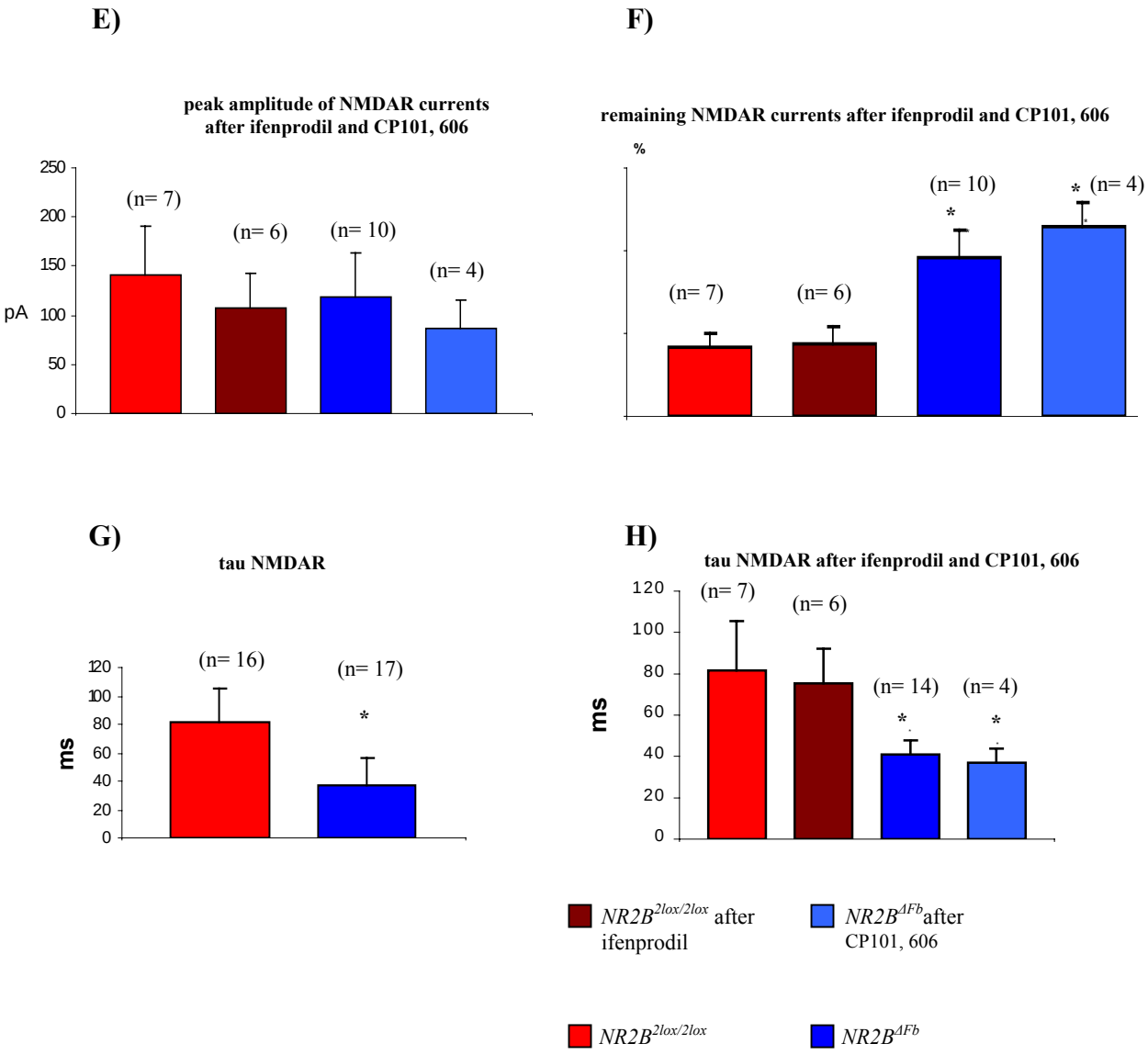

Figure 26: Nucleated Patches.

Somatic recordings were performed in P42-P45 animals. There was no difference in peak amplitude and decay time of the AMPAR component between the two genotypes (A), (B). Somatic recordings indicated an increase AMPA/NMDA ratio and significant decrease of NMDAR currents in *NR2B*$^{\Delta Fb}$ mice compared to littermates (*NR2B*$^{2lox/2lox}$) (C), (D). Sensitivity to NR2B antagonists (E) (F) and decay time (G) were significantly reduced in *NR2B*$^{\Delta Fb}$ mice compared to control littermates. Decay time of NMDAR currents after application of the NR2B antagonists in *NR2B*$^{2lox/2lox}$ mice was unchanged (H). Differences between two groups were evaluated using the unpaired two-tailed Student's t-test. P values <0.05 were considered statistically significant ($p<0.05$=*; $p<0.01$=**; $p<0.001$=***).

3.4.4 Impaired Hippocampal Long Term Potentiation

Recent studies propose that activation of NR2A containing receptors solely controls induction of LTP (Liu et al., 2004; Massey et al., 2004). This view has been challenged by other studies where NR2B subunit contribution was shown to be critical for the induction of LTP in hippocampal and anterior cingulate cortex (ACC) (Berberich et al., 2005; Zhao et al., 2005). The latter are consistent with the results from the transgenic mice overexpressing *NR2B*, which showed enhanced LTP (Tang et al., 1999). NR2A and NR2B containing NMDARs coexist in synapses of CA1 pyramidal cells. Their relative contribution to synaptic transmission and plasticity is still unclear.

We therefore wanted to determine whether synaptic transmission undergoes LTP in the absence of the NR2B subunit. LTP could be induced in hippocampal CA1 pyramidal cells from wild-type mice, by pairing Schaffer collateral stimulation with postsynaptic depolarisation (depolarisation to 0 mV for 3 min with low frequency presynaptic stimulation) under whole-cell conditions. This resulted in a twofold increase of synaptic currents (Figure 27 A). To quantify the level of LTP averaged EPSC amplitudes between 30-40 min after pairing were normalised to baseline (Figure 27 C). In $NR2B^{\Delta Fb}$ mice cellular LTP in hippocampal CA1 pyramidal cells was strongly impaired ($NR2B^{2lox/2lox}$= 1.71± 0.2 n= 7, $NR2B^{\Delta Fb}$= 1.00± 0.2, n= 6) (Figure 27 B).

The charge transfer during the induction of LTP (calculated from the integral of the current over the time) showed a significant decrease in the $NR2B^{\Delta Fb}$ mice ($NR2B^{2lox/2lox}$= 2.70± 1.25 pC, n= 7, $NR2B^{\Delta Fb}$= 0.37± 0.30 pC, n= 6). Since the AMPAR mediated currents were not altered in the $NR2B^{\Delta Fb}$ mice compared to $NR2B^{2lox/2lox}$ mice (Chapter 3.4.2.), the reduction in charge can be attributed to the decreased NMDAR component since our previous results from the synaptic and somatic recordings also revealed a significant decrease in the peak amplitude of the NMDAR mediated currents and faster decay time in the mutant (Chapter 3.4.1, 3.4.3). Ca^{2+} influx through the NMDA receptors is important for the induction of LTP. Therefore we assume that the reduction in charge transfer (Figure 27.D) could be related to a decreased Ca^{2+} influx, and consequently to impaired LTP.

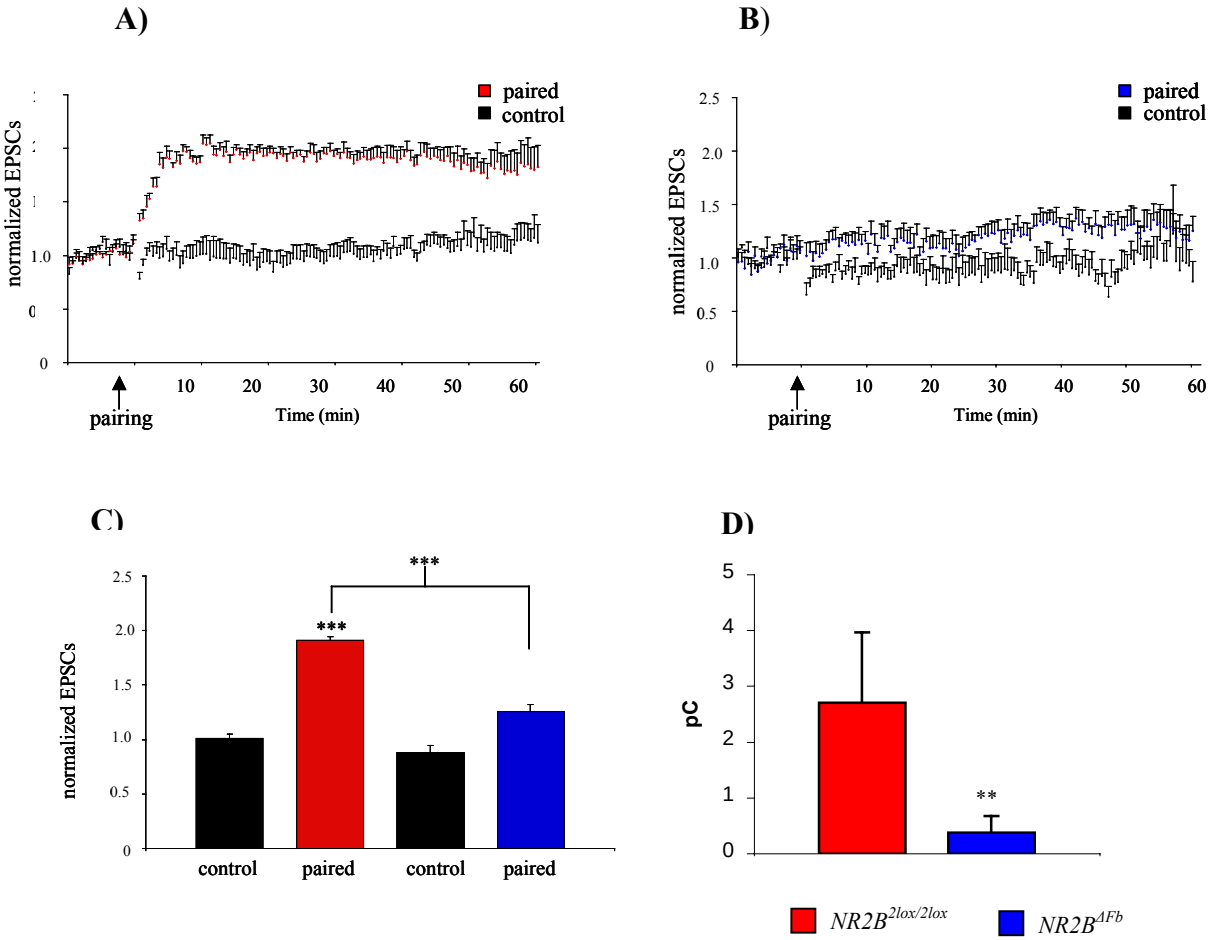

Figure 27: A) Normalised EPSC amplitudes evoked at CA3 to CA1 synapses in brain slices of *NR2B*$^{2lox/2lox}$ and *NR2B*$^{\Delta Fb}$ mice (P42-P47) in paired and control pathways. The mean of the 10 min baseline EPSCs was taken for normalisation. Cellular LTP was induced by pairing postsynaptic depolarisation to 0 mV for 3 min with low frequency presynaptic stimulation (0.67 Hz). Plotted area mean + SEM. B) Mean LTP (+SD) is given as an averaged normalised EPSC amplitudes from 30-40 min after pairing (n= 7 for *NR2B*$^{2lox/2lox}$ mice, n= 6 for *NR2B*$^{\Delta Fb}$ mice). P values <0.05 were considered statistically significant (p<0.05= *; p<0.01= **; p<0.001= ***). Asterisks indicate the significance between control and paired pathway and between paired pathway of *NR2B*$^{2lox/2lox}$ and *NR2B*$^{\Delta Fb}$ mice (two tailed Student´s t-test).

These results collectively show the significance of the NR2B subunit in hippocampal synaptic plasticity.

4 DISCUSSION

4.1 Altering *NR2B* Allele in Germ Line

4.1.1Embryonic Stem Cells and Removal of the Neomycin Cassette

When a fragment of genomic DNA is introduced into a mammalian cell it can recombine with endogenous homologous sequences. This type of homologous recombination has been widely used, particularly in mouse embryonic stem (ES) cells to generate so-called gene targeted mutations. ES cell lines are probably the most remarkable cell lines ever established since they can be cultured and manipulated relatively easily *in vitro* without losing their potential to step right back into their normal developmental programme when returned into the early stage embryo. They correspond closely to cells of the inner mass of the blastocyst. Even after extended periods of cell culture, ES cell lines can remain multipotent and participate in the formation of all tissues, including the gametes. Given the possibility of transmitting the altered gene through the germline of a chimeric animal, they are frequently used in gene targeting experiments (Robertson et al., 1991). Therefore, in the present work mouse ES cells from a clone positive for the homologous recombination were injected into mouse blastocysts derived from the strain C57Bl6 to generate the $NR2B^{2lox}$ mouse line.

Nearly all constructs used for homologous recombination rely on the positive selection of a drug resistance in order to differentiate homologous recombination from random integrations. A marker gene, such as the neomycin resistance gene (*neo*), is routinely used to select for targeted ES-cell clones. However, the placement of *neo* in introns, or in 5'- or 3'- flanking or untranslated regions, can interfere with the expression of the targeted or neighboring genes. In some cases, it has been determined that cryptic splice sites in *neo* interfere with normal splicing and therefore reduce wild-type mRNA levels. Therefore it is desirable to flank the neomycin cassette with loxP or frt sites for later removal either *in vitro* in ES cells by transiently introducing a Cre or Flp expressing plasmid or by breeding with a mouse line which expresses Cre or Flp in the germ line, such that the cassette can be removed. Taking out the neomycin cassette in stem cells

increases the passage number of the cells and by this may lead to differentiation of the ES cells. Although both approaches were tried in parallel, due to the shorter time span, the line *NR2B*^{2lox} was established from ES cells in which the removal of the cassette was performed in culture by using the Flp/Frt system (Schaft et al., 2001).

4.1.2 Conditional Ablation of the *NR2B* Gene

The ability to inactivate an endogenous gene in the mouse in a temporally and spatially controlled manner is not only useful for circumventing early lethal phenotypes but also allows biological questions to be addressed with exquisite accuracy. Strategies exploiting site specific DNA recombination have been incorporated into transgenic and gene targeting procedures to allow *in vivo* manipulation of DNA in embryonic stem (ES) cells (Gu et al., 1993; Orban et al., 1992) or living animals (Lakso et al., 1992; Gu et al., 1994). In this study we used Cre mediated DNA recombination for conditional ablation of the *NR2B* gene. Success of the experiments depends on the availability of tissue-specific regulatory elements to drive Cre expression. Nonspecific expression could render a Cre transgene useless because of the effective irreversibility of the recombination event. Nevertheless, even if the appropriate Cre line is not available, it is an alternative for investigators to produce floxed alleles rather than standard 'knock-outs'. This is because they can generate the recombined null allele by using one of the many Cre deleter strains and have mice that carry the floxed allele when the right Cre expressing mouse comes along in the future. The α-CaMKII promoter in the Tg^{Cre4} line guarantees the expression of Cre recombinase exclusively in postnatal principal neurons of the forebrain. Since α-CaMKII is not expressed in inhibitory GABAergic interneurons, this cell population lacks Cre recombinase expression in *NR2B*$^{\Delta Fb}$ mice. To delete NR2B expression specifically in inhibitory neurons, we will use transgenic animals in which Cre recombinase is expressed under the control of the parvalbumin promoter or the GAD67 promoter. These experiments will allow the further investigations of the NR2B physiological function in distinct neuronal cell populations.

4.2 Lentiviral Expression of Cre Recombinase

Lentivirus vectors based on the human immunodeficiency virus (HIV) represent a complex form of retrovirus that can infect and stably transduce dividing as well as terminally differentiated cells such as neurons (Naldini et al., 1996). It was also shown that a lentiviral vector is able to transduce efficiently and stably *in vivo* without a detectable decrease of transgene expression over time (Blömer et al., 1997). Advantages of this system are stable gene expression as well as the lack of immune or cytotoxic responses from the host organism. Stereotactic delivery of lentiviral particles to brain tissue *in vivo* allows efficient transduction of populations of neurons in selected brain regions, resulting essentially in a creation of local transgenic cells. Moreover, the vector system can be modified by including tissue or cell-specific promoters to express genes of interest in a subpopulation of cells in the brain. As the particles are pseudotyped with the envelope of the vesicular stomotitis virus (VSV), the vector can serve to introduce genes into a broad range of tissues and can be used *in vivo* (Schlegel et al., 1983). Therefore, in the present work, a lentiviral vector expressing Cre recombinase and GFP under the control of a 1.3 kb α-CaMKII promoter fragment was delivered stereotactically to the hippocampal CA1 region of $NR2B^{2lox/2lox}$ mice for the purpose of *in vivo* Cre/loxP recombination. Since the local area of injection limits further behavioural studies, which would elucidate the phenotypical consequence of the deletion of the *NR2B* gene in a broader area like the whole forebrain, we also used the Tg^{Cre4} line.

4.3 AMPA/NMDA Ratio

In most excitatory synapses AMPA and NMDA receptors coexist together (Bekkers and Stevens 1989). Since these receptors have distinct kinetics and the NMDAR is important for Ca^{2+} dependent plasticity (Bliss and Colligridge, 1993; Malenka and Nicoll, 1999), the ratio of NMDAR to AMPAR mediated currents is likely to be a key determinant of both short-term integration of synaptic inputs and their long-term modification.

We wanted to demonstrate *NR2B* ablation and its effects in the hippocampus by using a combination of biochemical and electrophysiological studies. Western blot analysis of hippocampal homogenates of $NR2B^{\Delta Fb}$ mice showed a reduction of NR2B subunit expression by 70%. Synaptic recordings from CA1 pyramidal cells revealed a twofold increase in the AMPA/NMDA ratio in $NR2B^{\Delta Fb}$ mice, which is probably due to the decreased amplitude of the current mediated by NMDARs. To exclude that the currents mediated by AMPARs were responsible for the increased AMPA/NMDA ratio, mEPSCs were recorded. Since the mEPSCs showed no significant difference in initial peak amplitude and frequency between $NR2B^{2lox/2lox}$ and $NR2B^{\Delta Fb}$ the number of AMPA receptors in the postsynaptic site in mutant mice appeared to be unaltered. Furthermore, the data from the western blot analysis of the hippocampal homogenates revealed comparable expression of GluR-A and GluR-B between the two genotypes. On the other hand a previous study (Kim et al., 2004) reported that in mature neurons NR2A and NR2B subunits have opposing actions on the surface insertion of the GluR-A subunit with NR2B subunit inhibiting its insertion. They found that overexpression of NR2B in culture inhibits the surface expression of GluR-A. Our results from the western blots of the hippocampal homogenates strongly suggest that in the absence of NR2B, there is no significant difference in the expression level of the GluR-A subunit , however, we did not check specifically the surface expression of the GluR-A. It is known that AMPA receptors mediate fast synaptic currents and NMDA receptors mediate currents that are slower and longer lasting (Dingledine et al., 1999). In line with this we viewed the reduced amplitude of mEPSCs after 50 ms as a measure for the reduced NMDAR contribution. By this way, in the present study we propose that the increased AMPA/NMDA ratio in $NR2B^{\Delta Fb}$ mice is solely due to the reduction in the number of NMDA receptors.

4.4 Kinetic Properties

During postnatal development, the duration of currents mediated by NMDA receptors decreases. Primary neuronal cultures expressing NR2A subunit mRNA had faster NMDAR EPSCs than cells with no expression of this subunit (Flint et al., 1997).

Increasing the contribution of NR2A-containing receptors to the synaptic current decreases the contribution from the NR2B subunit. The gradual supplementation of NR2B by NR2A during postnatal development has been implicated in the speeding of the decay of synaptic NMDAR mediated currents (Monyer et al., 1994; Flint et al., 1997; Cull-Candy et al., 2001). *In vitro*, NR2B containing receptors have slower decay times compared to NR2A containing receptors (Monyer et al., 1994; Cull-Candy et al., 2001). In accordance with this, our results from synaptic recordings of CA1 pyramidal cells lacking the NR2B subunit showed a dramatic reduction in the decay time (see results). Our findings are in line with a study which reported that NMDAR mediated EPSCs from cultured hippocampal neurons lacking the NR2B subunit have very fast deactivation kinetics compared to those from wild-type neurons (Tovar et al., 2000). Moreover, our finding is consistent with data from genetically modified mice overexpressing the NR2B subunit, which revealed 1.8 fold slower decay of NMDAR mediated currents in mature neurons (Tang et al., 1999). Application of the NR2B specific antagonist ifenprodil (10 μM) did not show a significant reduction in the currents mediated by NMDARs in CA1 pyramidal cells lacking NR2B. Lack of sensitivity to ifenprodil and faster decay time confirmed the absence of synaptic NR2B containing receptors in $NR2B^{\Delta lenti}$ and $NR2B^{\Delta Fb}$ mice. Additionally, western blot analysis of hippocampal homogenates also showed a comparable NR2A subunit expression in mutant and wild-type mice. Therefore, the faster decay time of the NMDAR mediated EPSCs in absence of NR2B can be explained by the predominance of NR2A containing receptors.

4.5 Cellular Plasticity

Both NR2A- and NR2B-type NMDA receptors activate signalling pathways that lead to LTP formation (Köhr et al., 2003). The NR2B subunit predominates early in development whereas expression of NR2A starts shortly after birth and gradually increases to the adult levels (Monyer et al., 1994). Increasing incorporation of NR2A subunits could underlie some of the changes in NMDA receptor properties observed during postnatal development. It has been hypothesized that a developmental switch from NR2B to NR2A

at synaptic sites may be responsible for the decreased plasticity observed in older animals (Carmignoto and Vicini, 1992; Crair and Malenka, 1995).

In young animals, both NR2A and NR2B contribute to LTP, whereas in adult animals, NR2A mediated signalling dominates (Köhr et al., 2003). Interestingly, studies of transgenic mice overexpressing *NR2B* in the adult forebrain demonstrate the important contribution made by NR2B subunits to hippocampal LTP (Tang et al., 1999) and behavioural learning (Tang et al., 1999; Wong et al., 2002). These mice exhibit enhanced LTP and a superior ability in learning and memory in various behavioural tasks. However, the authors did not try to prove that the beneficial effects of the transgenic overexpression of *NR2B* are not simply due to the higher number of total NMDA receptors and not specific for the NR2B subunit. A possible control would have been transgenic overexpression of NR2A. Whereas mice with targeted disruption of the NR2A subunit have reduced LTP and deficiencies in certain learning tests (Sakimura et al., 1995), mice lacking a functional *NR2B* gene die at birth (Kutsuwada et al., 1996). It is likely that both NR2A and NR2B dependent pathways are involved in memory formation in adult mice because, in contrast to mice that lack all NMDARs in CA1 pyramidal cells (McHugh et al., 1996), NR2A knock-out mice are less impaired in learning tests (Kiyama et al., 1998), and activation of NR2B-type NMDARs restores LTP in mice with absent or impaired NR2A signalling (Kiyama et al., 1998; Köhr et al., 2003) Alternatives to NR2 knock-out mice are gene-manipulated mice which express C-terminally truncated NR2 subunits. Mice in which the C-terminal domains of NR2 subunits are truncated show the same phenotype as the knock-out of the corresponding NR2 subunit with the NR2B showing the most severe phenotype (Sprengel et al., 1998; Mori et al., 1998). Most of these mice express gateable receptors that are synaptically activated, but are defective in intracellular signalling and less prominent in synaptic localisation. A recent study reports that hippocampal LTP is mediated by NMDARs containing the NR2A but not the NR2B subunit (Liu et al., 2004). This finding suggests that the NR2B receptors in the hippocampus may not contribute to learning-related synaptic potentiation, however, no behavioural study has demonstrated the inhibitory effect that NR2B antagonists may have on learning when injected locally in the hippocampus. Although yet another study also claims that activation of NR2A containing receptors solely controls induction of LTP

(Massey et al., 2004), this view has been challenged by other studies which reported the important contribution of NR2B for LTP induction (Berberich et al., 2005; Zhao et al., 2005). NR2A and NR2B subunits predominate in the forebrain, but their relative contribution to synaptic transmission and plasticity is still a challenge and not clearly understood.

To expand the knowledge in this field we examined if synaptic transmission undergoes LTP in the absence of the NR2B subunit. Our results demonstrated that cellular LTP in hippocampal CA1 pyramidal cells was strongly impaired in the absence of the NR2B subunit. Our finding is consistent with those results on genetically modified mice, in which *NR2B* expression was upregulated (Tang et al., 1999; Wong et al., 2002;) or NR2A signalling was impaired (Kiyama et al., 1998; Köhr et al., 2003). In summary, our results do not support the model that only NR2A-type NMDARs are responsible for LTP induction (Collingridge et al., 2004; Liu et al., 2004; Massey et al., 2004). It was reported in a CA3 specific knock out of the NR2B subunit that LTP could not be induced. However in contrast to our western blot analysis NR2A protein expression was drastically reduced, and NMDAR responses were hardly detected the CA3 synapses (Toshikazu et al., 2004 SFN Abstract). On the other hand, one can still argue and propose with our findings that the impaired LTP can be due to the decreased number of NMDA receptors rather than absence of the NR2B subunit. In order to elucidate if the impaired LTP is due to the lack of signalling cascades triggered specifically by the NR2B subunit, detailed investigation can be performed via overexpression of the NR2A in the absence of NR2B and further analysis of cellular LTP. One way to achieve this can be the stereotactic delivery of lentiviral particles co-expressing NR2A and GFP to the CA1 region of $NR2B^{\Delta Fb}$ mice. This way we want to find out if NR2A overexpression can rescue the impaired cellular plasticity in the absence of the NR2B subunit by increasing the total number of NMDA receptors. Whole-cell LTP can be induced by different stimulation paradigms, such as HFS (high frequency stimulation), pairing of action potentials with EPSPs with appropriate timing or pairing of postsynaptic depolarisation with low frequency stimulation (the protocol which was used in this study). Moreover, with another method the increase in synaptic transmission from a population of CA1

neurons can be recorded (field LTP). Our future electrophysiological studies will include LTP induction experiments by application of different protocols.

4.6 Somatic NMDAR Currents

NR2A subunits are incorporated synaptically late in development, whereas NR2B subunits are still highly persistent at extrasynaptic sites (Stocca and Vicini, 1998; Rumbaugh and Vicini, 1999; Tovar and Westbrook, 1999). In order to explore this view somatic currents were recorded in nucleated whole-soma patches from CA1 neurons in the absence of the NR2B subunit. In accordance with our results from the synaptic recordings the data showed that the AMPAR component was not changed in mutant mice. Therefore the observed increase in the AMPA/NMDA ratio could be due to the reduced number of NMDA receptors at extrasynaptic sites as it was found at synaptic sites. Lack of NR2B subunit was verified by reduced peak amplitudes of the NMDAR mediated currents and lack of sensitivity to NR2B antagonists at somatic sites. In conformity with synaptic recordings, the kinetics of NMDAR currents became faster. It has been suggested that some native NMDAR channels contain more than one type of NR2 subunit in the same assembly (Dunah et al., 1998; Sheng et al., 1994; Luo et al., 1997). Although studies in a heterologous system report the formation of functional triheteromeric assemblies of NR1/NR2A/NR2B (Vicini et al., 1998; Tovar and Westbrook, 1999), it is still unknown to what extent these assemblies are formed *in vivo*. Our rather surprising finding of the unchanged decay time after NR2B antagonist application (ifenprodil and CP101,606) in wild-type mice could be explained by the possible contribution of these triheteromeric NR1/NR2A/NR2B complexes at extrasynaptic sites, which might be less sensitive to these antagonists (Vicini et al., 1998; Tovar and Westbrook 1999).

4.7 Future Perspectives

We believe that the conditional knock-out of the *NR2B* gene will bring new insight into the field by elucidating the specific function of NR2B in learning and memory which is

still enigmatic. We observed that *NR2B*$^{\Delta Fb}$ mice grow and mate normally compared to wild-type littermates. Since the overexpression or upregulation of the NR2B subunit showed superior ability in learning and memory in the behavioural tests (Tang et al., 1999; Wong et al., 2002), whereas the global knock-out of the NR2B was lethal (Kutsuwada et al., 1996) we want to explore the effect of the NR2B ablation on learning and memory by performing specific behavioural studies, as for example novel object recognition, contextual, cued fear conditioning, and spatial reference, working memory by water maze and T maze.

5 ABBREVIATIONS

α	alpha
α^{32}P-dCTP	deoxicytosin triphosphate labelled with ^{32}P in alpha position
A	amphere
D-AP5	D-5-amnino phosphonate pentanic acid
ATP	adenosine triphosphate
AAV	adeno-associated virus
BIP	bovine immunodeficiency virus
BAPTA	1,2-bis-(2-aminophenoxy)ethane-N,N,N,N,N- tetracetic acid
BDNF	brain-derived neurotropic factor
bp	baise pairs
C	Celsius
CA	cornu ammonis
CaMKII	Ca^{2+}/calmodulin-dependent proteinkinase II
CMV	cytomegalovirus
CNS	central nervous system
CNQX	6-Cyano-7-nitroquinoxaline-2,3-dione, Ampa antagonist
cDNA	complementary DNA, obtained by reverse transcription of mRNA
Δ	delta
DEPC	diethyl pyrocarbonate
DNA	deoxyribonucleic acid
dNTPs	deoxyribonucleotides
E.coli	ecsherichia coli
EDTA	ethylene diaminetetraacetic acid
EGTA	ethylene glycol-bis(2-aminoethyl)-N,N,N,N-tetraacetic acid
EGFP	enhanced green fluoroscent protein
EPSC	excitatory postsynaptic current
EPSP	excitatory postsynaptic potential
ES cells	embryonic stem cells
et al.	et alii

FIV	feline immunodeficiency virus
G-protein	guanosine nucleotide-binding protein
GABA	γ-aminobutiric acid
γ	gamma
GluR	glutamate receptor
G418	Genetecin
GTP	guanosine triphosphate
h	hour
HEPES	N-(2-Hydroxyethyl)piperazine-N`-ethanesulforinic acid
HSV	herpes simplex virus
IPSP	inhibitory postsynaptic current
IRES	internal ribosomal entry site from the encephalomyelitis virus gene
IC50	concentration required for half maximal response
KA	kainite
kb	kilobase
kD	kilodalton
K.O	knock-out gene
LTD	long term depression
LTP	long term potentiation
LTR	long terminal repeats
M	mol
m	milli
μ	micro
mEPSC	miniature evoked postsynaptic current
MMLV	Moloney Murine Leukaemia Virus
N	asparagine
neo	neomycin resistance gene
NMDA	*N*-methyl-D-aspartate
NMDAR	*N*-methyl-D-aspartate receptor
NO	nitric oxide

NOS	nitric oxide synthase
NR1	NMDAR subunit 1
NR2	NMDAR subunit 2
NR3	NMDAR subunit 3
NBQX	1,2,3,4-Tetrahydro-6-nitro-2,3-dioxo-benzo(f)quinoxaline-7-sulfoamide
Neo	neomycin resistance gene
NVP-AAM077	(1RS,1'S)-PEAQX, NR2A subunit specific antagonist
p	pico
P	postnatal
p	probability
PBS	phosphate-buffered saline
PCR	polymerase chain reaction
PDZ domain	post synaptic density/disc large/zona ocludens-1 homology domain
PFA	paraformaldehyde
PKA	cyclic AMP-dependent protein kinase A
PKC	protein kinase C
PSD	postsynaptic densitiy
Q	glutamine
R	arginine
RNA	ribonucleic acid
RT-PCR	reverse transcription coupled to ploymerase chain reaction
s	second
SDS	sodium-dudecyl-sulfat
SDS-PAGE	SDS-PloyAcrylamide Gel Electrophoresis
STEDV	standart deviation
Taq	therminus aquaticus
TE	tris/EDTA buffer
TENS	tris-EDTA_Sodium chloride-SDS buffer
Tris-HCl	Tris(hydroxymethyl)aminomethane-hydrochloride

TTX	tetrodoxin
U	units
WRE	woodchuck regulatory element
Wt	wild-type
VSV-G	vesicular stomatitis virus glycoprotein

6 REFERENCES

Ault, B., and Hildebrand, L.M. (1993) Activation of nociceptive reflexes by peripheral kainate receptors. *J Pharmacol Exp Ther* **265**: 927-932

Ayalon, G., and Stern-Bach, Y. (2001) Functional assembly of AMPA and kainate receptors is mediated by several discrete protein-protein interactions. *Neuron* **31**: 103-113

Azzouz, M., Kingsman, S.M., and Mazarakis, N.D. (2004) Lentiviral vectors for treating and modeling human CNS disorders. *J Gene Med* **6**: 951-962

Barria, A., and Malinow, R. (2002) Subunit-specific NMDA receptor trafficking to synapses. *Neuron* **35**: 345-353

Barry, M.F., and Ziff, E.B. (2002) Receptor trafficking and the plasticity of excitatory synapses. *Curr Opin Neurobiol* **12**: 279-286

Behe, P., Stern, P., Wyllie, D.J., Nassar, M., Schoepfer, R., and Colquhoun, D. (1995) Determination of NMDA NR1 subunit copy number in recombinant NMDA receptors. *Proc Biol Sci* **262**: 205-213

Berberich, S., Punnakkal, P., Jensen, V., Pawlak, V., Seeburg, P.H., Hvalby, O., and Kohr, G. (2005) Lack of NMDA receptor subtype selectivity for hippocampal long-term potentiation. *J Neurosci* **25**: 6907-6910

Bliss, T.V., and Collingridge, G.L. (1993) A synaptic model of memory: long-term potentiation in the hippocampus. *Nature* **361**: 31-39

Bliss, T., and Schoepfer, R. (2004) Neuroscience. Controlling the ups and downs of synaptic strength. *Science* **304**: 973-974.

Bourne, H.R., and Nicoll, R. (1993) Molecular machines integrate coincident synaptic signals. *Cell* **72 Suppl**: 65-75

Burnashev, N., Monyer, H., Seeburg, P.H., and Sakmann, B. (1992) Divalent ion permeability of AMPA receptor channels is dominated by the edited form of a single subunit. *Neuron* **8**: 189-198

Burns, J.C., Friedmann, T., Driever, W., Burrascano, M., and Yee, J.K. (1993) Vesicular stomatitis virus G glycoprotein pseudotyped retroviral vectors: concentration to very high titer and efficient gene transfer into mammalian and nonmammalian cells. *Proc Natl Acad Sci U S A* **90**: 8033-8037

Capecchi, M.R. (1989) Altering the genome by homologous recombination. *Science* **244**: 1288-1292

Chatterton, J.E., Awobuluyi, M., Premkumar, L.S., Takahashi, H., Talantova, M., Shin, Y., Cui, J., Tu, S., Sevarino, K.A., Nakanishi, N., Tong, G., Lipton, S.A., and Zhang, D. (2002) Excitatory glycine receptors containing the NR3 family of NMDA receptor subunits. *Nature* **415**: 793-798

Chazot, P.L., and Stephenson, F.A. (1997) Biochemical evidence for the existence of a pool of unassembled C2 exon-containing NR1 subunits of the mammalian forebrain NMDA receptor. *J Neurochem* **68**: 507-516

Chen, N., Luo, T., Wellington, C., Metzler, M., McCutcheon, K., Hayden, M.R., and Raymond, L.A. (1999) Subtype-specific enhancement of NMDA receptor currents by mutant huntingtin. *J Neurochem* **72**: 1890-1898

Chenu, C., Serre, C.M., Raynal, C., Burt-Pichat, B., and Delmas, P.D. (1998) Glutamate receptors are expressed by bone cells and are involved in bone resorption. *Bone* **22**: 295-299

Clayton, D.A., Mesches, M.H., Alvarez, E., Bickford, P.C., and Browning, M.D. (2002) A hippocampal NR2B deficit can mimic age-related changes in long-term potentiation and spatial learning in the Fischer 344 rat. *J Neurosci* **22**: 3628-3637

Cull-Candy, S., Brickley, S., and Farrant, M. (2001) NMDA receptor subunits: diversity, development and disease. *Curr Opin Neurobiol* **11**: 327-335

Cull-Candy S. (2002). Ionotropic glutamate receptors. In: Egebjerg J., Schousboe A., Krogsgaard-Larsen P. (Eds), *Glutamate and GABA Receptors and Transporters. Taylor&Francis*, pp 11-40

Das, S., Sasaki, Y.F., Rothe, T., Premkumar, L.S., Takasu, M., Crandall, J.E., Dikkes, P., Conner, D.A., Rayudu, P.V., Cheung, W., Chen, H.S., Lipton, S.A., and Nakanishi, N. (1998) Increased NMDA current and spine density in mice lacking the NMDA receptor subunit NR3A. *Nature* **393**: 377-381

Dingledine, R., Borges, K., Bowie, D., and Traynelis, S.F. (1999) The glutamate receptor ion channels. *Pharmacol Rev* **51**: 7-61

Dudek, S.M., and Bear, M.F. (1992) Homosynaptic long-term depression in area CA1 of hippocampus and effects of N-methyl-D-aspartate receptor blockade. *Proc Natl Acad Sci U S A* **89**: 4363-4367

Dunah, A.W., Luo, J., Wang, Y.H., Yasuda, R.P., and Wolfe, B.B. (1998) Subunit composition of N-methyl-D-aspartate receptors in the central nervous system that contain the NR2D subunit. *Mol Pharmacol* **53**: 429-437

Dzubay, J.A., and Jahr, C.E. (1996) Kinetics of NMDA channel opening. *J Neurosci* **16**: 4129-4134

Ebralidze, A.K., Rossi, D.J., Tonegawa, S., and Slater, N.T. (1996) Modification of NMDA receptor channels and synaptic transmission by targeted disruption of the NR2C gene. *J Neurosci* **16**: 5014-5025

Flint, A.C., Maisch, U.S., Weishaupt, J.H., Kriegstein, A.R., and Monyer, H. (1997) NR2A subunit expression shortens NMDA receptor synaptic currents in developing neocortex. *J Neurosci* **17**: 2469-2476

Forrest, D., Yuzaki, M., Soares, H.D., Ng, L., Luk, D.C., Sheng, M., Stewart, C.L., Morgan, J.I., Connor, J.A., and Curran, T. (1994) Targeted disruption of NMDA receptor 1 gene abolishes NMDA response and results in neonatal death. *Neuron* **13**: 325-338

Forsythe, I.D., Westbrook, G.L., and Mayer, M.L. (1988) Modulation of excitatory synaptic transmission by glycine and zinc in cultures of mouse hippocampal neurons. *J Neurosci* **8**: 3733-3741

Gao, X.M., Sakai, K., Roberts, R.C., Conley, R.R., Dean, B., and Tamminga, C.A. (2000) Ionotropic glutamate receptors and expression of N-methyl-D-aspartate receptor subunits in subregions of human hippocampus: effects of schizophrenia. *Am J Psychiatry* **157**: 1141-1149

Ghosh, K., and Van Duyne, G.D. (2002) Cre-loxP biochemistry. *Methods* **28**: 374-383

Gill, S.S., Pulido, O.M., Mueller, R.W., and McGuire, P.F. (1998) Molecular and immunochemical characterization of the ionotropic glutamate receptors in the rat heart. *Brain Res Bull* **46**: 429-434

Gu, H., Marth, J.D., Orban, P.C., Mossmann, H., and Rajewsky, K. (1994) Deletion of a DNA polymerase beta gene segment in T cells using cell type-specific gene targeting. *Science* **265**: 103-106

Guillaud, L., Setou, M., and Hirokawa, N. (2003) KIF17 dynamics and regulation of NR2B trafficking in hippocampal neurons. *J Neurosci* **23**: 131-140

Hammond C. (2001). Ionotropic glutamate receptors. In: Hammond C., (Ed), *Cellular and Molecular Neurobiology.* Academic Press, pp 251-273

Hardingham, G.E., Fukunaga, Y., and Bading, H. (2002) Extrasynaptic NMDARs oppose synaptic NMDARs by triggering CREB shut-off and cell death pathways. *Nat Neurosci* **5**: 405-414

Hebb, D.O. (1949) The organization of the behavior. New-York: Willey

Hollmann, M., and Heinemann, S. (1994) Cloned glutamate receptors. *Annu Rev Neurosci* **17**: 31-108

Huh, K.H., and Wenthold, R.J. (1999) Turnover analysis of glutamate receptors identifies a rapidly degraded pool of the N-methyl-D-aspartate receptor subunit, NR1, in cultured cerebellar granule cells. *J Biol Chem* **274**: 151-157

Ikeda, K., Araki, K., Takayama, C., Inoue, Y., Yagi, T., Aizawa, S., and Mishina, M. (1995) Reduced spontaneous activity of mice defective in the epsilon 4 subunit of the NMDA receptor channel. *Brain Res Mol Brain Res* **33**: 61-71

Inagaki, N., Kuromi, H., Gonoi, T., Okamoto, Y., Ishida, H., Seino, Y., Kaneko, T., Iwanaga, T., and Seino, S. (1995) Expression and role of ionotropic glutamate receptors in pancreatic islet cells. *Faseb J* **9**: 686-691

Jahr, C.E., and Stevens, C.F. (1993) Calcium permeability of the N-methyl-D-aspartate receptor channel in hippocampal neurons in culture. *Proc Natl Acad Sci U S A* **90**: 11573-11577

Kennedy, M.B. (1997) The postsynaptic density at glutamatergic synapses. *Trends Neurosci* **20**: 264-268

Kennedy, M.B. (1998) Signal transduction molecules at the glutamatergic postsynaptic membrane. *Brain Res Brain Res Rev* **26**: 243-257

Kilby, N.J., Snaith, M.R., and Murray, J.A. (1993) Site-specific recombinases: tools for genome engineering. *Trends Genet* **9**: 413-421

Kim, J.H., and Huganir, R.L. (1999) Organization and regulation of proteins at synapses. *Curr Opin Cell Biol* **11**: 248-254

Kim, J., Dittgen, T., Nimmerjahn, A., Waters, J., Pawlak, V., Helmchen, F., Schlesinger, S., Seeburg, P.H., and Osten, P. (2004) Sindbis vector SINrep(nsP2S726): a tool for rapid heterologous expression with attenuated cytotoxicity in neurons. *J Neurosci Methods* **133**: 81-90

Kiyama, Y., Manabe, T., Sakimura, K., Kawakami, F., Mori, H., and Mishina, M. (1998) Increased thresholds for long-term potentiation and contextual learning in mice lacking the NMDA-type glutamate receptor epsilon1 subunit. *J Neurosci* **18**: 6704-6712

Kohr, G., and Seeburg, P.H. (1996) Subtype-specific regulation of recombinant NMDA receptor-channels by protein tyrosine kinases of the src family. *J Physiol* **492 (Pt 2)**: 445-452

Köhr, G., Jensen, V., Koester, H.J., Mihaljevic, A.L., Utvik, J.K., Kvello, A., Ottersen, O.P., Seeburg, P.H., Sprengel, R., and Hvalby, O. (2003) Intracellular domains of NMDA receptor subtypes are determinants for long-term potentiation induction. *J Neurosci* **23**: 10791-10799

Kornau, H.C., Schenker, L.T., Kennedy, M.B., and Seeburg, P.H. (1995) Domain interaction between NMDA receptor subunits and the postsynaptic density protein PSD-95. *Science* **269**: 1737-1740

Kuhn, R., and Torres, R.M. (2002) Cre/loxP recombination system and gene targeting. *Methods Mol Biol* **180**: 175-204

Kuryatov, A., Laube, B., Betz, H., and Kuhse, J. (1994) Mutational analysis of the glycine-binding site of the NMDA receptor: structural similarity with bacterial amino acid-binding proteins. *Neuron* **12**: 1291-1300

Kutsuwada, T., Sakimura, K., Manabe, T., Takayama, C., Katakura, N., Kushiya, E., Natsume, R., Watanabe, M., Inoue, Y., Yagi, T., Aizawa, S., Arakawa, M., Takahashi, T., Nakamura, Y., Mori, H., and Mishina, M. (1996) Impairment of suckling response, trigeminal neuronal pattern formation, and hippocampal LTD in NMDA receptor epsilon 2 subunit mutant mice. *Neuron* **16**: 333-344

Lakso, M., Sauer, B., Mosinger, B., Jr., Lee, E.J., Manning, R.W., Yu, S.H., Mulder, K.L., and Westphal, H. (1992) Targeted oncogene activation by site-specific recombination in transgenic mice. *Proc Natl Acad Sci U S A* **89**: 6232-6236

Laube, B., Kuhse, J., and Betz, H. (1998) Evidence for a tetrameric structure of recombinant NMDA receptors. *J Neurosci* **18**: 2954-2961

Lee, J.M., Zipfel, G.J., and Choi, D.W. (1999) The changing landscape of ischaemic brain injury mechanisms. *Nature* **399**: A7-14

Leonard, A.S., and Hell, J.W. (1997) Cyclic AMP-dependent protein kinase and protein kinase C phosphorylate N-methyl-D-aspartate receptors at different sites. *J Biol Chem* **272**: 12107-12115

Lester, R.A., Clements, J.D., Westbrook, G.L., and Jahr, C.E. (1990) Channel kinetics determine the time course of NMDA receptor-mediated synaptic currents. *Nature* **346**: 565-567

Lewandoski, M. (2001) Conditional control of gene expression in the mouse. *Nat Rev Genet* **2**: 743-755

Li, Y., Erzurumlu, R.S., Chen, C., Jhaveri, S., and Tonegawa, S. (1994) Whisker-related neuronal patterns fail to develop in the trigeminal brainstem nuclei of NMDAR1 knockout mice. *Cell* **76**: 427-437

Linden, D.J. (1999) The return of the spike: postsynaptic action potentials and the induction of LTP and LTD. *Neuron* **22**: 661-666

Lisman, J., and Harris, K. (1994) Who's been nibbling on my PSD: is it LTD? *J Physiol Paris* **88**: 193-195

Liu, L., Wong, T.P., Pozza, M.F., Lingenhoehl, K., Wang, Y., Sheng, M., Auberson, Y.P., and Wang, Y.T. (2004) Role of NMDA receptor subtypes in governing the direction of hippocampal synaptic plasticity. *Science* **304**: 1021-1024

Loftis, J.M., and Janowsky, A. (2003) The N-methyl-D-aspartate receptor subunit NR2B: localization, functional properties, regulation, and clinical implications. *Pharmacol Ther* **97**: 55-85

Lomeli, H., Sprengel, R., Laurie, D.J., Kohr, G., Herb, A., Seeburg, P.H., and Wisden, W. (1993) The rat delta-1 and delta-2 subunits extend the excitatory amino acid receptor family. *FEBS Lett* **315**: 318-322

Luo, J., Wang, Y., Yasuda, R.P., Dunah, A.W., and Wolfe, B.B. (1997) The majority of N-methyl-D-aspartate receptor complexes in adult rat cerebral cortex contain at least three different subunits (NR1/NR2A/NR2B). *Mol Pharmacol* **51**: 79-86

Lynch, M.A. (2004) Long-term potentiation and memory. *Physiol Rev* **84**: 87-136

MacDermott, A.B., Mayer, M.L., Westbrook, G.L., Smith, S.J., and Barker, J.L. (1986) NMDA-receptor activation increases cytoplasmic calcium concentration in cultured spinal cord neurones. *Nature* **321**: 519-522

Malenka, R.C., and Nicoll, R.A. (1997) Silent synapses speak up. *Neuron* **19**: 473-476

Malenka, R.C., and Bear, M.F. (2004) LTP and LTD: an embarrassment of riches. *Neuron* **44**: 5-21

Mantamadiotis, T., Lemberger, T., Bleckmann, S.C., Kern, H., Kretz, O., Martin Villalba, A., Tronche, F., Kellendonk, C., Gau, D., Kapfhammer, J., Otto, C., Schmid, W., and Schutz, G. (2002) Disruption of CREB function in brain leads to neurodegeneration. *Nat Genet* **31**: 47-54

Massey, P.V., Johnson, B.E., Moult, P.R., Auberson, Y.P., Brown, M.W., Molnar, E., Collingridge, G.L., and Bashir, Z.I. (2004) Differential roles of NR2A and NR2B-containing NMDA receptors in cortical long-term potentiation and long-term depression. *J Neurosci* **24**: 7821-7828

Mayer, M.L., Westbrook, G.L., and Guthrie, P.B. (1984) Voltage-dependent block by Mg2+ of NMDA responses in spinal cord neurones. *Nature* **309**: 261-263

Miyamoto, Y., Yamada, K., Noda, Y., Mori, H., Mishina, M., and Nabeshima, T. (2001) Hyperfunction of dopaminergic and serotonergic neuronal systems in mice lacking the NMDA receptor epsilon1 subunit. *J Neurosci* **21**: 750-757

Mohn, A.R., Gainetdinov, R.R., Caron, M.G., and Koller, B.H. (1999) Mice with reduced NMDA receptor expression display behaviors related to schizophrenia. *Cell* **98**: 427-436

Mohrmann, R., Kohr, G., Hatt, H., Sprengel, R., and Gottmann, K. (2002) Deletion of the C-terminal domain of the NR2B subunit alters channel properties and synaptic targeting of N-methyl-D-aspartate receptors in nascent neocortical synapses. *J Neurosci Res* **68**: 265-275

Monyer, H., Sprengel, R., Schoepfer, R., Herb, A., Higuchi, M., Lomeli, H., Burnashev, N., Sakmann, B., and Seeburg, P.H. (1992) Heteromeric NMDA receptors: molecular and functional distinction of subtypes. *Science* **256**: 1217-1221

Monyer, H., Burnashev, N., Laurie, D.J., Sakmann, B., and Seeburg, P.H. (1994) Developmental and regional expression in the rat brain and functional properties of four NMDA receptors. *Neuron* **12**: 529-540

Moon, I.S., Apperson, M.L., and Kennedy, M.B. (1994) The major tyrosine-phosphorylated protein in the postsynaptic density fraction is N-methyl-D-aspartate receptor subunit 2B. *Proc Natl Acad Sci U S A* **91**: 3954-3958

Mori, H., Manabe, T., Watanabe, M., Satoh, Y., Suzuki, N., Toki, S., Nakamura, K., Yagi, T., Kushiya, E., Takahashi, T., Inoue, Y., Sakimura, K., and Mishina, M. (1998) Role of the carboxy-terminal region of the GluR epsilon2 subunit in synaptic localization of the NMDA receptor channel. *Neuron* **21**: 571-580

Moriyoshi, K., Masu, M., Ishii, T., Shigemoto, R., Mizuno, N., and Nakanishi, S. (1991) Molecular cloning and characterization of the rat NMDA receptor. *Nature* **354**: 31-37

Mulkey, R.M., and Malenka, R.C. (1992) Mechanisms underlying induction of homosynaptic long-term depression in area CA1 of the hippocampus. *Neuron* **9**: 967-975

Mulkey, R.M., Herron, C.E., and Malenka, R.C. (1993) An essential role for protein phosphatases in hippocampal long-term depression. *Science* **261**: 1051-1055

Mulkey, R.M., Endo, S., Shenolikar, S., and Malenka, R.C. (1994) Involvement of a calcineurin/inhibitor-1 phosphatase cascade in hippocampal long-term depression. *Nature* **369**: 486-488

Nagy, A., Rossant, J., Nagy, R., Abramow-Newerly, W., and Roder, J.C. (1993) Derivation of completely cell culture-derived mice from early-passage embryonic stem cells. *Proc Natl Acad Sci U S A* **90**: 8424-8428

Naldini, L., Blomer, U., Gallay, P., Ory, D., Mulligan, R., Gage, F.H., Verma, I.M., and Trono, D. (1996) In vivo gene delivery and stable transduction of nondividing cells by a lentiviral vector. *Science* **272**: 263-267

Neyton, J., and Paoletti, P. (2006) Relating NMDA receptor function to receptor subunit composition: limitations of the pharmacological approach. *J Neurosci* **26**: 1331-1333

Nicoll, R.A., and Malenka, R.C. (1995) Contrasting properties of two forms of long-term potentiation in the hippocampus. *Nature* **377**: 115-118

Nowak, L., Bregestovski, P., Ascher, P., Herbet, A., and Prochiantz, A. (1984) Magnesium gates glutamate-activated channels in mouse central neurones. *Nature* **307**: 462-465

Omkumar, R.V., Kiely, M.J., Rosenstein, A.J., Min, K.T., and Kennedy, M.B. (1996) Identification of a phosphorylation site for calcium/calmodulindependent protein kinase II in the NR2B subunit of the N-methyl-D-aspartate receptor. *J Biol Chem* **271**: 31670-31678

Orban, P.C., Chui, D., and Marth, J.D. (1992) Tissue- and site-specific DNA recombination in transgenic mice. *Proc Natl Acad Sci U S A* **89**: 6861-6865

Philpot, B.D., Sekhar, A.K., Shouval, H.Z., and Bear, M.F. (2001) Visual experience and deprivation bidirectionally modify the composition and function of NMDA receptors in visual cortex. *Neuron* **29**: 157-169

Philpot, B.D., Weisberg, M.P., Ramos, M.S., Sawtell, N.B., Tang, Y.P., Tsien, J.Z., and Bear, M.F. (2001) Effect of transgenic overexpression of NR2B on NMDA receptor function and synaptic plasticity in visual cortex. *Neuropharmacology* **41**: 762-770

Quinonez, R., and Sutton, R.E. (2002) Lentiviral vectors for gene delivery into cells. *DNA Cell Biol* **21**: 937-951

Ramezani, A., Hawley, T.S., and Hawley, R.G. (2000) Lentiviral vectors for enhanced gene expression in human hematopoietic cells. *Mol Ther* **2**: 458-469

Rumbaugh, G., and Vicini, S. (1999) Distinct synaptic and extrasynaptic NMDA receptors in developing cerebellar granule neurons. *J Neurosci* **19**: 10603-10610

Sakimura, K., Kutsuwada, T., Ito, I., Manabe, T., Takayama, C., Kushiya, E., Yagi, T., Aizawa, S., Inoue, Y., Sugiyama, H., and et al. (1995) Reduced hippocampal LTP and spatial learning in mice lacking NMDA receptor epsilon 1 subunit. *Nature* **373**: 151-155

Sauer, B., and Henderson, N. (1988) Site-specific DNA recombination in mammalian cells by the Cre recombinase of bacteriophage P1. *Proc Natl Acad Sci U S A* **85**: 5166-5170

Sauer, B. (1998) Inducible gene targeting in mice using the Cre/lox system. *Methods* **14**: 381-392

Schaft, J., Ashery-Padan, R., van der Hoeven ,F., Gruss, P. and Stewart, F.A. (2001) Efficient FLP recombination in mouse ES cells and oocytes. *Genesis* **31**: 6-10

Schorge, S., and Colquhoun, D. (2003) Studies of NMDA receptor function and stoichiometry with truncated and tandem subunits. *J Neurosci* **23**: 1151-1158

Seeburg, P.H. (1993) The TINS/TiPS Lecture. The molecular biology of mammalian glutamate receptor channels. *Trends Neurosci* **16**: 359-365

Sheng, M., Cummings, J., Roldan, L.A., Jan, Y.N., and Jan, L.Y. (1994) Changing subunit composition of heteromeric NMDA receptors during development of rat cortex. *Nature* **368**: 144-147

Sheng, M. (1996) PDZs and receptor/channel clustering: rounding up the latest suspects. *Neuron* **17**: 575-578

Sommer, B., Kohler, M., Sprengel, R., and Seeburg, P.H. (1991) RNA editing in brain controls a determinant of ion flow in glutamate-gated channels. *Cell* **67**: 11-19

Sprengel, R., Suchanek, B., Amico, C., Brusa, R., Burnashev, N., Rozov, A., Hvalby, O., Jensen, V., Paulsen, O., Andersen, P., Kim, J.J., Thompson, R.F., Sun, W., Webster, L.C., Grant, S.G., Eilers, J., Konnerth, A., Li, J., McNamara, J.O., and Seeburg, P.H. (1998) Importance of the intracellular domain of NR2 subunits for NMDA receptor function in vivo. *Cell* **92**: 279-289

Steece-Collier, K., Chambers, L.K., Jaw-Tsai, S.S., Menniti, F.S., and Greenamyre, J.T. (2000) Antiparkinsonian actions of CP-101,606, an antagonist of NR2B subunit-containing N-methyl-d-aspartate receptors. *Exp Neurol* **163**: 239-243

Steigerwald, F., Schulz, T.W., Schenker, L.T., Kennedy, M.B., Seeburg, P.H., and Kohr, G. (2000) C-Terminal truncation of NR2A subunits impairs synaptic but not extrasynaptic localization of NMDA receptors. *J Neurosci* **20**: 4573-4581

Sternberg, N. (1981) Bacteriophage P1 site-specific recombination. III. Strand exchange during recombination at lox sites. *J Mol Biol* **150**: 603-608

Stevens, C.F., and Sullivan, J. (1998) Synaptic plasticity. *Curr Biol* **8**: R151-153

Stocca, G., and Vicini, S. (1998) Increased contribution of NR2A subunit to synaptic NMDA receptors in developing rat cortical neurons. *J Physiol* **507 (Pt 1)**: 13-24

Sugihara, H., Moriyoshi, K., Ishii, T., Masu, M., and Nakanishi, S. (1992) Structures and properties of seven isoforms of the NMDA receptor generated by alternative splicing. *Biochem Biophys Res Commun* **185**: 826-832

Tang, Y.P., Shimizu, E., Dube, G.R., Rampon, C., Kerchner, G.A., Zhuo, M., Liu, G., and Tsien, J.Z. (1999) Genetic enhancement of learning and memory in mice. *Nature* **401**: 63-69

Tingley, W.G., Ehlers, M.D., Kameyama, K., Doherty, C., Ptak, J.B., Riley, C.T., and Huganir, R.L. (1997) Characterization of protein kinase A and protein kinase C phosphorylation of the N-methyl-D-aspartate receptor NR1 subunit using phosphorylation site-specific antibodies. *J Biol Chem* **272**: 5157-5166

Tovar, K.R., and Westbrook, G.L. (1999) The incorporation of NMDA receptors with a distinct subunit composition at nascent hippocampal synapses in vitro. *J Neurosci* **19**: 4180-4188

Tovar, K.R., Sprouffske, K., and Westbrook, G.L. (2000) Fast NMDA receptor-mediated synaptic currents in neurons from mice lacking the epsilon2 (NR2B) subunit. *J Neurophysiol* **83**: 616-620

Toyoda, H., Zhao, M.G., and Zhuo, M. (2005) Roles of NMDA receptor NR2A and NR2B subtypes for long-term depression in the anterior cingulate cortex. *Eur J Neurosci* **22**: 485-494

Tsien, J.Z., Chen, D.F., Gerber, D., Tom, C., Mercer, E.H., Anderson, D.J., Mayford, M., Kandel, E.R., and Tonegawa, S. (1996) Subregion- and cell type-restricted gene knockout in mouse brain. *Cell* **87**: 1317-1326

Tsien, J.Z., Huerta, P.T., and Tonegawa, S. (1996) The essential role of hippocampal CA1 NMDA receptor-dependent synaptic plasticity in spatial memory. *Cell* **87**: 1327-1338

Verdoorn, T.A., Burnashev, N., Monyer, H., Seeburg, P.H., and Sakmann, B. (1991) Structural determinants of ion flow through recombinant glutamate receptor channels. *Science* **252**: 1715-1718

Vicini, S., Wang, J.F., Li, J.H., Zhu, W.J., Wang, Y.H., Luo, J.H., Wolfe, B.B., and Grayson, D.R. (1998) Functional and pharmacological differences between recombinant N-methyl-D-aspartate receptors. *J Neurophysiol* **79**: 555-566

Wang, Y.T., and Salter, M.W. (1994) Regulation of NMDA receptors by tyrosine kinases and phosphatases. *Nature* **369**: 233-235

Wei, F., Wang, G.D., Kerchner, G.A., Kim, S.J., Xu, H.M., Chen, Z.F., and Zhuo, M. (2001) Genetic enhancement of inflammatory pain by forebrain NR2B overexpression. *Nat Neurosci* **4**: 164-169

Wisden, W., and Seeburg, P.H. (1993) Mammalian ionotropic glutamate receptors. *Curr Opin Neurobiol* **3**: 291-298

Wong, R.W., Setou, M., Teng, J., Takei, Y., and Hirokawa, N. (2002) Overexpression of motor protein KIF17 enhances spatial and working memory in transgenic mice. *Proc Natl Acad Sci U S A* **99**: 14500-14505

Zhao, M.G., Toyoda, H., Lee, Y.S., Wu, L.J., Ko, S.W., Zhang, X.H., Jia, Y., Shum, F., Xu, H., Li, B.M., Kaang, B.K., and Zhuo, M. (2005) Roles of NMDA NR2B subtype receptor in prefrontal long-term potentiation and contextual fear memory. *Neuron* **47**: 859-872

Zheng, X., Zhang, L., Wang, A.P., Bennett, M.V., and Zukin, R.S. (1999) Protein kinase C potentiation of N-methyl-D-aspartate receptor activity is not mediated by phosphorylation of N-methyl-D-aspartate receptor subunits. *Proc Natl Acad Sci U S A* **96**: 15262-15267

Zuo, J., De Jager, P.L., Takahashi, K.A., Jiang, W., Linden, D.J., and Heintz, N. (1997) Neurodegeneration in Lurcher mice caused by mutation in delta2 glutamate receptor gene. *Nature* **388**: 769-773

7 ABSTRACTS

B. Doganci., J. vEngelhardt., P. H. Seeburg and H. Monyer (2005) Conditional knock-out of the NMDAR subunit NR2B. Presented at SFB 488 Symposium/ IZN (Interdisciplinary Center for Neurosciences) Retreat.

B. Doganci., J. vEngelhardt., P. H. Seeburg and H. Monyer (2005) Conditional knock-out of the NNMDAR subunit NR2B. Presented at Society for Neuroscience Meeting (Washington D.C).